




# Research Progress of Nanomedicine-Based Mild Photothermal Therapy in Tumor

Xiang He , Shentao Zhang, Yuhang Tian, Wen Cheng , Hui Jing 

Department of Ultrasound, Harbin Medical University Cancer Hospital, Harbin, People's Republic of China

Correspondence: Hui Jing; Wen Cheng, Department of Ultrasound, Harbin Medical University Cancer Hospital, No. 150, Haping Road, Nangang District, Harbin, 150081, People's Republic of China, Tel +86 13304504935; +86 13313677182, Email jinghuihrb@163.com; chengwen@hrbmu.edu.cn

**Abstract:** With the booming development of nanomedicine, mild photothermal therapy (mPTT, 42–45°C) has exhibited promising potential in tumor therapy. Compared with traditional PTT (>50°C), mPTT has less side effects and better biological effects conducive to tumor treatment, such as loosening the dense structure in tumor tissues, enhancing blood perfusion, and improving the immunosuppressive microenvironment. However, such a relatively low temperature cannot allow mPTT to completely eradicate tumors, and therefore, substantial efforts have been conducted to optimize the application of mPTT in tumor therapy. This review extensively summarizes the latest advances of mPTT, including two sections: (1) taking mPTT as a leading role to maximize its effect by blocking the cell defense mechanisms, and (2) regarding mPTT as a supporting role to assist other therapies to achieve synergistic antitumor curative effect. Meanwhile, the special characteristics and imaging capabilities of nanoplateforms applied in various therapies are discussed. At last, this paper puts forward the bottlenecks and challenges in the current research path of mPTT, and possible solutions and research directions in future are proposed correspondingly.

**Keywords:** nanomedicine, nanotechnology, mild photothermal therapy, tumor therapy

## Introduction

No more words are needed to emphasize the harm brought to people by tumors, and the traditional treatments like surgery, chemotherapy, and radiotherapy are still unable to improve the prognosis of patients effectively due to various contraindications, serious adverse reactions, and other limitations.<sup>1–3</sup> There is an urgent need for a novel therapeutic modality for Cancer. Fortunately, with the rapid development of nanotechnology in recent years, nanomedicine has gradually entered people's vision. Photothermal therapy (PTT), as an important part of nanomedicine, is a new effective tumor treatment method that makes use of photothermal agents (PTAs) to transform light energy into heat energy to kill tumor cells under the irradiation of external light sources, especially near-infrared light (NIR).<sup>4,5</sup> PTT has been broadly applied in tumor therapy research due to the spatiotemporal controllability, non-invasiveness, and minimal side effects compared with traditional tumor treatments.<sup>4,5</sup> The heat produced by PTAs is the key factor of PTT and directly determines the therapeutic effect of tumor as well as some biological reactions, and PTT is divided into conventional PTT and mild PTT (mPTT) according to temperature. As for conventional PTT, high local temperature (>50°C) is used to completely ablate the tumor tissues mainly through necrosis.<sup>6</sup> However, such excessive hyperthermia inevitably damages the surrounding normal tissues by non-specific heat diffusion, and the necrosis induced by PTT will cause severe local inflammation which may further impair normal tissues and even increase the risk of tumor metastasis.<sup>7</sup> Moreover, it has been proved that the host antitumor immunity is also suppressed attributed to the lesion of immune antigens at an overheating tumor microenvironment (TME) during PTT,<sup>8</sup> which is extremely unfavorable for clinical translation as the fact that the antitumor immune response plays an important role in inhibiting the metastasis and recurrence of tumors.<sup>9</sup> Therefore, mPTT at a relatively low temperature (usually 42–45°C) has been more and more widely used in recent years to avoid the drawbacks mentioned above.

Compared to the high-temperature PTT, mPTT produces negligible side effects by inducing apoptosis rather than necrosis while treating tumors, and the non-specific heat diffusion generated by such a relatively low temperature can be inconsiderable.<sup>10</sup> In addition, the biological effects of mPTT in favor of treatment make it more promising in tumor therapy. For instance, mPTT is able to loosen the dense structure in tumor tissues, enhance blood perfusion, and alleviate the hypoxic microenvironment, which can increase the infiltration of immune cells, improve the delivery of antitumor drugs, and boost the generation of reactive oxygen species (ROS), respectively.<sup>11–13</sup> However, mPTT utilizes low temperature that rarely causes harm to normal tissues, but the therapeutic efficacy is largely discounted and cannot ablate tumors as effectively as harsh PTT (hPTT). For this reason, extensive researches have been conducted to investigate how to improve the efficacy of mPTT in tumor therapy, mainly consisting of three aspects: (1) improving the property of PTAs and constructing multifunctional nanosystems, (2) taking mPTT as the leading role to maximize its effect by blocking the cell defense mechanisms, and (3) regarding mPTT as a supporting role to assist other therapies to achieve synergistic antitumor curative effect.

Since mPTT is a nanomedicine-based therapeutic method, the performance of nanomaterials directly determines the application prospects of mPTT. Researches on PTAs have emerged endlessly in recent years, which can be categorized into inorganic PTAs and organic PTAs. Inorganic PTAs have the advantages of excellent stability and high photothermal conversion efficiency (PCE), mainly comprising precious metals,<sup>14,15</sup> transition metals,<sup>16</sup> and some carbon-based nanomaterials,<sup>17,18</sup> while organic PTAs have the advantages of good biosafety and biodegradability, mainly including cyanine dyes,<sup>19,20</sup> conjugated polymers and polyaniline nanomaterials.<sup>21</sup> Whether inorganic PTAs or organic PTAs, the most basic but the most significant point is that they are supposed to possess extremely strong NIR absorption capacity and superb PCE, by reason of only with these features can lower quality NIR lasers and lower drug concentrations be employed during mPTT, as milder conditions undoubtedly improve the biosafety of therapy. In addition to developing novel PTAs with excellent PCE, researchers have issued a wide variety of multifunctional nanosystems to optimize the application of mPTT in tumor treatment. For instance, PTAs are endowed with the ability of active targeting to enhance accumulation in tumor tissues by being wrapped with biomimetic nanomaterials like cancer cell hybrid membranes.<sup>22</sup> Furthermore, the breakthrough in nanomaterials allows mPTT to apply laser radiation in the NIR-II window (1000–1350nm, especially 1064nm) with deeper penetration, higher maximum exposure to the skin, and lower signal-to-noise ratio than initial NIR-I window (750–1000nm, especially 808nm).<sup>23,24</sup> Last but not the least, imaging capabilities such as fluorescence imaging (FLI), Ultrasound (US), photoacoustic imaging (PAI), computed tomography (CT), and magnetic resonance imaging (MRI), also provide mPTT with favorable information for tumor diagnosis and treatment. For instance, the biodistribution of nanodrugs can be detected by imaging techniques, which identify tumors to provide diagnostic information, help determine the optimal starting irradiation time to obtain the maximum utilization of nanocomposites, and monitor the treatment process and outcomes. Each imaging modality has its own outstanding advantages. FLI has superior sensitivity and US can realize real-time monitoring of deep tissue, while PAI and MRI have excellent spatial resolution.

Although great efforts have been put into promoting mPTT by optimizing the performance of PTAs, mPTT monotherapy is still unable to fully eradicate tumors owing to the existence of a series of defense mechanisms of tumor cells. On the one hand, heat shock proteins (HSPs), a sort of molecular chaperone that involves in the process of repairing misfolded or denatured protein, are elevated to weaken the heat injury during mPTT when the tissue temperature rises to 41°C.<sup>25</sup> On the other hand, autophagy is activated under heat pressure and able to provide nutrition and energy for cell regeneration by degrading misfolded proteins and organelles, ultimately playing a protective role to resist mPTT.<sup>26</sup> Therefore, various strategies and multifunctional nanosystems have been meticulously designed to reduce HSPs expression or regulate the autophagy process to maximize mPTT efficacy. Besides, the combinations of mPTT with other therapies have also shown great clinical transformation value in tumor treatment due to its outstanding regulation ability and unique biological effects. Mild hyperthermia can realize controlled release and enhanced internalization of agents for combined application with chemotherapy and gene therapy, alleviate tumor hypoxia and increase ROS production for combined application with radiotherapy (RT), photodynamic therapy (PDT), and sonodynamic therapy (SDT), catalyze Fenton/Fenton-like reactions for combined application with chemodynamic therapy (CDT), decompose azo initiator to generate oxygen-independent alkyl radicals (R) for combined application with thermodynamic therapy (TDT), and convert “cold” tumors into “hot” tumors to improve immunosuppressive microenvironment for combined application with immunotherapy.

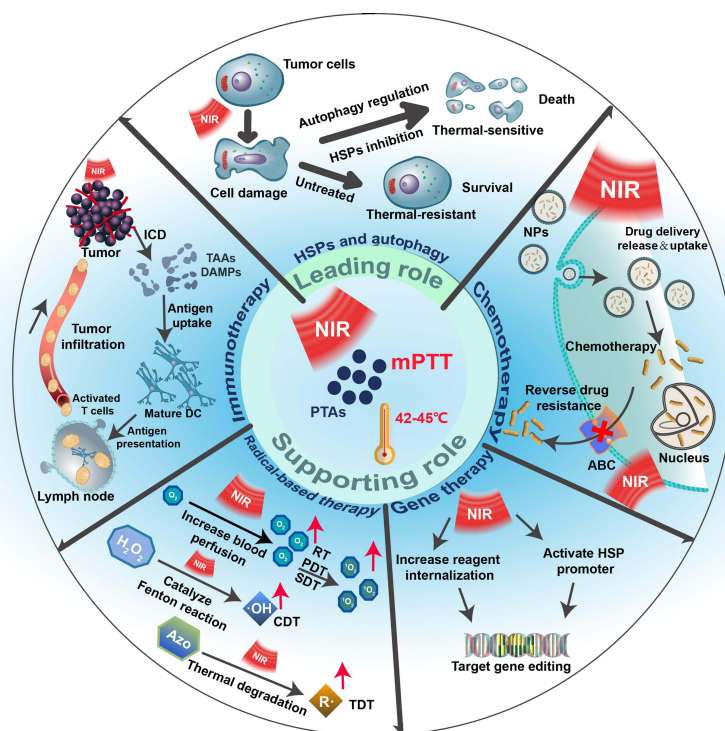


**Figure 1** Schematic illustration of mPTT playing a leading role or a supporting role in tumor therapy.

In this review, we extensively summarize the latest advances in the therapeutic applications of mPTT in cancer, mainly including two sections: (1) taking mPTT as a leading role to maximize its effect by blocking the cell defense mechanisms, and (2) regarding mPTT as a supporting role to assist other therapies to achieve synergistic antitumor curative effect (Figure 1). Meanwhile, we also summarize the special characteristics and imaging capabilities of nanoplatforms applied in various therapies. At last, we put forward the bottlenecks and challenges in the current research path of mPTT, and at the same time, possible solutions and research directions in future are proposed correspondingly.

## mPTT Plays a Leading Role in Tumor Therapy

Unlike hPTT at an overheating temperature, which rudely degrades all the protective proteins produced by tumors under heat stress, mPTT cannot bypass the stress protector mechanisms at a relatively mild temperature, and therefore the efficacy is largely diminished. Among defensive mechanisms, HSPs and autophagy play an important role in keeping tumors from heat injury. Primarily, heat-induced misfolding and dysfunctional proteins are prevented from aggregating by activated HSPs, and subsequently, HSPs can restore the function of impaired proteins, then repair the thermal damage.<sup>27,28</sup> In addition to HSPs, autophagy also plays a critical role in protecting cells from stress and various kinds of tumor treatments. Autophagy, as a highly conserved catabolic process and an important mechanism for maintaining intracellular homeostasis, exists in most cells, and autophagy mainly includes three steps: autophagosome formation, fusion with lysosome, and autolysosome degradation.<sup>29,30</sup> Once the progression of autophagy proceeds smoothly, the degradation of autolysosome which engulfed damaged organelles and dysfunctional proteins provides nutrition and energy for cell regeneration,<sup>31</sup> resulting in the survival of cancer cells and contributing to the inefficiency of a broad range of tumor treatment methods. As a result of HSPs and autophagy, cancer cells are able to escape heat injury and be highly resistant to therapies. To this end, studies on potentiating mPTT by inhibiting HSPs and manipulating autophagic process have been widely reported, including initial drug treatment and various novel strategies in the latest years. Of note, whether it is the inhibition of HSPs or the regulation of autophagy process, mPTT is always the key factor to kill tumor cells, so we call it the leading role in this part.

## mPTT Plays a Leading Role Through HSPs Inhibition

Based on their molecular mass, HSPs are usually classified into small HSPs (HSPB, molecular mass < 40 kDa), HSP40 (DNAJ), HSP60 (HSPD), HSP70 (HSPA), HSP90 (HSPC), and HSP110 (HSPH).<sup>32,33</sup> It has been demonstrated that HSPs with different molecular mass not only carry out many of the protein chaperone functions independently, but also collaborate on other protein structure-modifying functions. HSP70 involves in the early stage of folding and is related to a wide range of protein regions, while HSP90 recognizes specific conformations, and HSP60 promotes the folding, unfolding, and degradation of mitochondrial proteins.<sup>34,35</sup> These three types of HSPs are currently the most extensively studied among all HSPs due to their thermal resistance and antitumor apoptotic properties. Recently, heat resistance has been overcome by a variety of HSPs inhibition strategies based on the rapid development of nanomedicine, mainly including HSPs inhibitors-mediated HSPs inhibition, ATP-mediated HSPs inhibition, gas-mediated HSPs inhibition, and gene editing-mediated HSPs inhibition (Table 1).

**Table 1** mPTT Plays a Leading Role Through HSPs Inhibition

Strategy	Nanoplatfrom	PTAs	Therapeutic Agent	Target	Irradiation Wavelength	Imaging Capability	Ref.
Inhibitors	Virus-like SiO <sub>2</sub> /CeO <sub>2</sub> /VO <sub>x</sub> (SCV) nanoplatfrom	SiO <sub>x</sub>	VO <sup>2+</sup>	HSP60	1064nm	\	[36]
	ICG-loaded VO <sub>2</sub> (VO <sub>2</sub> -ICG)	ICG	VO <sup>2+</sup>	HSP60	785nm	FLI	[37]
	PEG-PAu@SiO <sub>2</sub> -SNO	Au@SiO <sub>2</sub>	PES	HSP70	808nm	\	[38]
	Liposome-supported gold nanoparticles (lipoAu) and PES	Lipoau	PES	HSP70	808nm	\	[39]
	COF-GA	COF	GA	HSP90	635nm	\	[25]
	HSA/dc-IR825/GA	dc-IR825	GA	HSP90	808nm	FLI	[40]
	Thermo-sensitive organic lauric acid-coated mesoporous organosilica NPs loading PB and GA (GA-PB@MONs@LA)	PB	GA	HSP90	808nm	PAI/MRI	[41]
	Mn-ICG@pHis-PEG/GA	ICG	GA	HSP90	808nm	FLI/PAI/MRI	[42]
	GA-loaded and PEGylated hollow mesoporous carbon spheres (HMCS-PEG-GA)	HMCS	GA	HSP90	808nm	PAI	[43]
	HA-functionalized and GA-loaded Bi <sub>2</sub> Se <sub>3</sub> hollow nanocube (HNC-s-s-HA/GA)	Bi <sub>2</sub> Se <sub>3</sub>	GA	HSP90	808nm	Multispectral optoacoustic tomography (MSOT)/CT	[44]
	PEGylated liposome (LP)-coated gold nanostars (AuNS) loading GA and tetrakis(4-carboxyphenyl) porphyrin (TCPP) with Zr <sup>4+</sup> (AuNS@ZrTCPP-GA@LP)	AuNS	GA	HSP90	980nm	FLI	[45]
	PEG-IR780-BIIB021 nano-micelles	IR780	BIIB021	HSP90	808nm	\	[46]
	17AAG and AIPH loaded mesoporous polydopamine (M-17AAG-AIPH)	PDA	17AAG	HSP90	808nm	FLI	[47]
	AIPH, ICG, and 17-AAG-loaded and HA-functionalized ZIF (A/I@aZIF@AAG@HA)	ICG	17-AAG	HSP90	808nm	\	[48]
	Star-PEG-PCL (sPP) and HA-functionalized hollow mesoporous PB loading 17-DMAG (17-DMAGHMPB@sPP@HA)	PB	17-DMAG	HSP90	808nm	\	[49]
	Lu:Nd@NiS <sub>2</sub> -EGCG	NiS <sub>2</sub>	EGCG	HSP90	808nm	Short-wave infrared imaging (SWIR)/MRI	[50]
	PI3K inhibitor LY294002-loaded Bi <sub>2</sub> S <sub>3</sub> -Tween 20 nanoplatfrom(Bi <sub>2</sub> S <sub>3</sub> -Tween 20@LY294002)	Bi <sub>2</sub> S <sub>3</sub>	LY294002	PI3K(PI3K/Akt/GSK-3/HSP)	808nm	\	[51]
	MPEG-coated-AuNR and VER-155008 micelles (MPEG-AuNR@VER-M)	AuNR	VER-155008	HSP70 HSP90	808nm	FLI/PAI	[14]

(Continued)



Table I (Continued).

Strategy	Nanoplatform	PTAs	Therapeutic Agent	Target	Irradiation Wavelength	Imaging Capability	Ref.
ATP regulation	pH-sensitive charge-transfer nanoparticles (CTNs) and GOx-loaded hydrogel (CAG)	CTNs	GOx	Glucose	1064nm	FLI	[52]
	Fe-PDAP/GOx/ICG	ICG	GOx	Glucose	808nm	FLI/PAI/MRI	[53]
	Lonidamine-loaded cancer cell membrane-cloaked Prussian blue (PB) nanoparticles (HmPGTL NPs)	PB	LN	Glucose	808nm	PAI	[54]
	PBLM@CCM	PB	LN	Glucose	793nm	US/PAI	[55]
	Platelet membrane (PM)-coated mesoporous Fe single-atom nanozyme (PMS)	Fe-Sazyme	OH	Mitochondria	1064nm	FLI	[56]
Gene regulation	PEGylated polydopamine (PDA)-coated nucleic acid nanogel (PP-NG)	PDA	SiRNA	HSP70	808nm	FLI	[57]
	Hypoxia-responsive gold nanorods (AuNRs)-based nanocomposite of CRISPR-Cas9 (APACPs)	AuNRs	Cas9 RNP	HSP90 $\alpha$	808nm	\	[58]
	CuS-RNP/DOX@PEI	CuS	Cas9 RNP	HSP90 $\alpha$	808nm	\	[59]
Gas regulation	NIR light responsive CuS-based NO gas nanogenerator (CuS-PEI/NO-TPP)	CuS	NO	Mitochondria	1064nm	\	[60]
	ENBS-PEG@L-TiO <sub>2</sub> -GNR	GNR	H <sub>2</sub>	HSP90	808nm	FLI	[61]
	PBPTV@mPEG (CO)	AIE polymer PBPTV	CO	HSP70	808nm	FLI	[62]
Ferroptosis	Pd-Sazyme	Pd-Sazyme	LPO/ROS	HSPs	1064nm	\	[15]

### HSPs Inhibitors-Mediated HSPs Inhibition

Up to today, researchers have exploited a variety of inhibitors to directly target different types of HSPs. Among them, VO<sup>2+</sup>, which can be transformed from vanadium oxide under a mildly acidic condition (pH 6.5–6.9), is able to inhibit the expression of HSP60.<sup>63</sup> For example, Zhao et al ingeniously developed a PEG-modified virus-like silicon oxide nanoplatform (SiO<sub>x</sub>/CeO<sub>2</sub>/VO<sub>x</sub>, SCV-PEG) loading CeO<sub>2</sub> and VO<sub>x</sub> simultaneously to achieve VO<sup>2+</sup>-mediated HSP60 inhibition for enhancing mPTT (Figure 2a).<sup>36</sup> Virus-like structures could load more drugs and transfer them into cells due to a large specific surface area, which facilitated the cell adhesion and phagocytosis of nanodrugs in tumors,<sup>64</sup> and SiO<sub>x</sub> was able to maintain the local temperature at 45°C under a 1064nm laser excitation in the NIR-II window. In addition, VO<sup>2+</sup> converted from VO<sub>x</sub> significantly inhibited the expression of HSP60 at a mild acidic TME. Accordingly, immunofluorescence staining assay results showed that the expression level of HSP60 in SCV-PEG+NIR group was obviously lowered than any other group. At the same time, SCV-PEG could also serve as a peroxidase (POD) due to the existence of CeO<sub>2</sub> capable of reacting with hydrogen peroxide (H<sub>2</sub>O<sub>2</sub>) to generate hydroxyl radical ( $\cdot$ OH). Synergistic with nanozyme catalytic therapy, SCV-PEG+NIR exhibited the highest tumor-killing efficiency in vitro and the smallest tumor volume in vivo, which resulted from the down-regulation of HSP60 that magnified the curative effect of mPTT and the production of toxic free radicals. Similarly, a novel VO<sub>2</sub>-ICG nanocomposite fabricated by Wang et al also realized the degradation of VO<sub>2</sub>-ICG under weak acidic TME and downregulated the expression of HSP60 to enhance photothermal tumor ablation.<sup>37</sup> Moreover, indocyanine green (ICG), a US Food and Drug Administration (FDA)-approved small molecular chromophor, not only endowed the nanocomposite with the ability of photothermal conversion but also the capacity of FLI to achieve imaging-guided enhanced mPTT.<sup>65</sup>

Besides HSP60 inhibitors, HSP70 inhibitors are also widely employed in mPTT for accomplishing satisfactory tumor treatment outcomes. Although researchers have demonstrated that HSPs expressions are decided by temperature, where the maximum expression content is reached at 43 °C for HSP70 and 45 °C for HSP90 in tumor cells, the correlation between HSPs expression and PTT temperature in vivo remains unclear.<sup>66</sup> In order to realize the precise management of HSPs expression, Xia et al made use of liposome-templated gold nanoparticles which had low-temperature fluctuation (smaller than 1°C) to

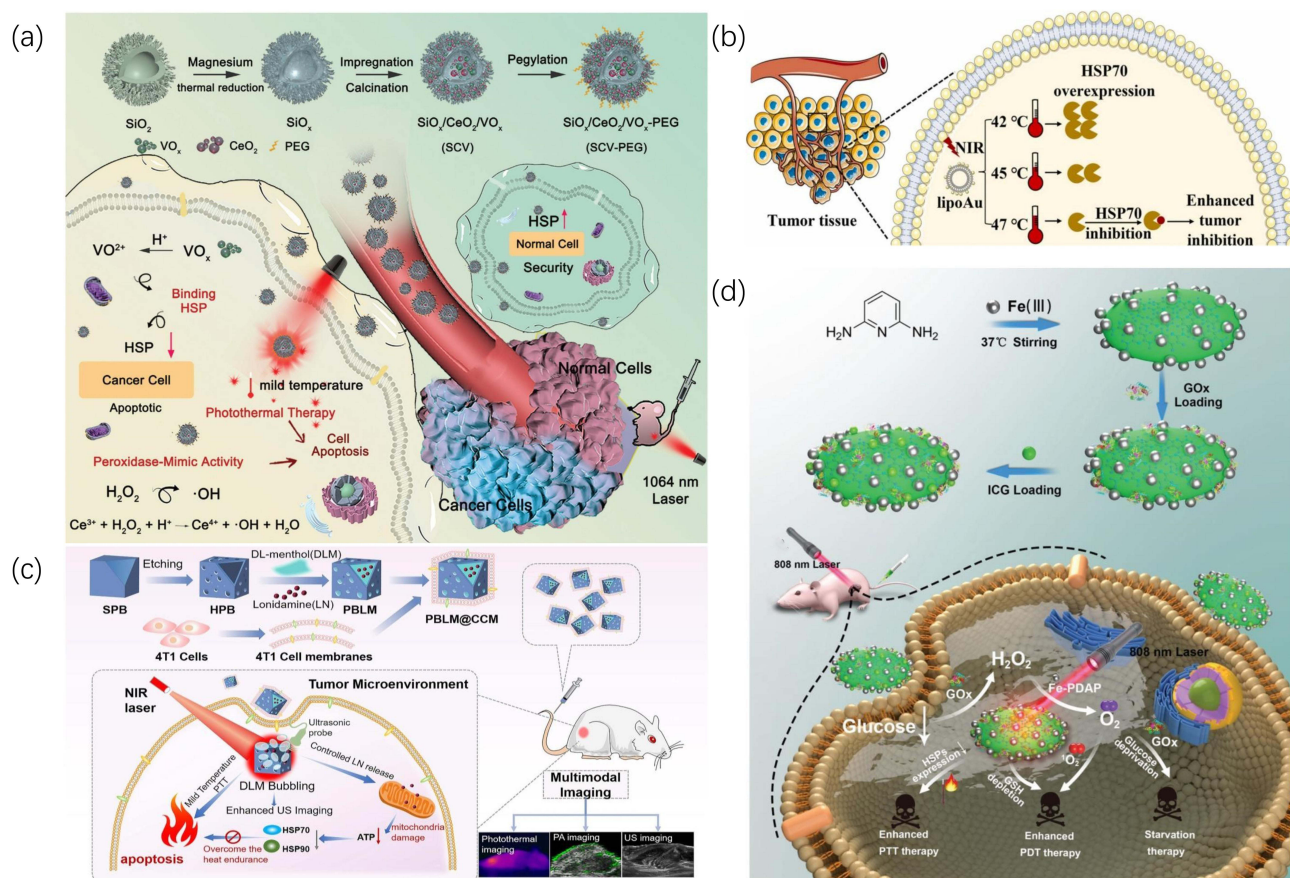


**Figure 2** (a) Schematic depicting the synthesis of virus-like SCV-PEG and its application in  $\text{VO}_2^{2+}$ -mediated HSP60 inhibition for enhancing mPTT. Reprinted with permission from Zhao R, Zhang R, Feng L, et al. Constructing virus-like SiO<sub>2</sub>/CeO<sub>2</sub>/VO<sub>2</sub> nanozymes for 1064 nm light-triggered mild-temperature photothermal therapy and nanozyme catalytic therapy. *Nanoscale*. 2022;14(2):361–372. Copyright 2022 Royal Society of Chemistry. (b) Schematic illustrating the temperature-mediated precise management of HSPs expression, where 47°C with the least HSP70 expression was applied for mPTT. Reprinted from *Colloids Surf B Biointerfaces*, 217, Xia Y, Li C, Cao J, et al. Liposome-templated gold nanoparticles for precisely temperature-controlled photothermal therapy based on heat shock protein expression. *Colloids Surf B Biointerfaces*. 2022;217:112686. Copyright 2022, with permission from Elsevier. (c) Schematic showing the synthesis of PBLM@CCM and its application for multimodal imaging-guided and multimodal-targeted mPTT. Reprinted from *J Control Release*, 347, Shu X, Chen Y, Yan P, et al. Biomimetic nanoparticles for effective mild temperature photothermal therapy and multimodal imaging. *J Control Release*. 2022;347:270–281. Copyright 2022, with permission from Elsevier. (d) Synthesis of the nanoplatform and its application for multimodal combination therapy. Reprinted with permission from Cao J, Qiao B, Luo Y, et al. A multimodal imaging-guided nanoreactor for cooperative combination of tumor starvation and multiple mechanism-enhanced mild temperature phototherapy. *Biomater Sci*. 2020;8(23):6561–6578. Copyright 2020 Royal Society of Chemistry.

probe the expression of HSP70 and HSP90 versus temperature (42,45,47,50,55°C) in 4T1 tumor-bearing Bal/b mice (Figure 2b).<sup>39</sup> Quantitative real time PCR analysis showed that the maximum expression of HSP70 and HSP90 were at 42°C and 47°C (3.9-fold and 2.3-fold compared to PBS group), similar to the in vitro results of Mantso's work,<sup>66</sup> while the minimal expression of HSP70 and HSP90 were both almost at 55°C (0.5-fold compared to PBS group). Interestingly, it found that the expression of HSP70 was more susceptible to temperature changes than HSP90, so the inhibition of HSP70 might be more beneficial to tumor treatment. Despite the lowest HSP70 expression and the best therapeutic efficacy at 55°C, it led to severe tumor necrosis and inflammation. Thus, the second lowest HSP70 expression, 47°C, was selected as the optimal temperature to combine 2-Phenylethanesulfonamide (PES, an HSP70 inhibitor) for enhancing mPTT, since lower expression of HSP70 meant less heat resistance and lower concentration of HSP inhibitors. Undoubtedly, the results showed that the introduction of PES greatly elevated the therapeutic outcome at a mild temperature. Such an accurate temperature-controlled mPTT based on the expression of HSPs strategy opened a new field of vision for tumor ablation.

Compared to HSP60 and HSP70 inhibitors, there is a greater variety of HSP90 inhibitors applied to mPTT. Among them, gambogic acid (GA) has almost occupied the largest proportion of HSP90 inhibitors in recent years' researches. For instance, Sun et al designed a nanoagent (COF-GA) for enhanced PTT against cancer at low temperature.<sup>25</sup> Covalent organic frameworks (COFs), a novel type of porous materials composing of molecules linked by covalent bonds, had shown great potential in bioMedical field because of their long-range ordered structure with large and regular pores and

components of only light atoms (such as C, H, O, N and B, etc.), which endowed them with high drug loading capacity and excellent biocompatibility.<sup>67–70</sup> The fabricated COF-GA nanoagent exerted a low-temperature (about 44°C) PTT on 4T1 tumor-bearing Balb/C mice upon 635nm NIR laser irradiation. After two weeks post treatment, the relative tumor volumes were obviously inhibited while neither the body weights of treated mice nor the serum biochemical measurements (ALT, AST, CRER, URER) significantly changed during the observation period, demonstrating excellent antitumor efficacy and negligible nonspecific thermal damage of this enhanced mPTT strategy and broadening our vision towards the different applications of COFs in biomedicine field. Apart from GA, other types of HSP90 inhibitors applied in mPTT had also achieved satisfactory cancer treatment outcomes. Zhang et al synthesized a mitochondria-targeted photosensitizer consisting of IR780 iodide and BIIB021 (an HSP90 inhibitor).<sup>46</sup> After selectively aggregating on mitochondria, the prepared PEG-IR780-BIIB021 released BIIB021 under 808nm laser irradiation to increase tumor heat sensitivity, which could reduce the mitochondrial membrane potential and induce the release of key intrinsic apoptotic factors (Cyt-C, Caspase-9, Bcl-2, and Bax) to activate the mitochondrial apoptotic pathway. In another example, Jiang group loaded phenolic epigallocatechin 3-gallate (EGCG, an HSP90 inhibitor) into the flower-like NiS<sub>2</sub> coated-NaLuF<sub>4</sub>:Nd nanoparticle (Lu:Nd@NiS<sub>2</sub>).<sup>50</sup> This novel therapeutic agent (Lu:Nd@NiS<sub>2</sub>-EGCG) achieved remarkable antitumor efficacy under the dual-mode imaging guidance of short-wave infrared light imaging and MRI. In addition, 17-allylamino-geldanamycin (17-AAG) and its second-generation derivative 17-dimethylamino-ethylamino-17-demethoxygeldanamycin (17-DMAG) had been proved to inhibit HSP90 expression for enhancing mPTT.<sup>48,49</sup>

### ATP-Mediated HSPs Inhibition

Since the expression, activation, and synthesis of HSPs primarily rely on intracellular adenosine triphosphate (ATP) levels, preventing intracellular ATP synthesis may assist to combat HSPs-dependent tumor heat tolerance and enhance the effectiveness of PTT at low temperature.<sup>71,72</sup> According to the Warburg effect, ATP produced by tumor cells occurs mainly through the glycolytic pathway rather than the oxidative phosphorylation pathway, even in the presence of sufficient oxygen, thus interfering with the process of glycolysis and reducing the level of glucose within the tumor are effective strategies to reduce ATP production.<sup>73,74</sup> Inspired by this, Shu et al loaded lonidamine (LN, a glycolysis inhibitor) and DL-menthol (DLM) into hollow mesoporous Prussian blue nanoparticles (HPB NPs) (Figure 2c).<sup>55</sup> DLM had the property of controllable solid-liquid-gas (SLG) triphasic change because of its boiling point of 212°C and melting point of 32–36°C, which made it not only a blocker agent of LN to avoid its early leakage, but also a US imaging agent.<sup>75,76</sup> After 793nm laser irradiation, the heat produced by HPB NPs was able to induce DLM vaporization and boost LN release, which could be observed by US imaging in real time. Moreover, the coating of 4T1 cancer cell membrane (CCM) endowed nanoparticles with the ability of homologous targeting and better biocompatibility. In conclusion, under the guidance of PAI and US imaging, PBLM@CCM NPs could specifically target tumors and decrease the level of intracellular ATP, thereby simultaneously reducing the expression of HSP70 and HSP90, so as to achieve enhanced mPTT.

Similarly, glucose oxidase (GO<sub>x</sub>), which can convert glucose into gluconic acid and H<sub>2</sub>O<sub>2</sub>, has been broadly applied in mPTT for tumors due to its property capable of reducing the level of glucose in tumor, which subsequently decreases the production of ATP and downregulates the expression of HSPs.<sup>77–79</sup> For instance, Cao et al elaborated a nanoreactor (Fe-PDAP/GO<sub>x</sub>/ICG) that simultaneously loaded GO<sub>x</sub> and ICG into Fe-doped polydiaminopyridine (Fe-PDAP) (Figure 2d).<sup>53</sup> As a nanozyme with intrinsic catalase-like activity, Fe-PDAP could not only convert H<sub>2</sub>O<sub>2</sub> generated from GO<sub>x</sub>-mediated glucose decomposition and naturally possessed H<sub>2</sub>O<sub>2</sub> within tumors to oxygen, but also consumed glutathione (GSH, ROS scavenger) via metal reduction reaction after releasing Fe<sup>3+</sup> to sensitize the ICG-mediated PDT. Meanwhile, the ICG-mediated mPTT could also be promoted attributed to the reduction of glucose and ATP as well as the decreased expression of HSPs. Moreover, Fe-PDAP/GO<sub>x</sub>/ICG nanoreactor had shown superior performance in imaging to simultaneously achieve FLI/PAI/MRI.

In addition to glucose-regulation-mediated downregulation of ATP, mitochondria, known as the factory of ATP production, plays an important role in ATP-dependent HSPs production, therefore interfering with the function of mitochondrial can also be used as a strategy to downregulate HSPs. Qi et al reported for the first time that biomimetic mesoporous Fe-SAzyme could realize mitochondrial damage-mediated mPTT (Figure 3a).<sup>56</sup> Although single-atom



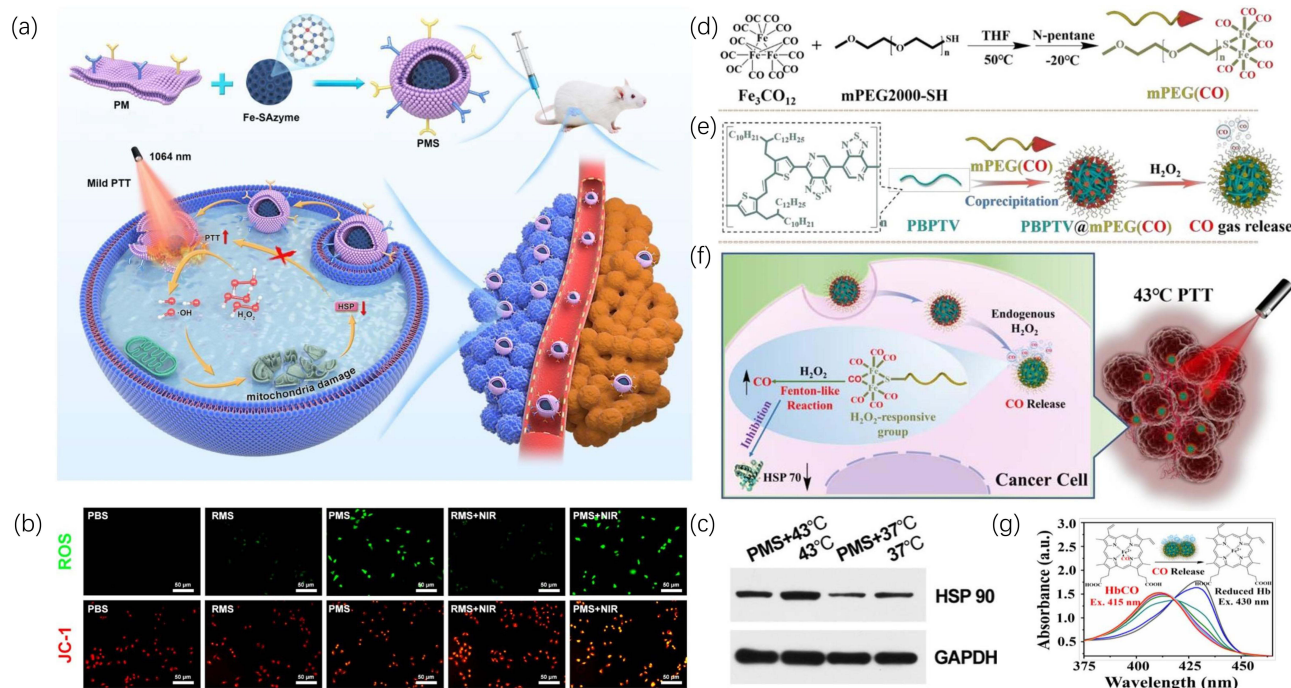


**Figure 3** (a) Schematic showing the synthesis of PMS and its working mechanisms in mPTT. (b) DCF fluorescence and JC-1 fluorescence intensity after the indicated treatments. (c) Western blot analysis of HSP90 after treatments. (a–c) Reprinted with permission from Qi P, Zhang J, Bao Z, et al. Nanozyme for mitochondrial damage-mediated mild-temperature photothermal therapy. *ACS Appl Mater Interfaces*. 2022;14(17):19081–19090.<sup>56</sup> Copyright 2022 American Chemical Society. (d) Schematic illustration of the synthesis of mPEG(CO). (e) Schematic depicting the nanobomb consisting of mPEG(CO) and PBPTV. (f) Schematic illustration of the working mechanisms of nanobomb. (g) The UV spectrum shift exhibits the release of CO into the aqueous nanobomb solution measured by reduced hemoglobin. (d–g) Reprinted with permission from Ma G, Liu Z, Zhu C, et al. Responsive NIR-II AIE nanobomb for carbon monoxide boosting low-temperature photothermal therapy. *Angew Chem Int Ed Engl*. 2022;61(36):e202207213. © 2022 Wiley-VCH GmbH.<sup>62</sup>

nanozyme (SAzyme) based on carbon material had emerged remarkable potential in cancer therapy and antibacterial therapy due to their distributed metallic architecture, which enabled SAzyme to maximize the usage of metal catalytic sites, the hard surface modification of carbon-based materials made it difficult for SAzyme to achieve tumor targeting.<sup>80–83</sup> For this reason, platelet membrane (PM) was coated onto the surface of Fe-SAzyme to attain tumor-targeting ability attributable to the tendency of PM to vascular injury areas and abnormal vascular structures in tumor tissue.<sup>84,85</sup> After specific aggregation to tumor tissue, PM-coated Fe-SAzyme (PMS) with POD activity could catalyze  $H_2O_2$  to produce  $\cdot OH$ , causing mitochondrial damage and down regulating HSPs, thereby enhancing mPTT under NIR-II excitation (Figure 3b and 3c). In another example of SAzyme, Chang et al added glutathione oxidase (GSHOx) activity on Pd-SAzyme with POD activity to induce ferroptosis that could produce a large number of lipid peroxides (LPO) to cleave HSPs, firstly achieving ferroptosis-boosted mPTT based on SAzyme.<sup>15</sup> These findings provided new insights into the current application of single-atom nanozyme in mPTT.

### Gas-Mediated HSPs Inhibition

In the latest research, gas-mediated HSPs downregulation which employs therapeutic auxiliary gases (such as CO,  $H_2$ , NO, etc.) or their precursor medications to inhibit the expression of HSPs has received a lot of interest in low-temperature PTT. For instance, Ma et al established a nanobomb (PBPTV@mPEG(CO)) based on the self-assembly of NIR-II AIE polymer PBPTV and carbon monoxide (CO) storage polymer mPEG, which could be destroyed by the excessive  $H_2O_2$  in TME to release CO and suppressed the overexpression of HSPs (Figure 3d–f).<sup>62</sup> In order to assess the CO release ability of the nanobomb, they used reduced hemoglobin (Hb) for measuring CO content that could be calculated in the light of the absorption peak value of reduced Hb and HbCO (Figure 3g).<sup>86</sup> In a simulated environment of TME, the nanobomb released CO vigorously at the speed of 1494/s, while barely released in the absence of  $H_2O_2$ . Western blot analysis proved that the expression of HSP70 was significantly inhibited by CO under a low temperature (43°C). With the guidance of FLI, this nanobomb exhibited excellent tumor inhibition effect both in vivo and in vitro.

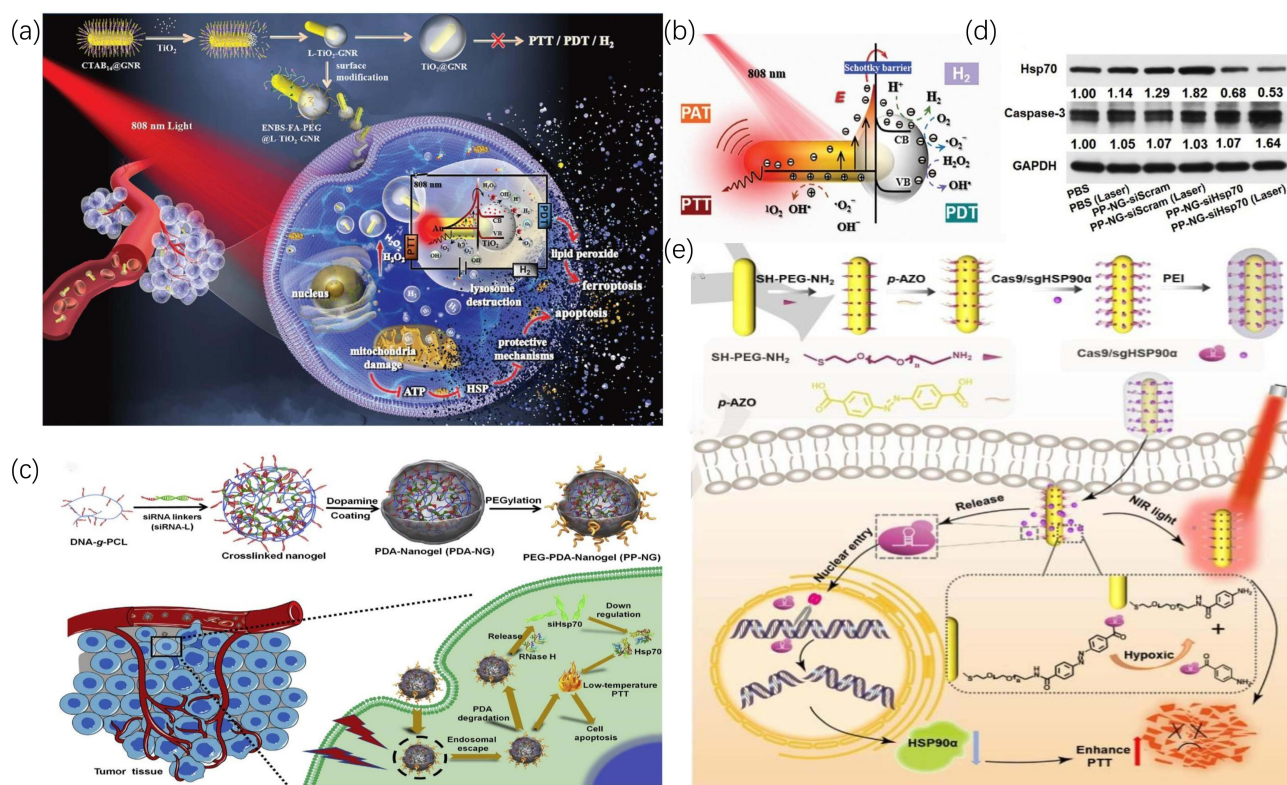


**Figure 4** (a) Schematic showing the construction of ENBS-PEG@L-TiO<sub>2</sub>-GNR nanoparticle and its application in synergistic PDT, mPTT, and H<sub>2</sub> therapy. (b) The mechanism of ROS generation and photothermal effect by ENBS-PEG@L-TiO<sub>2</sub>-GNR nanoparticle upon NIR irradiation. (a and b) Reprinted with permission from Ge H, Du J, Long S, et al. Near-Infrared Light Triggered H<sub>2</sub> Generation for Enhanced Photothermal/Photodynamic Therapy against Hypoxic Tumor. *Adv Healthc Mater.* 2022;11(3):e2101449. © 2021 Wiley-VCH GmbH.<sup>61</sup> (c) Schematic illustrating the synthesis of PP-NG and its working mechanisms in combination therapy. (d) Western blot analysis of HSP70 and Caspase-3 after the indicated treatments. (c and d) Reprinted from *Biomaterials*, 245, Ding F, Gao X, Huang X, et al. Polydopamine-coated nucleic acid nanogel for siRNA-mediated low-temperature photothermal therapy. 119976, Copyright 2022, with permission from Elsevier.<sup>57</sup> (e) The synthesis of Cas9/sgHSP90a and its application for gene editing and mPTT combination therapy. Reprinted with permission from Li X, Pan Y, Chen C, et al. Hypoxia-responsive gene editing to reduce tumor thermal tolerance for mild-photothermal therapy. *Angew Chem Int Ed Engl.* 2021;60(39):21200–21204. © 2021 Wiley-VCH GmbH.<sup>58</sup>

Equally, H<sub>2</sub> has been used to reduce the expression of HSPs to optimize mPTT. Different from the previous example, Ge group took advantage of the hot electron transfer property to produce H<sub>2</sub> in TME to damage mitochondria instead of carrying gas from the outside, thus reducing the expression of HSPs (Figure 4a).<sup>61</sup> The developed gold nanorod/titanium dioxide lollipop-like nanoparticle(L-TiO<sub>2</sub>-GNR) could generate abundant hot electrons on the GNRs under irradiation at 808nm. On the one hand, some of the electrons generated on the GNRs were able to raise local temperature to 48°C to produce mPTT effect on tumors (Figure 4b). On the other hand, the rest electrons could yield ·OH, <sup>1</sup>O<sub>2</sub>, and H<sub>2</sub> by irreversibly injecting into the conduction band of TiO<sub>2</sub> through the Schottky junction, thus inducing PDT effect and the simultaneous production of H<sub>2</sub> was capable of reducing the expression of HSPs (Figure 4b). Further, the introduction of Nile blue derivative ENBS and PEG enabled nanoparticles to have FLI ability and higher biocompatibility. Therefore, this ENBS-PEG@L-TiO<sub>2</sub>-GNR nanoparticle which had synergistic PDT, mPTT, and H<sub>2</sub> therapy only with the support of NIR irradiation opened a new window for gas-enhanced mPTT. Besides CO and H<sub>2</sub>, NO also played a role in gas-mediated HSPs degradation. A mitochondria-targeting CuS-PEI/NO-TTP nanoplatfrom that combined mPTT and NO gas treatment, two distinct therapeutic modalities, in a single nanomaterial to synergistically improve cancer therapy was described by Wu et al<sup>60</sup> Under 1064 nm laser irradiation, NO released from nanomaterial could interfere with the function of mitochondria to decrease ATP production, causing the suppression of HSP90 and enhancing mPTT.

### Gene Editing-Mediated HSPs Inhibition

Gene editing-mediated HSPs down-regulation by silencing HSPs at the genomic level which mainly includes small interfering RNA (siRNA) and the clustered regularly interspaced short palindromic repeats-associated protein 9 system



(CRISPR-Cas9) has become an indispensable part of mPTT. However, one of the biggest challenges is that the exposed siRNA will be degraded by various biological molecules such as nuclease, which increases the difficulty of its application. For this purpose, Ding et al elaborately designed a PEGylated PDA-coated siRNA-bearing nucleic acid nanogel (PEG-PDA-NG) with three shields (Figure 4c).<sup>57</sup> Under the protection of three-layered barriers comprising nucleic acid nanogel, PDA, and PEG, siRNA could be free from the degradation of lysosomes and effectively silenced HSP70. Under 808nm laser irradiation, the secondary barrier PDA also functioned as a PTA to realize mPTT. The Western blot results showed that the expression of HSP70 in PEG-PDA-NG+NIR group was significantly reduced compared with the rest groups, along with a remarkable increase level in caspase-3 (a representative protein of apoptosis) (Figure 4d). This work gave a classic example of the realization of gene-mediated mPTT while also providing an easily scalable and applicable nano-delivery platform that could be applied as a vehicle for other combination therapies.

In the recent development of gene editing technologies, CRISPR-Cas9 composing of Cas9 nuclease and single-guide RNA (sgRNA) undoubtedly occupies the most important position and has been increasingly applied in cancer research because of its high specificity, easy operation, well efficiency, and simultaneous silencing of multiple targets.<sup>87</sup> Li et al constructed a hypoxia-responsive nanoplatform by connecting CRISPR-Cas9 system with Au nanorods through azobenzene-4, 4'-dicarboxylic acid (P-AZO, a hypoxia-responsive azobenzene linker) to achieve Cas9-mediated mPTT (Figure 4e).<sup>58</sup> Under normal partial pressure of oxygen, CRISPR-Cas9 system was covalently cross-linked to Au nanorods through P-AZO, but by reaching the tumor area, a hypoxic microenvironment, the N-N double bond of P-AZO would be cleaved, causing the release of Cas9/sgRNA ribonucleoprotein mixture (Cas9 ribonucleoprotein, Cas9 RNP) and specifically knocking down Hsp90 $\alpha$  (a subunit of Hsp90). Similarly, Chen et al took another approach to regulate the release of Cas9 RNP.<sup>59</sup> According to the principle of base complementary pairing, Cas9 RNP was assembled with Thiol-modified DNA (DNA-SH) fragments which were conjugated to CuS NPs. Under 808nm light irradiation, heat introduced by CuS could break the double chain and promote the release of Cas9 RNP to knock out Hsp90 $\alpha$ . Both studies, although utilizing different modes of regulation, were successful in achieving Cas9-mediated mPTT by specifically knocking down Hsp90 $\alpha$ .

In general, various approaches of inhibiting HSPs mentioned above to sensitize mPTT all achieved favorable efficacy. We believe that there is no best but only the most suitable strategy to down regulate the expression of HSPs, which mainly benefits from the rapid development of nanotechnology which allows the drawbacks of different therapies to be addressed one by one. For instance, nanoplatform can realize non-targeted drugs to reach tumor tissue specifically, make gas-mediated therapy possible, and prevent nucleic acid from being degraded by biomolecules. Therefore, it is undoubtedly the wisest to select a strategy for HSPs inhibition based on the unique properties of the nanoplatform.

## mPTT Plays a Leading Role Through Autophagy Regulation

Autophagy, a highly conserved catabolic process and an important mechanism for maintaining intracellular homeostasis, has been argued as a double-edged sword in tumorigenesis.<sup>29,30</sup> Autophagy can lead to the survival of tumor cells and the inefficiency of a wide range of tumor therapeutic approaches by alleviating cellular stress, but autophagy, in turn, can limit tumorigenesis through multiple pathways.<sup>31,88</sup> The fact is, in recent years of researches on tumor therapy, autophagy mostly plays a protective role (Table 2). The inhibition of autophagy has therefore emerged as an effective approach to enhance mPTT.

All kinds of novel nanoplatforms have been designed to block the process of autophagy to potentiate mPTT, where the targeted delivery of autophagy inhibitors is initial and the most typical method. Among them, chloroquine (CQ), which can inhibit the fusion of autophagosome with lysosome to block autophagic progression, is widely used to enhance mPTT. Shi et al applied poly(lactic-co-glycolic acid) (PLGA) as a carrier to load IR820 (PTA), ZnCdSe/ZnS quantum dots (QDs, FLI agent), and CQ to afford a multifunctional nanoplatform.<sup>26</sup> Under the mild acidic TME, the developed PLGA/IR820/QDs/CQ nanoparticles (PIFC NPs) would be biodegraded and released CQ that could greatly reduce degradation of autolysosome and effectively prevent damaged cells from repairing. With 808nm laser irradiation, the PIFC NPs showed enhanced tumor-killing effect both in vitro and in vivo under a relatively low temperature (45°C). At the same time, the PIFC NPs achieved excellent real-time FLI capability attributed to the introduction of inorganic fluorescent emitter QDs, which had stronger fluorescence intensity and higher light stability compared with organic fluorescent dyes.<sup>95</sup>

**Table 2** mPTT Plays a Leading Role Through Autophagy Regulation

Strategy	Nanoplatfrom	PTAs	Therapeutic Agent	Mechanism	Irradiation Wavelength	Imaging Capability	Ref.
Autophagy inhibition	PDA-PEG/CQ	PDA	CQ	Reduce degradation of autolysosome	808nm	FLI	[89]
	PLGA/IR820/QDs/CQ	IR820	CQ	Reduce degradation of autolysosome	808nm	FLI	[26]
	Bi@SiO <sub>2</sub> -CQ	Bi@SiO <sub>2</sub>	CQ	Reduce degradation of autolysosome	808nm	\	[90]
	Red blood cell-cancer hybrid membrane-coated ICGCQ NPs (ICGCQ@RCm)	ICG	CQ	Reduce degradation of autolysosome	793nm	FLI	[22]
	CQ and phase-changing material (PCM)-loaded hollow mesoporous Prussian blue nanoparticles ((CQ+PCM)@HMPBs)	PB	CQ	Reduce degradation of autolysosome	808nm	\	[91]
	NPIADs	ICG	NDs	Deplete NUPR1 and regulate the late stage of autolysosome processing	808nm	FLI/PAI	[92]
	BNN-Bi <sub>2</sub> S <sub>3</sub>	Bi <sub>2</sub> S <sub>3</sub>	NO	Downregulate autophagy level	808nm	MSOT/CT	[93]
Autophagy activation	Beclin-1-derived peptide and Arg-Gly-Asp (RGD) peptide-conjugated PDA (PPBR)	PDA	Beclin-1 peptide	Activate the beclin-1-involved the pathway of autophagic cell death	808nm	FLI	[94]

As research continues to deepen, methods to inhibit autophagy are being gradually excavated. Nanodiamonds (NDs), known as a kind of nanocarrier possessing numerous advantages like large specific surface area, have been reported to serve as an autophagy inhibitor by blocking the NUPR1-mediated autophagy process.<sup>96–98</sup> NUPR1 (nuclear protein 1), a transcriptional coregulator, is aberrantly expressed in tumor cells and dramatically induced upon stress conditions.<sup>99</sup> Since NUPR1 involves in regulating the late stage of autolysosome processing, it may downregulate autophagic flux and reduce degradation of autolysosome by depleting NUPR1.<sup>99</sup> Encouraged by the unique performance of NDs, Cui et al formulated a multifunctional NDs-based nanoplatfrom consisting of ICG, apotozole (APZ, an HSP70 inhibitor), and doxorubicin (DOX) through a layer-by-layer self-assembly approach (Figure 5a).<sup>92</sup> This nanoplatfrom achieved robust antitumor efficacy by using two strategies to simultaneously increase the sensitivity of tumor cells to the combination therapy of mPTT/chemotherapy. Firstly, APZ enhanced mPTT by reducing the expression of HSP70. Secondly, NDs-mediated inhibition of autophagy further increased the efficacy of mPTT while reducing the resistance of tumor cells to chemotherapy agent. This work proved that autophagy could be blocked not only by specific autophagy inhibitors, but also by unique nanocarriers, thus realizing enhanced mPTT.

Apart from specific autophagy inhibitors and nanocarriers, gas like NO has also been demonstrated to inhibit the progression of autophagy and optimize mPTT. Zhang et al synthesized a heat-triggered NO controlled release nanocomposites based on bismuth sulfide (Bi<sub>2</sub>S<sub>3</sub>) nanoparticles loading hydrophobic NO donor, N, N'-Di-sec-butylN,N'-dinitroso-1,4-phenylenediamine (BNN) (Figure 5b).<sup>93</sup> Compared with Bi<sub>2</sub>S<sub>3</sub> NPs, BNN-Bi<sub>2</sub>S<sub>3</sub> NPs with NO assistance showed a stronger tumor inhibition effect under mPTT. Besides the partial toxic effect of NO itself, the author further explored the in-depth molecular mechanism to explain this synergistic effect. Hence, autophagy inducer rapamycin (Rapa) and inhibitor 3-methyladenine (3-MA) were used to analogize the role of NO in autophagy regulation under a mild temperature. The results demonstrated that Rapa could relieve tumor cell death, whereas 3-MA, like NO, could promote tumor cell death during the mPTT. Subsequently, Western blot and flow cytometry further validated that NO could inhibit the progression of autophagy to promote tumor cell apoptosis (Figure 5c and d). This study for the first time reported NO-sensitized mPTT and provided a new strategy for autophagy inhibition.

In contrast to the above examples, activation of autophagy has been similarly exploited to augment mPTT for tumor therapy. For example, Zhou et al constructed a multifunctional nanoparticle (PPBR) with autophagy activation characteristic, which consisted of PEGylated PDA modified by Arg-Gly-Asp (RGD) peptides and beclin-1 peptide.<sup>94</sup> The modification of RGD peptides which could specifically bind overexpressed  $\alpha\text{v}\beta\text{3}$  integrin receptor on the tumor cell

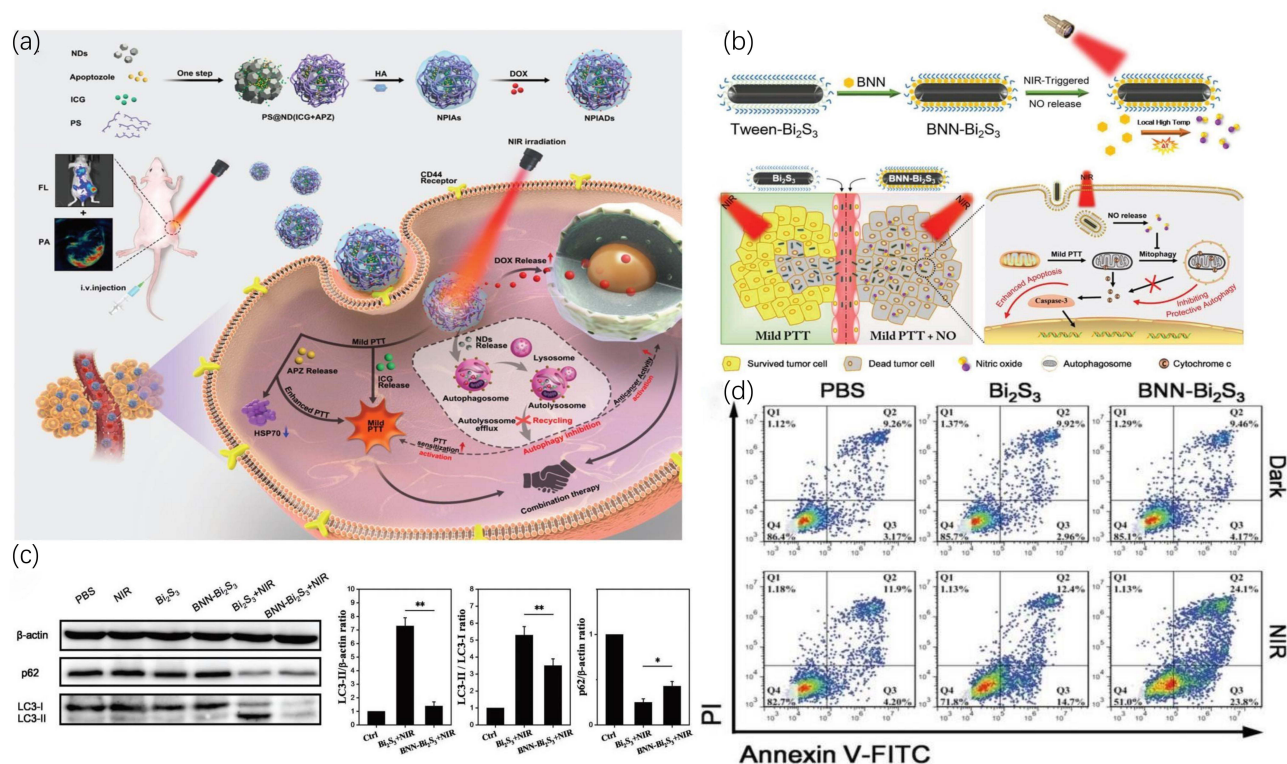


**Figure 5** (a) Schematic showing the synthesis of NDs-based nanoplatform and its application for multimodal imaging-guided combination therapy. Reprinted with permission from Cui X, Liang Z, Lu J, et al. A multifunctional nanodiamond-based nanoplatform for the enhanced mild-temperature photothermal/chemo combination therapy of triple negative breast cancer via an autophagy regulation strategy. *Nanoscale*. 2021;13(31):13375–13389.<sup>92</sup> Copyright 2021 Royal Society of Chemistry. (b) The synthesis of BNN-Bi<sub>2</sub>S<sub>3</sub> NPs and their working mechanisms for enhanced mPTT. (c) Western blot analysis of p62 and LC3-I/LC3-II was examined to evaluate autophagic flux after the indicated treatments. (d) Flow cytometry was examined to determine the percentages of apoptosis with different treatments. (b–d) Reproduced from Zhang X, Du J, Guo Z et al Efficient Near Infrared Light Triggered Nitric Oxide Release Nanocomposites for Sensitizing Mild Photothermal Therapy. *Adv Sci (Weinh)*. 2019;6(3):1801122. © 2018 The Authors. Published by WILEY-VCH Verlag GmbH & Co. KGaA, Weinheim. To view a copy of this license, visit <http://creativecommons.org/licenses/by/4.0/>.<sup>93</sup>

surface enabled PPBR to selectively aggregate in tumor, and the modification of beclin-1 peptide could activate the beclin-1-involved the pathway of autophagic cell death.<sup>100</sup> As a result, the efficacy of mPTT was significantly improved with the assistance of beclin-1-induced autophagy.

Collectively, since autophagy acts as a double-edged sword in the progression of tumorigenesis, the priority is to identify the relationship between autophagy and mPTT, although it mainly plays a protective role. The examples mentioned above demonstrated that both inhibition of protective autophagy and promotion of pro-death autophagy were effective in potentiating mPTT.

## mPTT Plays a Supporting Role in Tumor Therapy

Although inhibiting the expression of HSPs and regulating the progression of autophagy can significantly increase the efficacy of single-mode mPTT by reducing the resistance of tumor cells to stress, it still has some limitations. Researchers have been plagued by the conundrum of uneven distribution of heat inside tumors, and the limited penetration ability of NIR fails to effectively cover deep tumor tissues. Residual tumor cells located at the edge and deep part of the tumor tissues inevitably result in tumor recurrence and metastasis. Furthermore, although the enhanced mPTT has exhibited powerful therapeutic effect on local lesions, it has little efficacy on distant tumors and cannot reduce the risk of tumor metastasis either. There is a desperate need to seek out suitable strategies to deal with the above problems. Fortunately, with the continuous efforts of researchers, the above-mentioned issues have been addressed by the combination therapy of mPTT with other therapies, including chemotherapy, gene therapy, radical-based therapy, and immunotherapy. Of note, besides the weak tumor-killing effect, mPTT mainly plays an adjuvant role to enhance the efficacy of the combination therapy when it is synergistic with other therapies, so we call it a supporting role in this part, and the synergistic mechanisms will be discussed in the corresponding section.

## mPTT Plays a Supporting Role in Synergizing with Chemotherapy

Chemotherapy, as one of the three traditional therapies for cancer, has a pivotal position in clinical application, however, its efficacy is still unsatisfactory due to serious systemic side effects and drug resistance. Thanks to the rapid development of nanotechnology, mPTT based on nanomedicine has raised the application of chemotherapy in tumors to a new level, mainly from the following aspects. (1) Most chemotherapeutics suffer from several disadvantages such as low solubility, low bioavailability, and non-targeting ability, causing severe side effects.<sup>101–103</sup> Compared with free chemotherapeutic agents, nanocarrier delivery systems can achieve a longer half-life and lower systemic toxicity.<sup>104</sup> Meanwhile, precision medicine is made possible under the auspices of passive targeting by enhanced permeability and retention (EPR) effect as well as active targeting by artificial modification. (2) Owing to the presence of distorted tumor vessels and dense extracellular matrix (ECM), nanocarriers are usually located at the edge of the tumor after reaching, which terribly compromises the therapeutic efficacy.<sup>10</sup> It has been well recognized that mild hyperthermia can destroy the dense ECM, improve the blood fluid of tumor tissue and the permeability of tumor blood vessels, and increase the permeability and fluidity of tumor cell membranes to assist the intracellular uptake of drugs.<sup>105,106</sup> At the same time, the chemical bonds or physical interactions between chemotherapeutic agents and nanocarriers will be disrupted by mild hyperthermia thus achieving spatiotemporally controllable on-demand release.<sup>107,108</sup> (3) Mild hyperthermia can also reverse drug resistance of tumor cells by regulating drug resistance-related markers like P-gp.<sup>109</sup> Therefore, both the nanocarriers on which mPTT depends and the biological effects exerted by mPTT itself circumvent the problems faced by mono chemotherapy and increase its efficacy (Table 3).

**Table 3** mPTT Plays a Supporting Role in Synergizing with Chemotherapy

Strategy	Nanoplatfrom	PTAs	Chemotherapeutic Agents	Irradiation Wavelength	Imaging Capability	Ref.
Promote release and uptake	Chlorin e6 and DOX co-loaded mesoporous silica (MS) shell and PGO(DOX-UMCG)	Polyethylene glycol-modified graphene (PGO)	DOX	808nm	\	[110]
	RGD-coated, DOX, and Ag <sub>2</sub> S QD co-loaded dendritic mesoporous silica (Ag <sub>2</sub> S@M/D-P-RGD)	Ag <sub>2</sub> S	DOX	808nm	FLI/PAI	[12]
	ICG/Cu-LDH@BSA-DOX	Cu-LDH	DOX	808nm	\	[111]
	Thermo-responsive DNA hydrogel-based nanoplatfrom	Ti <sub>3</sub> C <sub>2</sub> T <sub>x</sub> -based MXene	DOX	808nm	\	[112]
	Poly-tannic acid (pTA) coated PTX nanocrystals (PNC-pTA)	pTA	PTX	808nm	\	[113]
	Perfluoropentane (PFP), ICG, PTX co-loaded, and PEGylated hollow mesoporous organosilica nanoparticles (ICG/PFP@HMOP-PEG)	ICG	PTX	808nm	PAI/US	[114]
	PSN-HSA-PTX-IR780	IR780	PTX	808nm	FLI	[115]
	PTX/ICG/HAase-HSA-NPs	ICG	PTX	808nm	\	[116]
	TCPP-Iso	Tetra (4-carboxyphenyl) porphine (TCPP)	Isoliensinine(Iso)	650nm	\	[117]
	iRGD-PEG-PLGA/AuNC/EGCG	Gold nanocages (AuNC)	EGCG	808nm	MSOT	[118]
	GNRs-anchored thermosensitive liposomal complex co-loaded with Sodium tanshinone IIA sulfonate (STS) and celastrol (G-T/C-L)	GNRs	Celastrol	808nm	\	[119]
	7-ethyl-10-hydroxycamptothecin (SN38)-loaded and alendronate (ALN)-anchored polydopamine nanoparticle (PDA-ALN/SN38)	PDA	SN38	808nm	FLI/three-dimensional micro-computed tomography(3D micro-CT)	[120]

(Continued)

Table 3 (Continued).

Strategy	Nanopatform	PTAs	Chemotherapeutic Agents	Irradiation Wavelength	Imaging Capability	Ref.
	Dual stimuli-sensitive polydopamine-chlorambucil (CB) conjugate nanoparticles (PDCBs)	PDA	CB	808nm	FLI/3D PAI	[121]
	Obatoclax (OBX)-loaded melanin coated magnetic nanoparticles (MMNs)	MMNs	OBX	808nm	PAI/MRI	[122]
	AuNP-5-FU	Au	5-fluorouracil(5-FU)	808nm	\	[123]
	Etoposide (Eto) loaded bovine serum albumin (BSA) and polyacrylic acid (PAA) coated superparamagnetic iron oxide nanoparticles (SPIONs) (Eto-BSA@PAA@SPION)	SPIONs	Eto	808nm	\	[124]
	5-FU/Cu-LDH@nAb-PTX	Copper-doped layered double hydroxide (Cu-LDH)	Albumin-bound paclitaxel (nAb-PTX) 5-FU	808nm	\	[125]
	PTX/CUR/Au NRs@cRGD	Au	PTX Curcumin (CUR)	808nm	FLI	[126]
Reverse drug resistance	Liposomes coated and DOX-loaded gold nanocages (LAD)	AuNC	DOX	808nm	FLI	[109]
	HA-coated, gold (Au)-nanodot-decorated, and DOX-loaded hollow carbon nanospheres (DOX@AuHCNs-HA)	Au	DOX	808nm	\	[127]
	PNOC-PDA/DOX	PDA	DOX	808nm	3D PAI	[128]
	DOX@MoS <sub>2</sub> -PEI-HA	MoS <sub>2</sub>	DOX	808nm	PET	[129]
	F-Pt-NPs	Photothermal conjugated polymer DAP-F	Cisplatin	808nm	\	[130]
	Dual drug-paired polyprodrug nanoparticle (PDCN <sub>25</sub> -CDDP)	PDA	DOX Cisplatin	808nm	FLI/3D PAI	[131]

### mPTT Facilitates Drug Delivery, Release, and Uptake

As mentioned above, mPTT based on nanomedicine can accomplish the targeted delivery of chemotherapeutic drugs, spatiotemporally controllable on-demand release, and improve drug uptake in tumor cells, solving the shortcomings faced by single-mode chemotherapy and boosting its efficacy. Accordingly, in the following section, we will illustrate two aspects including the targeted delivery of chemotherapeutics and the role of mPTT after reaching the tumor.

Targeted delivery of chemotherapeutic drugs is one of the most effective methods to reduce systemic adverse effects. In addition to passive targeting by the EPR effect, researchers have dedicated themselves to mining for overexpressed biomolecules on tumor cells to achieve active targeting, such as hyaluronic acid (HA) targeting CD44 and RGD targeting integrin  $\alpha\beta3$ .<sup>132,133</sup> Although the dual targeting strategy including active targeting and passive targeting has further improved the delivery efficiency of chemotherapy drugs, it mainly focuses on the treatment of solid tumor, leaving metastasis unresolved, and we know that it is metastasis instead of the tumor itself that causes more than 90% cancer-related deaths in clinical.<sup>134,135</sup> Efforts are needed to find a strategy targeting tumor metastasis. Studies have shown that platelets can participate in all steps of the metastasis cascade to promote tumor metastasis.<sup>136</sup> When circulating tumor cells (CTCs) enter the blood circulation, they will activate platelets to upregulate P-selectin and bind to them via CD44.<sup>137</sup> With the help of platelet “coat”, the combined platelet-cancer cell complex can escape the surveillance of the immune system, promote the adhesion and exudation of cancer cells to the endothelium, and support the survival of CTCs in distant organs.<sup>138-140</sup> Encouraged by the metastasis-targeting property of platelets, Zhao et al realized the increased paclitaxel (PTX) aggregation both in the primary and metastatic foci through the “platelet bridge” induced by mild hyperthermia (Figure 6a).<sup>115</sup> They fabricated PSN (CDAEWVDVS)-modified human serum albumin (HSA) nanoparticles (PSN-HSA-PTX-IR780) loading IR780 (PTA) and PTX. In the presence of PSN, PSN-HSA-PTX-IR780



could target overexpressed P-selectin on activated platelets. After reaching the solid tumor via the EPR effect, the mild hyperthermia generated by IR780 under 808nm laser irradiation injured tumor tissue and subsequently led to the platelet recruitment and activation, which could guide more circulating nanoparticles into the tumor by recognizing P-selectin overexpressed on activated platelets in a positive feedback manner. Meanwhile, the intermolecular disulfide bonds were disrupted by GSH in tumor thereby releasing PTX, and the results showed that the amount of PTX released from PSN-HSA-PTX-IR780 was 2.86-fold higher than that from HSA-PTX-IR780 at 45°C (Figure 6b). Moreover, since activated platelets also involved in tumor metastasis, PSN-modified nanoparticles were able to complete the targeting and inhibition of metastasis via a ‘platelet bridge’. Taken together, with the assistance of mPTT, this work achieved significant efficacy in the treatment of primary and metastatic lesions by regarding platelets as a ‘bridge’ to lead the target delivery of chemotherapeutic drugs, providing new insights into the targeted delivery of drugs and the treatment of tumor metastasis.

Upon the targeted arrival of the nanocomplexes at the tumor tissues, mPTT can regulate the controllable on-demand release of chemotherapeutic agents and increase drug internalization into tumor cells according to the mechanisms discussed before. For example, He et al established a thermo-responsive DNA hydrogel-based nanoplatform integrating both DOX and  $Ti_3C_2Tx$ -based MXene, a PTA with excellent photothermal conversion efficiency (Figure 6c).<sup>112</sup> Upon 808nm light irradiation, the mild heat produced by  $Ti_3C_2Tx$ -based MXene could break the DNA duplex crosslinking

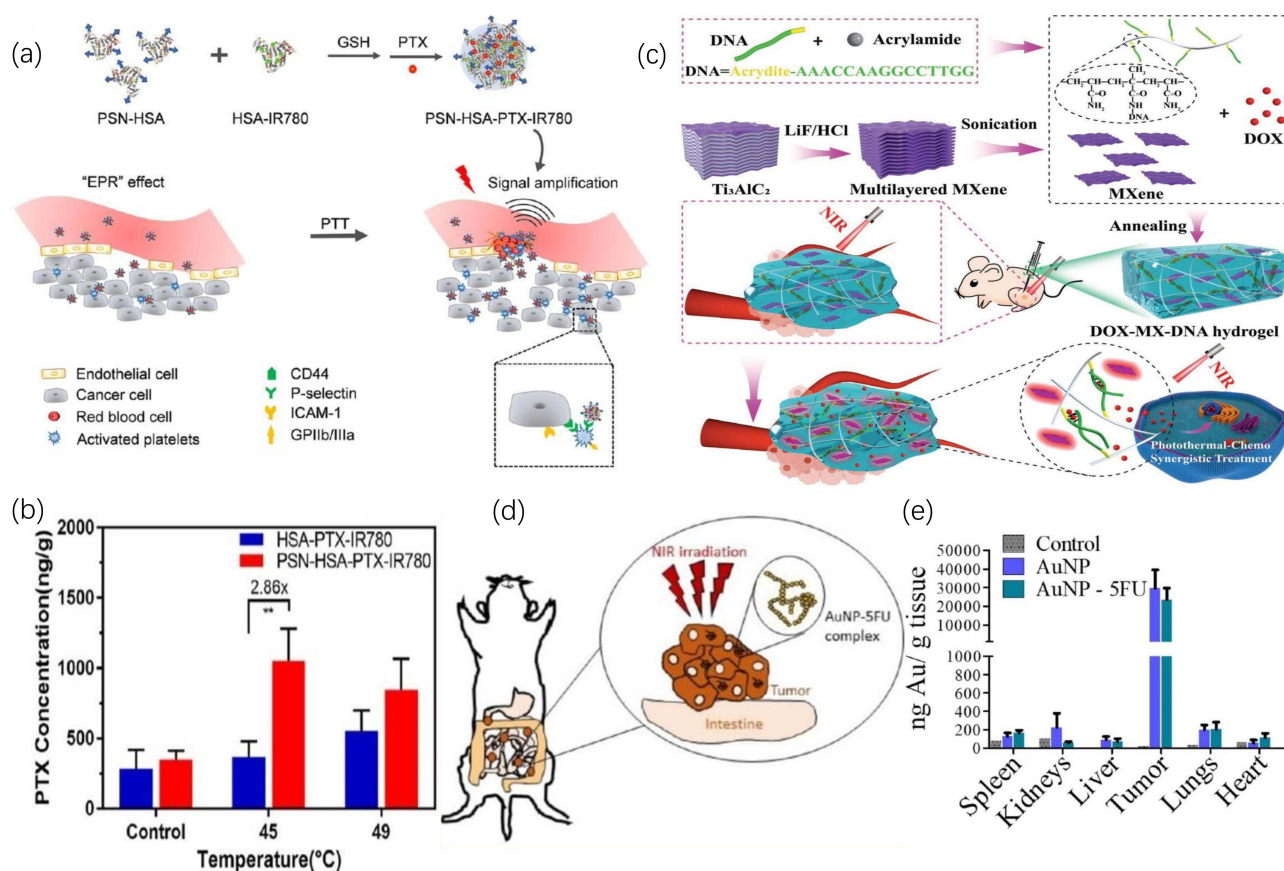


**Figure 6** (a) The working mechanisms of PSN-HSA-PTX-IR780: after aggregation in solid tumor via EPR effect, NPs could generate mild heat to induce tissue injury and then increased infiltration of platelets, which guided more circulating NPs into the tumor. (b) Quantification of intratumoral PTX concentration after treatments. (a and b) Reprinted with permission from Zhao W, Li T, Long Y, et al. Self-promoted albumin-based nanoparticles for combination therapy against metastatic breast cancer via a hyperthermia-induced “platelet bridge”. *ACS Appl Mater Interfaces*. 2021;13(22):25701–25714.<sup>115</sup> Copyright 2021 American Chemical Society. (c) Schematic showing the synthesis of DOX-loaded MXene-DNA hydrogel and its application in photothermal-chemo synergistic treatment. Reprinted with permission from He PP, Du X, Cheng Y, et al. Thermal-responsive MXene-DNA hydrogel for near-infrared light triggered localized photothermal-chemo synergistic cancer therapy. *Small*. 2022;18(40):e2200263. © 2022 Wiley-VCH GmbH.<sup>112</sup> (d) Schematic illustration of a tumor-selective heating approach induced by AuNP-5FU complex. (e) Biodistribution of Au after intratumoral injection. (d and e) Reprinted with permission from Mulens-Arias V, Nicolás-Boluda A, Pinto A, et al. Tumor-selective immune-active mild hyperthermia associated with chemotherapy in colon peritoneal metastasis by photoactivation of fluorouracil-gold nanoparticle complexes. *ACS Nano*. 2021;15(2):3330–3348.<sup>123</sup> Copyright 2021 American Chemical Society.

structures in the hydrogel matrix and lead to the localized release of DOX. Intriguingly, when the NIR irradiation was removed, the DNA duplex structures and the hydrogel matrix could be reformed with adaptive shapes and the recombination of free DOX could be achieved, thereby attaining on-demand release of DOX via the reversible gel-to-solution transition of the DNA hydrogel. With the enhanced drug uptake triggered by mPTT, this nanoplatform exhibited extraordinary antitumor efficacy with negligible side effects. In another example, Mulens-Arias et al combined 5-fluorouracil(5-FU) and spherical citrate-coated gold nanoparticles (AuNPs) to form a AuNP-5-FU complex to address the shortcomings of hyperthermic intraperitoneal chemotherapy (HIPEC).<sup>123</sup> HIPEC was mainly used to treat the residual disease after cytoreductive surgery (CRS) by circulating heated sterile solution containing a chemotherapeutic drug throughout the peritoneal cavity with the aid of a machine.<sup>141</sup> Nevertheless, with prolonged intraperitoneal heating (most recommended at 41°C for 90 minutes), HIPEC posed many side effects such as digestive fistula or peritonitis, seriously affecting the life quality of patients.<sup>142</sup> Luckily, the defects of HIPEC were subtly resolved by Mulens-Arias et al through a tumor-selective heating approach (Figure 6d). To begin with, they evaluated the ability of AuNP-5-FU to aggregate in tumors. The biodistribution of AuNP-5-FU was analyzed 24h after intraperitoneal injection, the time of light exposure, and quantitative analysis revealed that the vast majority of AuNP-5-FU accumulated in the tumor region, accompanied by a small fraction accumulated in spleen, liver, intestine, and kidneys (Figure 6e). After irradiation, the mild heat (<43 °C) induced 5-FU release and promoted its internalization by tumor cells. What's more, this synergistic therapy of mPTT combined with chemotherapy achieved reprogramming of the immune microenvironment, polarizing M2 macrophages to M1 macrophages and activating a "cold" immune TME into a "hot" one. In a word, this research, from the perspective of solving the current thorny problems faced by the clinic, proposed and verified a precise medical strategy of tumor-targeted heating combined with chemotherapy to replace HIPEC, making a great contribution to clinical translation.

### mPTT Reverses Drug Resistance

Multidrug resistance (MDR) has always been a major obstacle in the development of chemotherapy, greatly compromising the efficacy of treatment and contributing to tumor recurrence.<sup>1</sup> There are many mechanisms responsible for MDR, one of the most important is the overexpression of P-glycoprotein (P-gp) on tumor cells, an ATP binding cassette (ABC) that pumps chemotherapeutic drugs out of tumor cells and results in treatment failure.<sup>143</sup> As widely studied, different strategies of inhibiting P-gp combined with mPTT can reverse MDR to improve the efficacy of chemotherapy. For instance, Xu et al employed weak PDT and mPTT synergistic chemotherapy to combat MDR through an HA-coated nanosystem (DOX@AuHCNs-HA) incorporating gold (Au)-nanodot as a PTA, hollow carbon nanospheres (HCNs) as a photodynamic agent and DOX (Figure 7a).<sup>127</sup> Under low-level infrared irradiation, the mild heat (<40°C) induced by DOX@AuHCNs-HA accompanied by the generation of a small amount of ROS showed little killing effect on tumor cells, whereas was sufficient to achieve DOX unloading and interfere with the function of P-gp. Because P-gp was an ATP-dependent protein and mild heat as well as modest amounts of ROS were able to functionally impair mitochondrial ATP generation, the weak PTT and PDT could inhibit the drug efflux mediated by P-gp, thereby retaining drug within cells and augmenting curative effect of chemotherapy without damaging neighboring tissues. Further, it was found that MDR could be similarly reversed by NO by inhibiting the expression of P-gp.<sup>144</sup> Ding et al conjugated poly(L-cysteine) 20-poly(ethylene oxide)<sub>45</sub> (PC) with SNO, a heat-sensitive NO donor, to form PNOC, then PDA was coated on PNOC to prepare the NIR-responsive NO-releasing nanocomplexes, and finally DOX was loaded on the outer surface of PDA via  $\pi$ - $\pi$  stacking and hydrogen-bond interactions.<sup>128</sup> Upon mild hyperthermia, the synthesized PNOC-PDA/DOX released NO and DOX simultaneously in the local tumor, and NO could reduce the cellular efflux of DOX by interfering with P-gp so as to reverse MDR and enhance the therapeutic efficacy of DOX. Interestingly, as the study progressed, He et al reported that mono mPTT was sufficient to downregulate chemoresistance-related markers (Figure 7b).<sup>109</sup> They found a more pronounced antitumor effect of LAD (liposomes coated and DOX-loaded gold nanocages) compared to LAU (liposomes coated gold nanocages) and free DOX under laser irradiation. The intrinsic mechanisms revealed that mPTT could not only cut down the expression of P-gp, but also downregulated the expression of mutant p53 protein and heat shock factor-1 (HSF-1) protein. It was worth noting that mutant p53 protein could protect tumor cells from apoptosis and that HSF-1 could alleviate the stress imposed by chemotherapy agents, thus resulting in chemotherapeutic

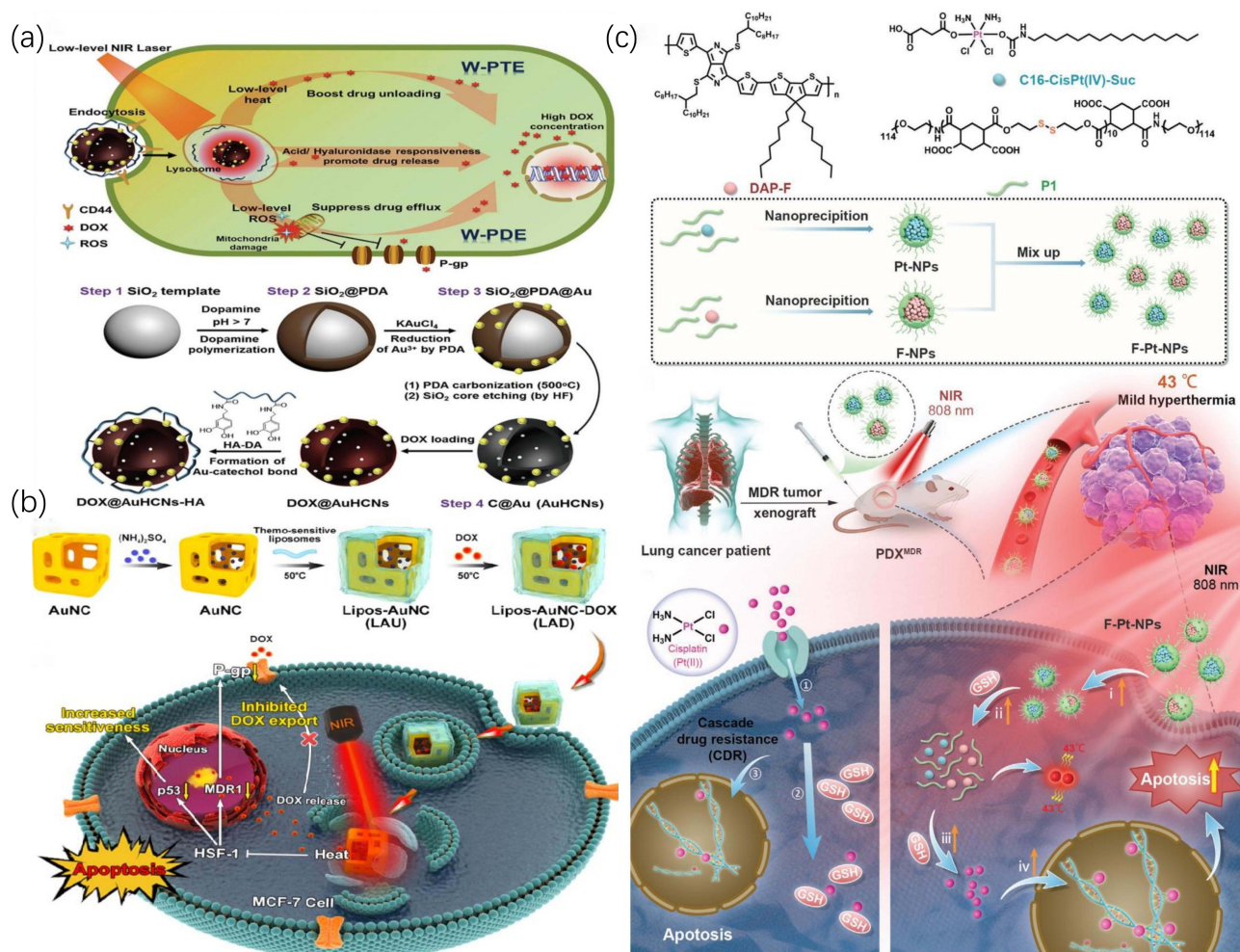


**Figure 7** (a) Schematic showing the construction of DOX@AuHCNs-HA and its application in mPTT and weak PDT-assisted chemotherapy. Reprinted with permission from Xu L, Liu J, Xi J, et al. Synergized multimodal therapy for safe and effective reversal of cancer multidrug resistance based on low-level photothermal and photodynamic effects. *Small*. 2018;2018:e1800785. © 2018 WILEY-VCH Verlag GmbH & Co. KGaA, Weinheim.<sup>127</sup> (b) Schematic illustration of the synthesis of LAD and its working mechanisms in reversing drug resistance. Reprinted from *J Control Release*, 323, He H, Liu L, Zhang S, et al. Smart gold nanocages for mild heat-triggered drug release and breaking chemoresistance. 387–397, Copyright 2020, with permission from Elsevier.<sup>109</sup> (c) Schematic depicting the construction of F-Pt-NPs and their application in combating CDR. Reprinted with permission from Wang L, Yu Y, Wei D, et al. Strategy of combinational blow for overcoming cascade drug resistance via NIR-light-triggered hyperthermia. *Adv Mater*. 2021;33(20):e21100599. © 2021 Wiley-VCH GmbH.<sup>130</sup>

resistance.<sup>145,146</sup> Thanks to mPTT, MDR was reversed through the downregulation of chemoresistance related markers, leading to the increased aggregation of chemotherapeutic agents and drug sensitivity.

Unfortunately, although the inhibition of chemoresistance-related proteins can alleviate MDR to some extent, drug resistance results from multiple mechanisms, including accelerating drug efflux, inhibiting drug activity, increasing drug detoxification, enhancing damage repair, etc., which are known as cascade drug resistance (CDR).<sup>147–150</sup> Failure to completely ruin CDR by interfering with one specific process in drug resistance necessitates efforts to find a systematic strategy to overcome CDR. Cisplatin, one of the most commonly used chemotherapeutic agents clinically, is a victim of the CDR due to several mechanisms, including the inhibition of drug internalization, detoxification mediated by GSH, and reduced formation of Pt-DNA adducts.<sup>151</sup> Given these, Wang et al combined GSH-responsive amphiphilic polymer (P1) with hydrophobic photothermal conjugated polymer (DAP-F) and Pt (IV) prodrug C16-CisPt-Suc to form F-NPs and Pt-NPs, and mixed them to synthesize the final NPs formulation, F-Pt-NPs (Figure 7c).<sup>130</sup> On the one hand, GSH in tumor tissues could not only disintegrate F-Pt-NPs to release C16-CisPt-Suc via disulfide bonds, but also allowed further reduction of C16-CisPt-Suc to cisplatin, which in turn greatly reduced detoxification mediated by GSH. On the other hand, mild hyperthermia could intervene almost the whole CDR process by facilitating the internalization of NPs,



catalyzing the dissociation of NPs and the reduction of C16-CisPt-Suc to cisplatin mediated by GSH, and accelerating the formation of Pt-adducts. In brief, this work, on the basis of fully understanding the CDR mechanism of cisplatin, formulated a systematic strategy and a step-by-step approach to break the CDR and improve the efficacy of cisplatin by using mPTT and GSH-sensitive multifunctional NPs.

## mPTT Plays a Supporting Role in Synergizing with Gene Therapy

Gene therapy has shown huge practical value in different cancer treatments by using exogenous nucleic acids to directly up- or down-regulate the expression of target genes.<sup>152,153</sup> However, numerous challenges such as degradation of naked nucleic acids, nonspecific biodistribution, and low transfection efficiency leave gene therapy less than satisfactory.<sup>154</sup> Therefore, it is highly necessary to exploit multifunctional gene delivery platforms for addressing the shortcomings of single-mode gene therapy. mPTT based on nanomedicine has contributed greatly to the successful realization of gene therapy. For one thing, various developed nanocarriers not only protect nucleic acids from degradation, but also allow them to specifically accumulate in tumor regions. For another, mild hyperthermia increases the uptake of gene therapeutic agents by tumor cells and facilitates the efficiency of transfection.<sup>155,156</sup> For instance, Odda et al fabricated  $\alpha$ -Fe<sub>2</sub>O<sub>3</sub> NPs via a hydrothermal method, and subsequently synthesized Fe<sub>2</sub>O<sub>3</sub>@PEDOT core-shell NPs with enhanced photothermal conversion efficiency by polymerizing EDOT monomers with Fe<sup>3+</sup> released from Fe<sub>2</sub>O<sub>3</sub> surface, and finally incorporated negatively charged siRNA through electrostatic interaction to form Fe<sub>2</sub>O<sub>3</sub>@PEDOT-siRNA NPs (Figure 8a).<sup>157</sup> All

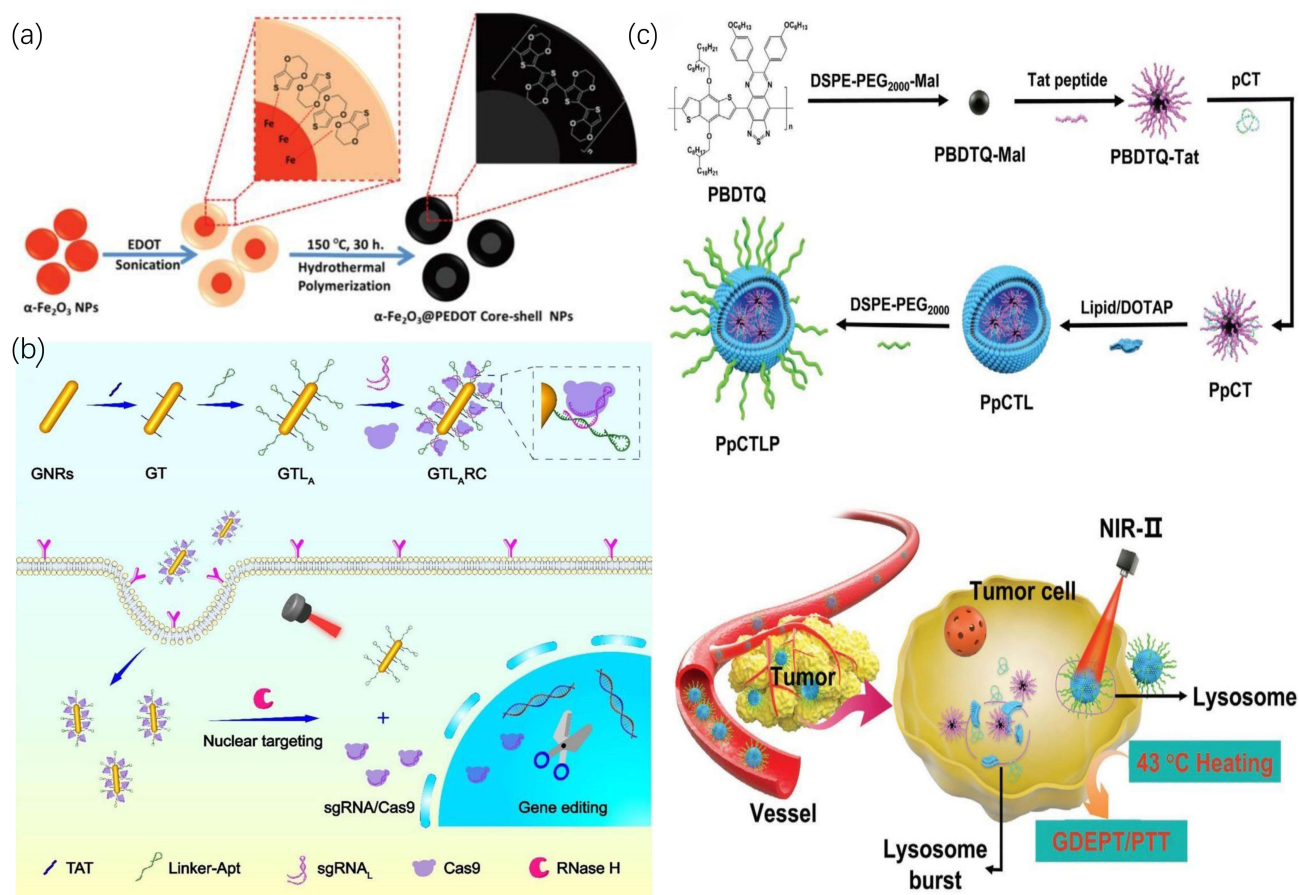


**Figure 8** (a) Schematic illustration of the construction process of as-made core-shell  $\alpha$ -Fe<sub>2</sub>O<sub>3</sub>@PEDOT NPs. Reprinted with permission from Odda AH, Cheang T-Y, Alesary HF, et al. A multifunctional  $\alpha$ -FeO@PEDOT core-shell nanoplatform for gene and photothermal combination anticancer therapy. *J Mater Chem B*. 2022;10(9):1453–1462.<sup>157</sup> Copyright 2022 Royal Society of Chemistry. (b) Schematic showing the synthesis of GTA<sub>A</sub>RC and its application in gene editing and mPTT combination therapy. Reprinted with permission from Tang W, Han L, Lu X, et al. A nucleic acid/gold nanorod-based nanoplatform for targeted gene editing and combined tumor therapy. *ACS Appl Mater Interfaces*. 2021;13(18):20974–20981.<sup>158</sup> Copyright 2021 American Chemical Society. (c) The preparation of PpCTL and its application in synergistic tumor GDEPT/PTT at mild hyperthermia. Reprinted with permission from Zhang X, Yang Y, Kang T, et al. NIR-II absorbing semiconducting polymer-triggered gene-directed enzyme prodrug therapy for cancer treatment. *Small*. 2021;17(23):e2100501. © 2021 Wiley-VCH GmbH.<sup>160</sup>

experimental results proved that  $\text{Fe}_2\text{O}_3@\text{PEDOT-siRNA+NIR}$  exhibited the strongest tumor inhibition compared with the remaining groups, which benefited from the mild hyperthermia-facilitated internalization of NPs and gene transfection efficiency. Further, Tang et al utilized gold nanorods (GNRs) as a vehicle to deliver CRISPR/Cas9 system and achieved excellent antitumor efficacy in combination with mPTT (Figure 8b).<sup>158</sup> They integrated a DNA linker (Linker-Apt), which enabled NPs to target tumor tissues, and a nuclear targeting peptide (TAT) onto GNRs through Au-S interaction to formulate  $\text{GTL}_A$ , and then loaded sgRNA/Cas9 complex into  $\text{GTL}_A$  through RNA-DNA hybridization between the 3' terminal extended sgRNA and the DNA linker to prepare the final product  $\text{GTL}_A\text{RC}$ .<sup>159</sup> After specific accumulation into tumor area, owing to the existence of endogenous RNase H which could selectively break the RNA strand of RNA-DNA hybrids, the sgRNA/Cas9 complex was released from  $\text{GTL}_A\text{RC}$  to edit the tumor-associated gene polo-like kinase 1 (PLK1). The qRT-PCR analysis and Western blot assay demonstrated that the mRNA and protein levels of PLK1 were obviously downregulated. Moreover, the therapeutic effect was further enhanced by mild hyperthermia.

Apart from increasing the uptake and transfection efficiency of gene therapy agents, mPTT acts as a “switch” to initiate precise gene regulation through HSP promoters. As an upstream regulator, HSP promoters that are triggered in response to mild hyperthermia can function as a controller to regulate the expression of downstream genes like suicide genes in addition to significantly inducing HSPs expression. In view of these mechanisms, Zhang et al designed and synthesized a kind of PEG<sub>2000</sub>-decorated nanocomposites (PBDTQ/pCT/Lipid-PEG, PpCTLP) by encapsulating a semiconducting polymer (PBDTQ) with excellent photothermal conversion performance under NIR-II and a CD-TK double suicide gene which conjugated with a heat-inducible plasmid (pDNA) (Figure 8c).<sup>160</sup> Under 1060nm NIR irradiation, the mild heat (43°C) produced by PBDTQ could activate HSP70 promoter to upregulate the downstream suicide gene expression of cytosine deaminase (CD) and herpes simplex virus type-I thymidine kinase (TK).<sup>161</sup> The upregulated CD-TK could further realize gene-directed enzyme prodrug therapy (GDEPT) by converting the prodrug of 5-fluorocytosine (5-FC) and ganciclovir (GCV) into their cytotoxic forms, thus killing tumor cells. In the same manner, Tang et al developed a supramolecular cationic gold nanorod (ANP/HSP-Cas9) carrying the CRISPR/Cas9 plasmid with a heat-inducible promoter to realize gene editing of PD-L1 by means of the NIR-II mild photothermal activation of CRISPR/Cas9.<sup>162</sup> These contributions opened a new avenue in the field of mPTT synergistic gene therapy, demonstrating the potential of mild hyperthermia as a promoter to trigger gene therapy.

## mPTT Plays a Supporting Role in Synergizing with Radical-Based Therapy

The radical with high oxidative potential has been recognized as an effective weapon to directly kill tumor cells, for it can oxidize DNA, proteins, and many other cellular substances, resulting in cellular dysfunction and leading to a variety of programmed cell death such as apoptosis, ferroptosis, and pyroptosis.<sup>163–167</sup> Similar to mPTT, many radical-dependent therapies based on nanomedicine have come to their golden age with the boom of nanotechnology. Radical-based nanomedical therapies are classified differently depending on the type of cytotoxic free radicals and the dependency on oxygen. According to the category of cytotoxic free radical they can be classified into ROS mediating type such as RT, PDT, SDT, and CDT as well as alkyl free radical mediating type such as TDT, while according to the dependence on oxygen they can be divided into oxygen-dependent type such as RT, PDT, and SDT as well as oxygen-independent type such as CDT and TDT. Nevertheless, these emerging therapies are confronted with several setbacks because of the unfavorable factors of TME. For RT/PDT/SDT, the amount of ROS generation that requires oxygen as a reactant directly determines the therapeutic efficacy, which is however greatly limited by the hypoxic TME. The poor catalytic efficiency of the Fenton or Fenton-like reaction at physiological temperature compromises the effect of CDT. In addition, the characteristic of thermo-sensitive alkane radical generator is hard to exert without the assistance of exogenous heating, making TDT a dilemma. As a result, the combination with mPTT, which can relieve tumor hypoxia, catalyze the Fenton or Fenton-like reaction, and degrade alkane radical generator, is highly warranted (Table 4).



**Table 4** mPTT Plays a Supporting Role in Synergizing with Radical-Based Therapy

Nanoplatform	PTAs	Combination Therapy	Irradiation Wavelength	Imaging Capability	Ref.
Dual-sensitizing GNPs system	Au	RT	808nm	PAI/CT	[168]
<sup>131</sup> I-hydrogel/DOX/GNPs	GNPs	RT	808nm	FLI/SPECT	[169]
Worm-like Pt nanoparticles(Pt-PEG nanoworms)	Pt	RT	1064nm	PAI/CT	[170]
Ti <sub>3</sub> C <sub>2</sub> @Au	Ti <sub>3</sub> C <sub>2</sub> -based Mxene	RT	1064nm	PAI/CT	[171]
PEGylated molybdenum oxide nanoparticles (PEG-MoO <sub>x</sub> NPs)	MoO <sub>x</sub>	PDT	1064nm	\	[172]
C <sub>16</sub> -Cypate-RRKK-PEG <sub>8</sub> -COOH(CCP)	Cypate	PDT	793nm	PAI	[173]
mPEG-ICG/L-Arg	ICG	PDT	808nm	FLI	[174]
Phthalocyanine (PcS) and mitoxantrone (MA) loaded uniform nanostructures (PcS-MA)	PcS	PDT	610nm	FLI	[13]
Au@Rh-ICG-CM	Au@Rh	PDT	808nm	FLI/PAI	[175]
Gd-doped, CuS-modified, and PEGylated hollow mesoporous organosilica nanoparticles (PEG-HMON@CuS/Gd)	CuS	PDT	808nm	FLI/MRI	[176]
(HMON@CuS/Gd <sub>2</sub> O <sub>3</sub> )	CuS	PDT	808nm	FLI/MRI	[177]
High-temperature treated and PEGylated Ti <sub>3</sub> C <sub>2</sub> MXene nanosheets (Ti <sub>3</sub> C <sub>2</sub> NSs) (H-Ti <sub>3</sub> C <sub>2</sub> -PEG NSs)	Ti <sub>3</sub> C <sub>2</sub> -based Mxene	SDT	1064nm	PAI	[178]
Titanium hydride (TiH <sub>1.924</sub> ) nanodots	TiH <sub>1.924</sub>	SDT	1064nm	PAI	[179]
Photothermogenic nanozyme Fe <sub>3</sub> O <sub>4</sub> nanoparticles (Ir@Fe <sub>3</sub> O <sub>4</sub> NPs)	Fe <sub>3</sub> O <sub>4</sub>	CDT	808nm	\	[180]
Molybdenum diphosphide nanorods (MoP <sub>2</sub> NRs)	MoP <sub>2</sub>	CDT	808nm	\	[181]
Mn-doped Prussian blue nanoparticles (MnPB NPs)	PB	CDT	808nm	PAI/MRI	[182]
Bi <sub>2-x</sub> Mn <sub>x</sub> O <sub>3</sub> hollow nanospheres (BM)	Bismuth (Bi)	CDT	808nm	\	[183]
Liposome-TiN-GO <sub>x</sub> -pH-PEG	TiN	CDT	808nm	\	[184]
A-Pt-IR NP	IR1048	CDT	1064nm	\	[185]
Virus-like Fe <sub>3</sub> O <sub>4</sub> @Bi <sub>2</sub> S <sub>3</sub> nanocatalysts (F-BS NCs)	Bi <sub>2</sub> S <sub>3</sub>	CDT	808nm	\	[186]
AIPH, ICG, and 17-AAG-loaded and HA-functionalized ZIF (A/I@aZIF@aAG@HA)	ICG	TDT	808nm	\	[48]
17AAG and AIPH loaded mesoporous polydopamine(M-17AAG-AIPH)	PDA	TDT	808nm	FLI	[47]
Chinse ink, AIPH, HY19991 loaded all-in-one hydrogel	Ink	TDT	1064nm	\	[187]
AIPH and Chinese Ink-loaded in situ hydrogel of sodium alginate (ALG)	Ink	TDT	1064nm	PAI	[188]
Au-integrated Fe single-atom nanozyme (Au-FeSAzyme)	Au	PDT/CDT	808nm	PAI	[189]
Si-Pt nanocomposites (Si-Pt NCs)	Si-Pt NCs	SDT/CDT	1064nm	PAI	[190]
Two-dimensional H-TiO <sub>2</sub> /C composite nanosheets(H-TiO <sub>2</sub> /C-PEG)	TiO <sub>2</sub>	SDT/CDT	1064nm	PAI	[191]

### RT/PDT/SDT

Despite different modes of exogenous excitation, the therapeutic mechanisms of RT/PDT/SDT are primarily the generation of ROS to exert cytotoxic effect. Nevertheless, this process requires the assistance of oxygen and is impeded by the hypoxic TME. It has been well recognized that mild hyperthermia can improve the blood fluid and microvascular permeation to increase oxygen supply, making mPTT available in coordination with various oxygen-dependent therapies. For instance, Zhang et al designed and developed an injectable multifunctional hybrid hydrogel nanoplatform (<sup>131</sup>I-hydrogel/DOX/GNPs aggregates) by treating radionuclide iodine-131 (<sup>131</sup>I) labeled polymeric hydrogels (<sup>131</sup>I-PEG-P(Tyr)<sub>8</sub>) as a skeleton simultaneously loading DOX and gold nanoparticle aggregates (GNPs aggregates)

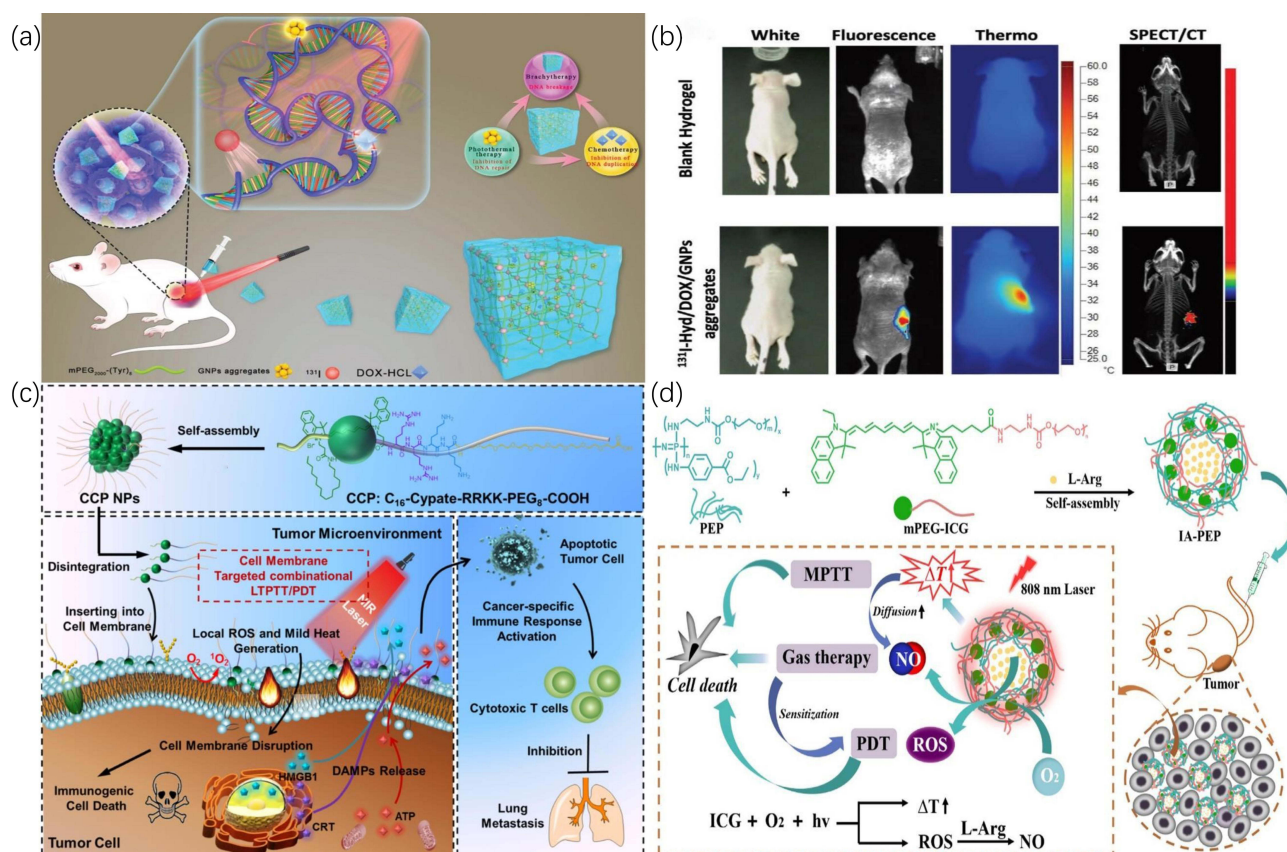


**Figure 9** (a) Schematic illustrating the mechanisms of the triple-combination therapy. (b) In vivo multi-modal imaging of multi-functional hybrid hydrogel. (a and b) Reprinted with permission from Zhang J, Yang L, Huang F, et al. Multifunctional hybrid hydrogel enhanced antitumor therapy through multiple destroying DNA functions by a triple-combination synergistic therapy. *Adv Healthc Mater.* 2021;10(21):e2101190. © 2021 Wiley-VCH GmbH.<sup>169</sup> (c) Schematic illustration of CCP NPs for effective and anti-metastatic combinational mPTT/PDT. Reprinted from *Biomaterials*, 286, Chen P-L, Huang P-Y, Chen J-Y, et al. A self-delivery chimeric peptide for high efficient cell membrane-targeting low-temperature photothermal/photodynamic combinational therapy and metastasis suppression of tumor. 121593, copyright 2022, with permission from Elsevier.<sup>173</sup> (d) Schematic showing the preparation of L-arginine and PEGylated ICG-modified nanovesicles and the mechanisms of synergistic cancer therapy. Reprinted from *Acta Biomater*, 140, Wang K, Jiang L, Qiu L. Near infrared light triggered ternary synergistic cancer therapy via L-arginine-loaded nanovesicles with modification of PEGylated indocyanine green. 506–517, Copyright (2022), with permission from Elsevier.<sup>174</sup>

(Figure 9a).<sup>169</sup> GNPs aggregates not only acted as a radiosensitizer to induce the RT effect by generating ROS to make DNA double strands destruction, but also as a photothermal sensitizer to produce mPTT effect which ameliorated tumor hypoxia and inhibited the self-repair of damaged DNA, thereby reaching a synergistic effect. With the additional effect of DOX, <sup>131</sup>I-hydrogel/DOX/GNPs aggregates exhibited the most favorable antitumor efficacy with negligible side effects. Moreover, the multifunctional hybrid hydrogel nanoplatform possessed both fluorescence and SPECT imaging properties (Figure 9b), thus constructing an integrated nanoplatform for multimodal imaging-guided cancer theranostic based on RT/mPTT/chemotherapy synergistic therapy.

Similarly, PDT, a treatment strategy that takes advantage of the light energy absorbed by photosensitizers to convert tumor-dissolved oxygen into cytotoxic ROS, is restricted by hypoxic TME.<sup>192</sup> Synergistic application of PDT with mPTT which relieves hypoxia has attracted increasing attention. Chen et al assembled hydrophobic palmitic acid-modified Cypate (an analog of ICG) and hydrophilic chimeric peptide Arg-Arg-Lys-Lys-PEG<sub>8</sub> (RRKK-PEG<sub>8</sub>-COOH) to construct a novel tumor cell membrane-targeting chimeric peptide (C<sub>16</sub>-Cypate-RRKK-PEG<sub>8</sub>-COOH, named as CCP) for synergistic therapy of PDT and mPTT (Figure 9c).<sup>173</sup> Different from the membrane-targeting ability which was previously exemplified to have homologous targeting property and increase the internalization of nanocomposites, membrane-targeting herein referred to the fact that CCP could be anchored on the tumor cell membrane through the insertion of alkyl chain of palmitic acid into the membrane and the electrostatic interaction between RRKK and cell membrane. Upon 793 nm light irradiation, the large amount of ROS produced by CCP directly disintegrated the cell membrane and led to

rapid cell death, meanwhile, the generated mild hyperthermia was able to accelerate the process by increasing the oxygen supply. Compared with conventional nanotherapies that required the cascade implementation of “CAPIR” (circulation, accumulation, penetration, internalization, and release) to exert toxic effect, the novel strategy of tumor cell membrane-targeting combined with mPTT/PDT in this report could circumvent various biological barriers to inhibit tumors and had great potential for synergistic antitumor therapy.<sup>193,194</sup> In another example, Wang et al achieved mPTT-promoted PDT-mediated NO release for the treatment of tumors by loading PEGylated ICG (mPEG-ICG) and water-soluble NO donor L-arginine (L-Arg) into a nanocontainer self-assembled by amphiphilic poly[(PEG)(ethyl-p-aminobenzoate)phosphazene] (PEP) (Figure 9d).<sup>174</sup> On the one hand, the ROS produced by the final product IA-PEP under 808 nm laser irradiation could not only kill tumor cells, but also oxidized L-Arg to release NO for further tumor suppression. On the other hand, the mild hyperthermia generated under the same laser increased the content of ROS and accelerated the oxidation of L-Arg to produce more NO. In this work, mPTT played a dual role of promoting the production of ROS and NO, and remarkably enhanced the curative effect of synergistic therapy. Interestingly, it seemed that investigators were not content with the alleviation of hypoxia through a single mPTT approach, and the elevated H<sub>2</sub>O<sub>2</sub> in tumors had emerged as a tool for oxygen production. Wang et al applied Au@Rh(rhodium) core-shell nanostructures with catalase-like activity and photothermal conversion performance as a basic platform to load ICG for constructing Au@Rh-ICG, which were coated by cancer cell membrane (CM) to form end products Au@Rh-ICG-CM (Figure 10a).<sup>175</sup> After specific aggregation in tumor guided by CM, the synthesized Au@Rh-ICG-CM catalyzed the excessive H<sub>2</sub>O<sub>2</sub> to oxygen in tumor, and at the same time, the mild hyperthermia generated under external laser irradiation could further improve the hypoxia.

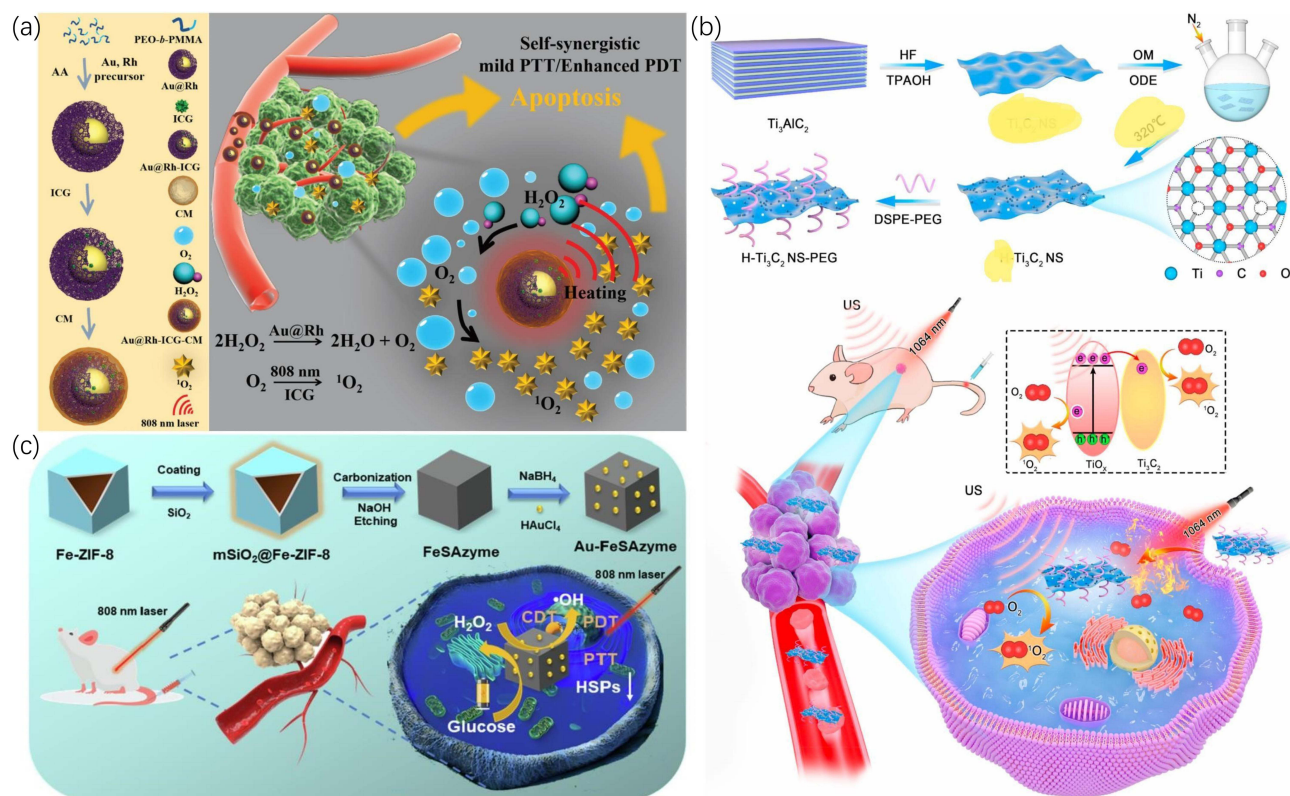


**Figure 10** (a) Schematic illustration of the synthesis of Au@Rh-ICG-CM and the mechanisms for self-synergistic mPTT/enhanced PDT. Reprinted with permission from Wang J, Sun J, Hu W, et al. A Porous Au@Rh Bimetallic core-shell nanostructure as an H<sub>2</sub>O<sub>2</sub>-driven oxygenator to alleviate tumor hypoxia for simultaneous bimodal imaging and enhanced photodynamic therapy. *Adv Mater.* 2020;32(22):e2001862. © 2020 WILEY-VCH Verlag GmbH & Co. KGaA, Weinheim.<sup>175</sup> (b) Schematic showing the construction of H-Ti<sub>3</sub>C<sub>2</sub>-PEG NSs and their application in synergistic mPTT/SDT antitumor therapy. Reproduced from Li G, Zhong X, Wang X et al. Titanium carbide nanosheets with defect structure for photothermal-enhanced sonodynamic therapy. *Bioact Mater.* 2022;8:409–419. To view a copy of this license, visit <http://creativecommons.org/licenses/by-nc-nd/4.0/>.<sup>178</sup> (c) Schematic illustration of the Au-FeSAzyme for biocatalysis and mPTT synergistic therapy. Reprinted from J Colloid Interface Sci, 618, Feng N, Li Q, Bai Q, et al. Development of an Au-anchored Fe Single-atom nanozyme for biocatalysis and enhanced tumor photothermal therapy. 68–77, Copyright (2022), with permission from Elsevier.<sup>189</sup>



The experimental results proved that the efficacy of oxygen-dependent PDT could be strikingly enhanced with a dual hypoxia-relieving strategy.

SDT, another novel and noninvasive nanomedical therapy, has been employed for cancer treatment via ROS generated by sonosensitizers under US irradiation.<sup>195,196</sup> Although SDT benefits from the deeper penetration characteristic of US for better efficacy on deep-seated tumors compared to PDT, it is still hampered by hypoxia, which makes it reasonable to collaborate with mPTT.<sup>197</sup> Li et al engineered Ti<sub>3</sub>C<sub>2</sub> nanosheets (Ti<sub>3</sub>C<sub>2</sub> NSs) with high photothermal conversion efficiency into H-Ti<sub>3</sub>C<sub>2</sub> NSs by two-step methods of chemical exfoliation and high-temperature treatment to promote their US-responsive ability, and then the biocompatibility of the synthesized H-Ti<sub>3</sub>C<sub>2</sub> NSs was increased by PEGylation (Figure 10b).<sup>178</sup> With sequential 1064 nm laser and US irradiation, H-Ti<sub>3</sub>C<sub>2</sub>-PEG NSs heated the local temperature to 42°C for accelerating blood circulation as well as relieving hypoxia, and subsequently generated a large amount of ROS to exert a cytotoxic effect. This research provided a typical paradigm for mPTT combined with SDT and demonstrated that it was feasible and promising for enhanced SDT by rational application of mPTT to overcome hypoxia.

### CDT/TDT

Different from the oxygen-dependent therapies mentioned above, CDT/TDT can eradicate tumors without being affected by hypoxia. CDT mainly uses metal ions such as Fe<sup>2+</sup>, Mn<sup>2+</sup>, and Cu<sup>1+</sup> to activate Fenton or Fenton-like reaction, which converts H<sub>2</sub>O<sub>2</sub> into highly toxic ·OH to elicit cancer cell death.<sup>198–201</sup> However, one of the most formidable challenges is that the low catalytic efficiency restricts the production of ·OH, giving rise to incomplete elimination of tumors and hindering its clinical transformation.<sup>202,203</sup> Encouraged by the fact that mild hyperthermia could accelerate Fenton or Fenton-like reaction, Qian et al synthesized MoP<sub>2</sub> nanorods with excellent PCE and POD activity via a facile liquid exfoliation to achieve mPTT-augmented CDT.<sup>181</sup> Additionally, building on the accelerated Fenton reaction by mPTT, Feng et al further enhanced CDT by increasing the amount of reactant H<sub>2</sub>O<sub>2</sub>.<sup>189</sup> They constructed a composite nanoplat-form (Au-FeSAzyme) by integrating Au NPs with glucose oxidase (GOD)-like catalytic property into the Fe single-atom nanozyme (FeSAzyme) with POD-like activity (Figure 10c). The as-prepared Au-FeSAzyme could convert glucose to gluconic acid and H<sub>2</sub>O<sub>2</sub> via GOD-like property, and then catalyzed H<sub>2</sub>O<sub>2</sub> generated from the reaction as well as excessive H<sub>2</sub>O<sub>2</sub> from tumor to ·OH through POD-like activity. Upon 808nm laser irradiation, the catalytic efficiency was advanced and much more OH was produced, thus realizing the boosted CDT. Nevertheless, considering the potential safety concern of excess metal ions, many efforts had been dedicated to finding alternative strategies to develop metal-free CDT. Artemisinin, an antimalarial drug, had been reported to function as a free radical generator due to its endoperoxide moieties that could react with iron ions to produce ROS.<sup>204,205</sup> Coincidentally, the rich iron ions in tumor cells met the artemisinin-iron reaction to induce CDT effect.<sup>206</sup> In view of these mechanisms, Zhang et al designed A-Pt-IR NP by employing HAS to encapsulate a Pt(IV) prodrug (A-Pt) containing two artesunates (ART, an artemisinin derivative) molecules and a NIR-II PTA IR1048 (Figure 11a).<sup>185</sup> A-Pt would be reduced to cisplatin and ART by a great quantity of GSH inside the tumor, subsequently achieving cisplatin-mediated chemotherapy and ART-mediated CDT, which was intensely facilitated under the mild heat generated by IR1048 upon 1064 nm laser irradiation. In addition, the mPTT-enhanced synergistic therapy of chemotherapy and CDT could induce a strong immune response and increase antitumor immunity.

Apart from CDT, TDT is another oxygen-independent radical-based therapy. The mechanism of TDT is to utilize thermally decomposable radical initiators such as azo to generate alkyl radicals (R) for cancer treatment.<sup>207,208</sup> By reason of the perfect fit between the condition for TDT to function and the thermal effect generated by mPTT, the combination of TDT and mPTT has attracted more and more attention in tumor treatment. For instance, Ouyang et al used a multifunctional injection hydrogel of sodium alginate (ALG) as the vehicle to carry a NIR-II PTA Ink and thermal-degradable 2,2'-azobis[2-(2-imidazolin-2-yl) propane]-dihydrochloride (AIPH, an azo initiator) (Figure 11b).<sup>188</sup> Under mild hyperthermia, AIPH was rapidly degraded accompanied by the production of massive lethal alkyl radicals to kill tumor cells. Similarly, Li et al also achieved well antitumor efficacy by co-loading 17-AAG and AIPH on mesoporous polydopamine (MPDA) to induce mPTT-mediated TDT without being affected by hypoxia TME (Figure 11c).<sup>47</sup>

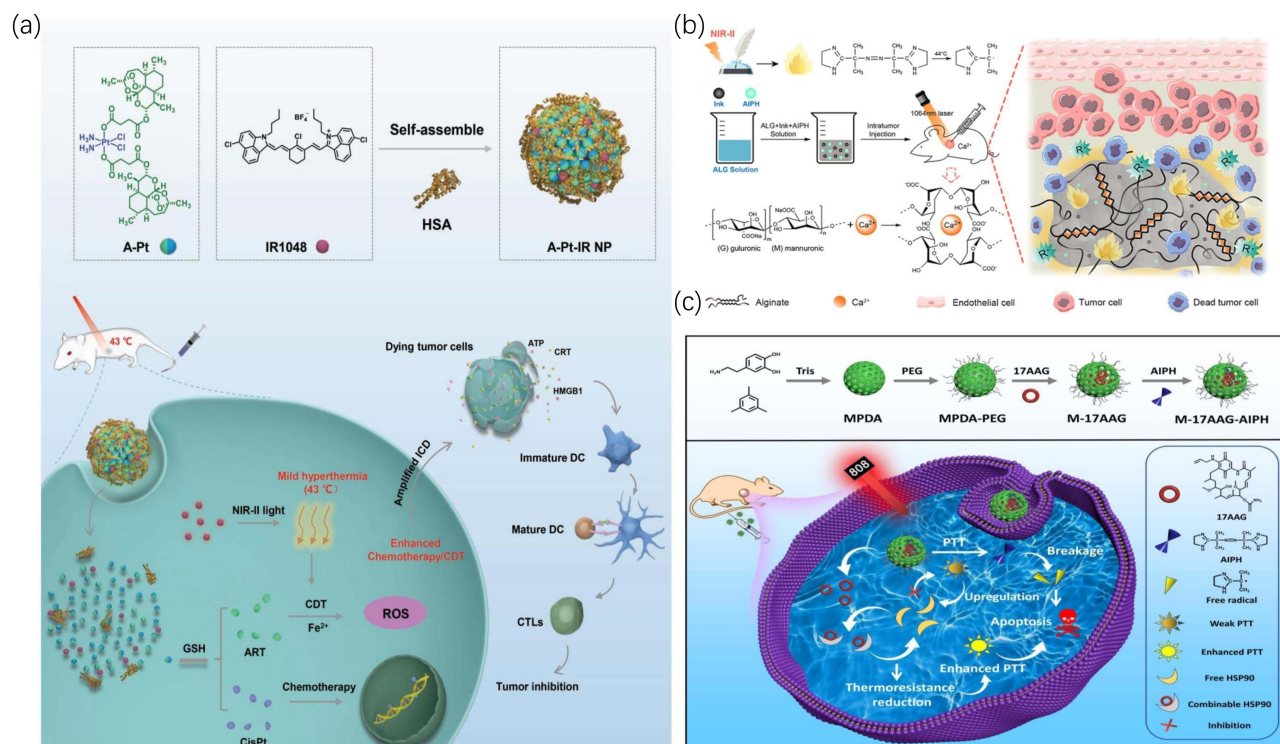


**Figure 11** (a) Schematic illustrating the preparation of A-Pt-IR NP and its application for NIR-II light-enhanced chemotherapy/CDT. Reprinted with permission from Xiong G, Huang D, Lu L, et al. Near-infrared-II light induced mild hyperthermia activate cisplatin-artemisinin nanoparticle for enhanced chemo/chemodynamic therapy and immunotherapy. *Small Methods*. 2022;6(9):e2200379. © 2022 Wiley-VCH GmbH.<sup>185</sup> (b) Schematic showing the mechanisms of alkyl free radicals generated by AIPH and their application in tumor therapy. Reprinted with permission from Ouyang B, Liu F, Ruan S, et al. Localized free radicals burst triggered by NIR-II Light for augmented low-temperature photothermal therapy. *ACS Appl Mater Interfaces*. 2019;11(42):38555–38567.<sup>188</sup> Copyright 2019 American Chemical Society. (c) The synthesis of M-17AAG-AIPH NPs and their synergistic mechanisms in tumor therapy. Reprinted from *Acta Biomater*, 148, Li R, Hu X, Shang F, et al. Treatment of triple negative breast cancer by near infrared light triggered mild-temperature photothermal therapy combined with oxygen-independent cytotoxic free radicals. 218–229, Copyright (2022), with permission from Elsevier.<sup>47</sup>

## mPTT Plays a Supporting Role in Synergizing with Immunotherapy

In recent decades, immunotherapy has played an incomparable role in tumor therapy due to its powerful ability to inhibit metastasis and prevent recurrence in addition to eradicating the primary tumor.<sup>209</sup> Immunotherapy exerts vigorous and long-term antitumor effect by activating host immune responses through various approaches, mainly including cancer vaccines, immune checkpoint blockade (ICB) therapy, and adoptive cell therapy (ACT).<sup>210–212</sup> However, a few unfavorable factors make mono immunotherapy far from satisfactory. It is well established that the immunosuppressive microenvironment, also known as “cold” tumor, characterizing the lost antigenicity, poor immunogenicity, abnormal tumor vessels, dense ECM, etc., is responsible for the deficiency of immune efficacy.<sup>213–215</sup> Substantial efforts are required to improve the immunosuppressive microenvironment for reinvigorating the immune response against tumor. Recently, mPTT has been reported to hold promising potential in transforming immunosuppressive “cold” tumor into immunosensitive “hot” tumor.<sup>216,217</sup> Mild heat can enhance the delivery of immunotherapeutic agents and the recruitment of tumor-infiltrating lymphocytes (TILs) by disrupting dense ECM, loosening compact tumor tissue, and normalizing blood vessels.<sup>218,219</sup> What’s more, mild heat has the potential to induce the release of tumor-associated antigens (TAAs), which can be presented by antigen-presenting cells (APCs) and promote their maturation, subsequently stimulating the proliferation and differentiation of T cells to fight against tumor.<sup>219,220</sup> Additionally, the slight increase of local temperature of tumor can lead to a switch in the phenotype of tumor-associated macrophages (TAMs) from an M2 immunosuppressive phenotype to an M1 immunosensitive phenotype, and inhibit immunosuppressive regulatory T cells (Tregs).<sup>221,222</sup> All in all, mPTT generates an overall immune-promoting microenvironment from multiple pathways, acting as possibly the best candidate for adjuvant immunotherapy.

Cancer vaccine aims to induce specific antitumor immune response against tumor antigens to defeat tumor, and generate immunological memory to prevent recurrence.<sup>223,224</sup> However, the clinical transformation of cancer vaccine has not achieved



encouraging results, since it is extremely strenuous to exploit specific vaccine for different tumors in different individuals due to the pronounced tumor heterogeneity.<sup>225,226</sup> In addition, the immunosuppressive microenvironment is not conducive to cancer vaccine either.<sup>227</sup> With these issues in mind, multiple NIR-responsive multifunctional nanovaccines, which generally include three components of nanocarriers, immunoadjuvants, and PTAs, have been developed.<sup>228</sup> On the one hand, the mild hyperthermia generated by PTAs under NIR irradiation can activate antigen presentation and recruit dendritic cells (DCs) via the exposure of TAAs, which are considered as “whole cancer cell vaccines” and optimal in situ cancer vaccines.<sup>10,222</sup> On the other hand, kinds of immunoadjuvants carried in nanovaccines are able to further improve the capture of tumor antigens by DCs and enhance the immune response of T cells.<sup>229,230</sup> Besides the initial nanovaccines combining mPTT with immunoadjuvants, certain smart nanovaccines are also expected to realize robust and long-term antitumor immune response.<sup>228</sup> For instance, Sun et al constructed intelligent DCs (iDCs) as an advanced nanovaccine by coating IR-797 (PTA) loaded nanodots with a mature DC membrane (Figure 12).<sup>9</sup> Unlike traditional NIR-responsive nanovaccines that activated immune responses in a single way by inducing antigen release, iDCs with mature DC membrane function could not only directly stimulate in situ T cells, but also entered draining lymph nodes to activate T cell responses, which subsequently migrated to tumor regions. The immunostimulatory cytokines such as tumor necrosis factor (TNF)- $\alpha$  secreted by activated T cells could modulate the immunosuppressive microenvironment to a certain extent and inhibit the expression of HSPs. After 808nm light radiation, mild heat impaired tumor cells without affecting the recruited immune cells, releasing large amounts of TAAs to restart the self-sustaining cycle of cancer immunity. This smart nanovaccine achieved dual immune activation using mature DC membrane function in combination with mPTT, significantly enhancing antitumor immunity against both primary and metastatic tumors.

Immunogenic cell death (ICD), as a major initiator of adaptive cascade immunity (TAAs release, DCs maturation, T cells activation, and TILs recruitment), is characterized by the exposure of TAAs with the release of damage-associated

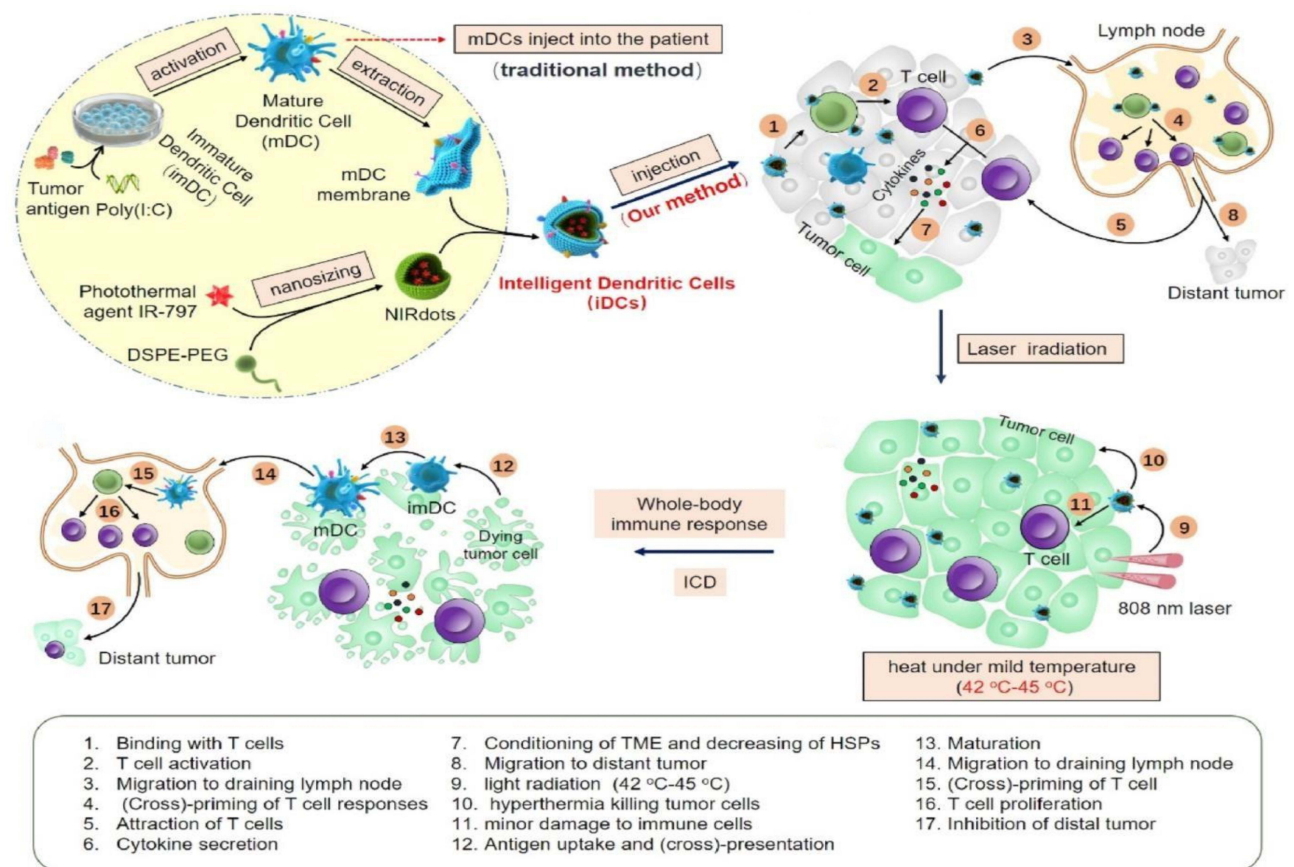


**Figure 12** Schematic illustration of the synthesis of iDCs and their working mechanisms in the synergistic treatment of mPTT with iDCs. Reprinted from *Biomaterials*, 279, Sun Z, Deng G, Peng X, et al. Intelligent photothermal dendritic cells restart the cancer immunity cycle through enhanced immunogenic cell death. 121228, Copyright (2021), with permission from Elsevier.<sup>9</sup>

molecular patterns (DAMPs) which subsequently activate systemic immune responses.<sup>231</sup> Various methods of inducing ICD have been reported, including chemotherapy, radical-based therapy, gas therapy, and PTT.<sup>187,232,233</sup> Although these therapies have shown to activate immune responses by inducing ICD, the immune efficacy generated by the recruited TILs is largely compromised due to the presence of immune checkpoints such as programmed death ligand 1 (PD-L1) expressed on tumor cells, which interacts with programmed cell death 1 (PD-1) expressed on cytotoxic T lymphocytes (CTLs) and limits their function.<sup>219,232</sup> From this, continuously growing studies are inclined to combine ICD with ICB to improve antitumor immune efficacy. It is worth noting that mPTT plays an appreciable adjuvant role in the combination of ICD and ICB by inducing ICD to release TAAs and DAMPs, increasing the recruitment of TILs and upregulating the expression of PD-L1 to sensitize ICB.<sup>234</sup> Considering these above, Ning et al developed an all-in-one hydrogel loading a photothermal agent of Chinese ink, a PD-L1 inhibitor of HY19991 (HY), and AIPH for mild photothermal immunotherapy (Figure 13a).<sup>187</sup> The mild heat generated by Chinese ink under 1064 nm light irradiation first improved the immunosuppressive environment and degraded AIPH, subsequently the released alkyl radicals amplified the ICD caused by mPTT, and finally, the intervention of HY blocked the binding of CTLs with PD-L1, achieving mPTT-enhanced alkyl radicals-mediated ICD synergistic immunotherapy with ICB. Similarly, Huang et al synthesized a drug-free nanoplatfrom (NO<sub>PS</sub>@BP) comprised of an outer cloak of nitrate-containing polymeric NO donor and an inner core of black phosphorus (BP, a PTA) to realize efficient multimodal therapy of mPTT, NO gas therapy, and ICB-based immunotherapy by taking advantage of the photothermal conversion function of BP as well as the dual function of NO which could induce ICD and interfere with PD-L1 activation.<sup>233</sup> Further, since the activation of immune response was a multistep cascade process, it was highly necessary to target multiple key steps in the cascade to promote a positive shift in the cancer-immunity cycle.<sup>235,236</sup> To this end, Feng et al adopted a strategy of sequential administration combined with mPTT to achieve the above objectives (Figure 13b).<sup>232</sup> On the first day, the prepared Au nanorod/DOX gel (AuNR/DOX gel) was administered via peri-tumoral injection, and the sustained release of DOX controlled by Pluronic gel could induce ICD to release TAAs and DAMPs. The next day, AuNR generated mPTT under 880nm irradiation to further induce ICD while improving the immunosuppressive microenvironment. On the third day, intratumorally administered maleimide-modified liposomes (L-Mals) which acted as an antigen capturing NPs could capture TAAs to enhance antigen uptake by DCs, and PD-L1 antibody (aPD-L1) administered intraperitoneally on the same day blocked the binding of CTLs and PD-L1. The experimental results proved that this sequential administration combined with mPTT tactic promoted the release of TAAs, accelerated the maturation of DCs, increased the infiltration of TILs, and magnified the toxicity of CTLs, thereby achieving enhanced antitumor immunity by targeting multiple cascade immunity events.

ACT is a highly potential strategy for cancer immunotherapy by harvesting immunocompetent cells from patients, expanding *in vitro*, genetically engineering, functionally characterizing, and reinfusing back into patients to achieve the goal of either killing tumor cells directly or provoking immune response in the body to kill tumor cells.<sup>237</sup> Among ACT, chimeric antigen receptor T cell (CAR-T) therapy, as a representative therapy of ACT, has provided a substantial breakthrough for tumor immunotherapy, especially with respect to hematological tumors.<sup>238</sup> However, CAR-T still faces great challenges in the field of solid tumor treatment owing to the limitation of several factors such as the physical and immune barriers.<sup>239</sup> Noteworthy, the potent immune environment reprogramming ability of mPTT makes it possible for CAR-T to achieve better antitumor immunity in solid tumors.<sup>240</sup> For instance, Shi et al reported the successful implementation of CAR-T-based immunotherapy for solid tumors via microenvironment reconstruction by utilizing as-prepared multimodal theranostic and imaging nanoplatfrom (FA-Gd-GERTs@Ibrutinib) (Figure 14a).<sup>241</sup> To be specific, after intravenous injection into the xenograft models of non-Hodgkin's lymphoma, FA-Gd-GERTs@Ibrutinib selectively aggregated in tumor through folate (FA) receptors and released chemotherapeutic agent (ibrutinib) and PTA (gadolinium-loaded gap-enhanced Raman tags (Gd-GERTs)) to partially kill tumor cells upon 808nm light irradiation. More importantly, the generated mild hyperthermia could not only break the physical barrier by destroying dense ECM, decreasing high interstitial fluid pressure (IFP), dilating blood vessels, and improving blood flow perfusion to enhance the infiltration and penetration of CAR-T cells, but also disrupted the immune barrier by increasing immunogenicity and the level of chemokines such as chemokine ligand 2 (CCL2) which further recruited CAR-T cells. After purging the barriers of immune response, CD19-specific CAR-T lymphocytes were intravenously injected. As expected, treatment with mPTT led to more activation and proliferation of CAR-T cells within the tumor and secreted more inflammatory

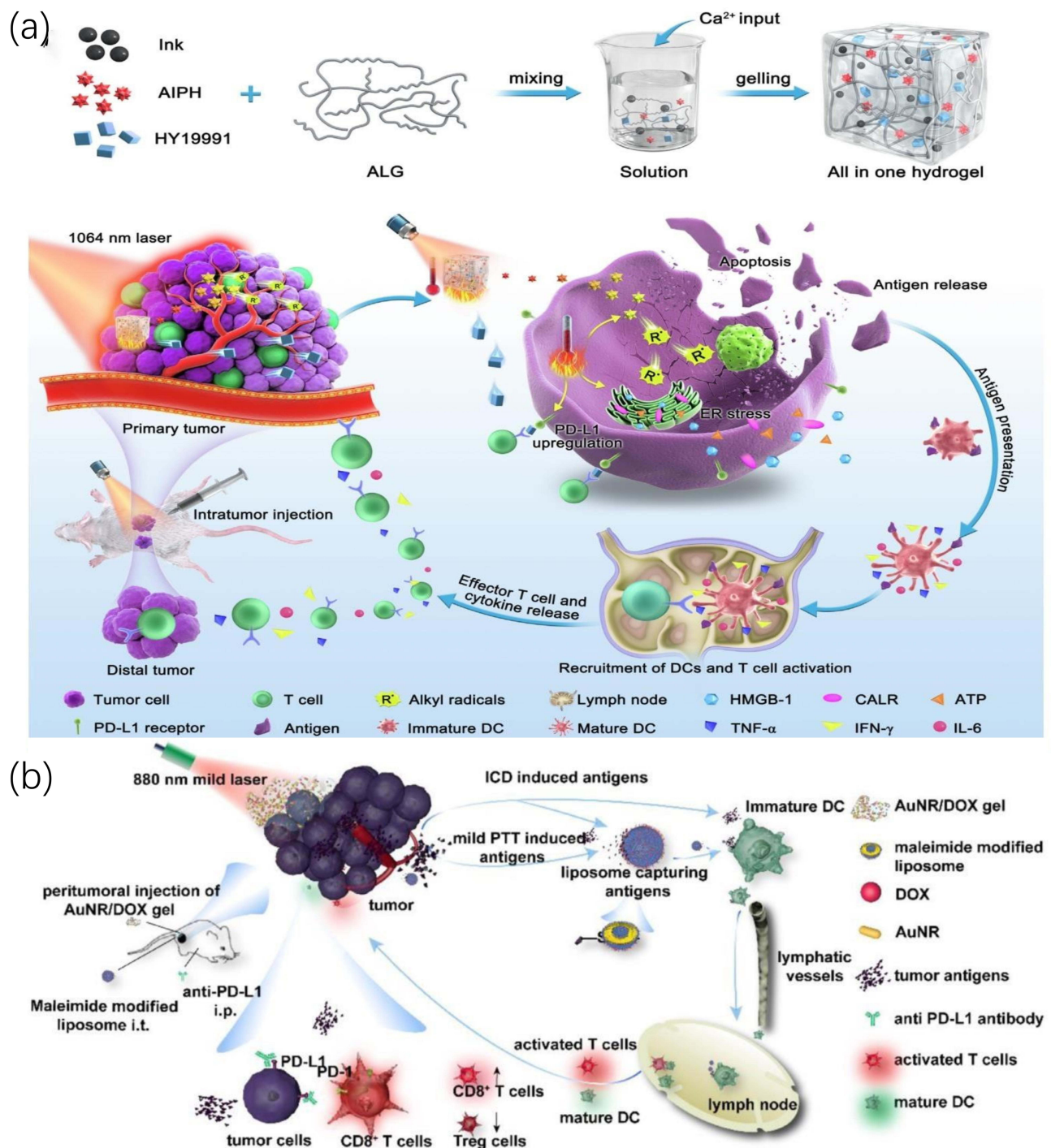


**Figure 13** (a) Schematic showing the preparation of the all-in-one hydrogel and its therapeutic mechanisms for potentiating immunotherapy. Reprinted from *J Colloid Interface Sci*, 614, Ning B, Liu Y, Ouyang B, et al. Low-temperature photothermal irradiation triggers alkyl radicals burst for potentiating cancer immunotherapy. 436–450, Copyright (2022), with permission from Elsevier.<sup>187</sup> (b) Schematic illustrating the mPTT combined with antigen-capturing liposomes and anti-PD-L1 for enhanced immunotherapy. Reprinted from *Acta Biomater*, 136, Feng Z-H, Li Z-T, Zhang S, et al. A combination strategy based on an Au nanorod/doxorubicin gel via mild photothermal therapy combined with antigen-capturing liposomes and anti-PD-L1 agent promote a positive shift in the cancer-immunity cycle. 495–507, Copyright (2021), with permission from Elsevier.<sup>232</sup>

cytokines such as interleukin (IL)-2 and interferon (IFN)- $\gamma$ , resulting in stronger antitumor immunity compared to the absence of mPTT treatment (Figure 14b and c). Additionally, the multimodal imaging characteristics of CT/MRI/SERS (surface-enhanced Raman scattering) enabled multifunctional therapeutic nanoplatform to accurately visualize cancer during treatment (Figure 14d–g). Intriguingly, considering the cumbersome and costly procedures of in vitro genetic



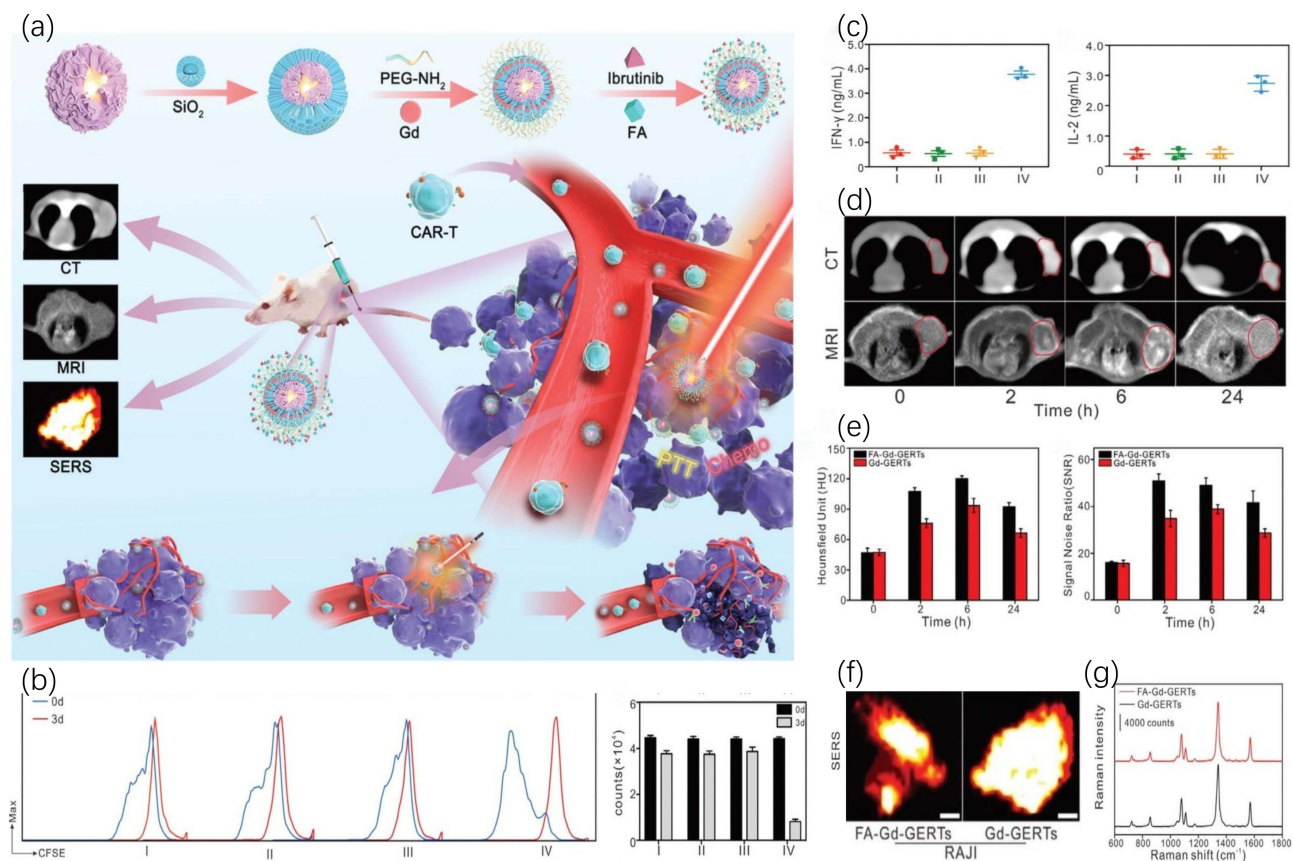


**Figure 14** Schematic illustration of FA-Gd-GERTs@Ibrutinib design and its application. (a) The preparation process of FA-Gd-GERTs@Ibrutinib and its application for multimodal imaging guidance and multiple immune microenvironment regulation to enhance CAR-T therapy in solid tumors. (b) Representative flow cytometry analysis of CD19 CAR-T cells labeled with CFSE and its mean fluorescence intensity and (c) the expression levels of IFN- $\gamma$  and IL-2 in the supernatants three days after the indicated treatments. Four groups: (I) untreated; (II) laser treated ( $0.5 \text{ W cm}^{-2}$ , 3min); (III) FA-Gd-GERTs@Ibrutinib treated; and (IV) FA-Gd-GERTs@Ibrutinib treated, followed by laser irradiation ( $0.5 \text{ W cm}^{-2}$ , 3min). (d) Representative transection CT and MR images at 0, 2, 6, and 24h after the intravenous injection of NPs (the red circles indicate tumor areas) and (e) their CT values and T1 MR SNRs. Representative SERS images (f) and Raman spectra (g) 6 h after the intravenous injection of NPs. Scale bars: 2 mm. Reprinted with permission from Shi B, Li D, Yao W, et al. Multifunctional theranostic nanoparticles for multi-modal imaging-guided CAR-T immunotherapy and chemophotothermal combinational therapy of non-Hodgkin's lymphoma. *Biomater Sci.* 2022;10(10):2577–2589.<sup>241</sup> Copyright 2022 Royal Society of Chemistry.

manipulation of immune cells, Lin et al realized nature killer (NK) cell-based ACT by modifying tumor cells and cooperating with mPTT to increase NK cell infiltration and activation.<sup>242</sup> In brief, they synthesized a gold-selenium-based nano-immunomodulator (AuNSP@ $\alpha$ CD16) which could, on the one hand, induce mild NIR-II PTT to remodel immunosuppressive microenvironment, and on the other hand, modify CD16 antibody ( $\alpha$ CD16) on tumor cells surface to further recruit and activate NK cells. These works demonstrated that mPTT could pave the way for immunotherapy by creating an immune favorable microenvironment, providing substantial insight for future application of ACT in solid tumors.

## Conclusions and Perspectives

In summary, as an emerging cancer treatment modality, mPTT has received increasing attention in recent years due to its numerous advantages. However, mono mPTT is not sufficient to completely eradicate tumors, which has prompted researchers to work on developing feasible strategies for the optimized application of mPTT. In this review, the applications of mPTT in tumor therapy are divided into two parts according to the function it exerts, where the first is taking mPTT as the leading role to directly kill tumors, and the second is regarding mPTT as an adjuvant role to synergize other therapies for inhibiting tumors. In the first section, we discuss the effects of HSPs and autophagy on mPTT and introduce various methods of inhibiting HSPs and regulating autophagy to make tumor cells more susceptible to thermal injury. Although the efficacy of mPTT is significantly improved by reducing thermal resistance, some

limitations such as uneven distribution of heat, poor efficacy on deep-seated tumors, and inability to prevent metastasis and recurrence limit its clinical transformation. Therefore, the corresponding resolutions, that is, the combination of mPTT with other therapies including chemotherapy, gene therapy, radical-based therapy, and immunotherapy, are discussed in the second part. It is worth noting that in this section, mPTT mainly plays an adjuvant role to enhance the efficacy of combination therapy rather than directly killing tumor cells, and the specific mechanisms of synergistic effects are elaborated in the corresponding part.

Meanwhile, several challenges remain with mPTT. Primarily, since mPTT is a nanomedicine-based therapy, the development level of nanotechnology directly determines its superior limit of application. The importance of exploiting novel PTAs with higher PCE cannot be overemphasized, for a higher PCE means less drug dose and lower radiation power, which will undoubtedly reduce the occurrence of side effects. In addition, the limited penetration ability of NIR makes mPTT have little efficacy against deep-seated tumors. It is feasible that NIR-II with characteristics of deeper penetration, higher maximum exposure to the skin, and lower signal-to-noise ratio may be a potential alternative for deep tumors. The targeting of nanocomposites is another issue worth paying attention to. At present, most nanoplatfroms are still dominated by passive targeting of EPR, although it can resolve the nonspecific distribution of drugs in vivo to some extent, there is much room for improvement. Conferring active targeting ability on the basis of EPR is the development trend of future precision medicine, among which CCMs are of great concern because of the excellent targeting ability to primary and metastasis as well as universality. Moreover, imaging capability, capable of precisely visualizing tumors, is also a key parameter for the comprehensive evaluation of nanoplatfroms. Despite some nanoplatfroms having been reported to achieve all the above characteristics simultaneously, it comes at the cost of a complicated preparation process, which is unfavorable for clinical translation. In view of the above, tremendous efforts are still required to develop nanoplatfroms integrating various characteristics for cancer diagnosis and treatment with as few components as possible.

Apart from the versatile properties of nanoplatfroms, mechanism of medical therapy is another key point closely related to mPTT. For the strategy of enhancing mPTT, although existing studies have demonstrated that the efficacy of mPTT can be significantly improved by blocking HSPs and regulating autophagy progression, and the mode of action has evolved from the initial drugs action to the subsequent materials and gases action, it seems that there is a lack of reagents that interfere with HSPs and autophagy at the same time to sensitize mPTT. Besides, whether there are other mechanisms of resistance to mPTT other than HSPs and autophagy waiting to be discovered is also a matter worth considering. As for the combination therapy of mPTT, the biological effects that mPTT can produce, such as destroying ECM, increasing blood perfusion, improving cell membrane permeability, and regulating immune microenvironment, should be first fully understood, and based on this, the biological characteristics of mPTT should be targeted use to address the difficulties faced by other therapies, so as to achieve synergistic therapy in a real sense, rather than simply rudimentary arrayed combinations of two or more therapies. Moreover, as mPTT is still at the initial stage of development, its therapeutic mechanisms as well as the combined treatment mechanisms need to be further explored. It is worth mentioning that mPTT has also achieved significant efficacy in antibacterial treatment and wound healing. Altogether, we believe that with the booming development of nanomedicine and the continuous depth of research mechanisms, mPTT will have a broader application platform in future.

## Funding

This review was supported by the National Natural Science Foundation of China (grant number 82171953 and 82171947).

## Disclosure

The authors report no conflicts of interest in this work.

---

## References

1. Shi J, Kantoff PW, Wooster R, Farokhzad OC. Cancer nanomedicine: progress, challenges and opportunities. *Nat Rev Cancer*. 2017;17(1):20–37.
2. Miller KD, Siegel RL, Lin CC, et al. Cancer treatment and survivorship statistics, 2016. *CA Cancer J Clin*. 2016;66(4):271–289.
3. McGranahan N, Swanton C. Clonal heterogeneity and tumor evolution: past, present, and the future. *Cell*. 2017;168(4):613–628.



4. Chen P, Ma Y, Zheng Z, Wu C, Wang Y, Liang G. Facile syntheses of conjugated polymers for photothermal tumour therapy. *Nat Commun.* 2019;10(1):1192.
5. Liu Y, Bhattarai P, Dai Z, Chen X. Photothermal therapy and photoacoustic imaging via nanotheranostics in fighting cancer. *Chem Soc Rev.* 2019;48(7):2053–2108.
6. Xiong R, Hua D, Van Hoeck J, et al. Photothermal nanofibres enable safe engineering of therapeutic cells. *Nat Nanotechnol.* 2021;16(11):1281–1291.
7. Orosz P, Echtenacher B, Falk W, Rüschoff J, Weber D, Männel DN. Enhancement of experimental metastasis by tumor necrosis factor. *J Exp Med.* 1993;177(5):1391–1398.
8. Gao J, Wang F, Wang S, et al. Hyperthermia-triggered on-demand biomimetic nanocarriers for synergetic photothermal and chemotherapy. *Adv Sci.* 2020;7(11):1903642.
9. Sun Z, Deng G, Peng X, et al. Intelligent photothermal dendritic cells restart the cancer immunity cycle through enhanced immunogenic cell death. *Biomaterials.* 2021;279:121228.
10. Jiang Z, Li T, Cheng H, et al. Nanomedicine potentiates mild photothermal therapy for tumor ablation. *Asian J Pharm Sci.* 2021;16(6):738–761.
11. Yu Q, Tang X, Zhao W, et al. Mild hyperthermia promotes immune checkpoint blockade-based immunotherapy against metastatic pancreatic cancer using size-adjustable nanoparticles. *Acta Biomater.* 2021;133:244–256.
12. Li C, Yang X-Q, An J, et al. A near-infrared light-controlled smart nanocarrier with reversible polypeptide-engineered valve for targeted fluorescence-photoacoustic bimodal imaging-guided chemo-photothermal therapy. *Theranostics.* 2019;9(25):7666–7679.
13. Li X, Yu S, Lee D, et al. Facile supramolecular approach to nucleic-acid-driven activatable nanotheranostics that overcome drawbacks of photodynamic therapy. *ACS Nano.* 2018;12(1):681–688.
14. Tang X, Tan L, Shi K, et al. Gold nanorods together with HSP inhibitor-VER-155008 micelles for colon cancer mild-temperature photothermal therapy. *Acta Pharm Sin B.* 2018;8(4):587–601.
15. Chang M, Hou Z, Wang M, et al. Single-atom Pd nanozyme for ferroptosis-boosted mild-temperature photothermal therapy. *Angew Chem Int Ed Engl.* 2021;60(23):12971–12979.
16. Gong L, Yan L, Zhou R, Xie J, Wu W, Gu Z. Two-dimensional transition metal dichalcogenide nanomaterials for combination cancer therapy. *J Mater Chem B.* 2017;5(10):1873–1895.
17. Zhou L, Jing Y, Liu Y, et al. Mesoporous carbon nanospheres as a multifunctional carrier for cancer theranostics. *Theranostics.* 2018;8(3):663–675.
18. Sun W, Zhang X, Jia H-R, et al. Water-dispersible candle soot-derived carbon nano-onion clusters for imaging-guided photothermal cancer therapy. *Small.* 2019;15(11):e1804575.
19. Zhu Y-X, Jia H-R, Gao G, et al. Mitochondria-acting nanomicelles for destruction of cancer cells via excessive mitophagy/autophagy-driven lethal energy depletion and phototherapy. *Biomaterials.* 2020;232:119668.
20. Jia H-R, Zhu Y-X, Liu X, et al. Construction of dually responsive nanotransformers with nanosphere-nanofiber-nanosphere transition for overcoming the size paradox of anticancer nanodrugs. *ACS Nano.* 2019;13(10):11781–11792.
21. Gao G, Jiang Y-W, Jia H-R, Wu F-G. Near-infrared light-controllable on-demand antibiotics release using thermo-sensitive hydrogel-based drug reservoir for combating bacterial infection. *Biomaterials.* 2019;188:83–95.
22. Huang P-Y, Zhu -Y-Y, Zhong H, et al. Autophagy-inhibiting biomimetic nanodrugs enhance photothermal therapy and boost antitumor immunity. *Biomater Sci.* 2022;10(5):1267–1280.
23. Luo J, Fan M, Xiong L, et al. 1T-phase dirac semimetal PdTe nanoparticles for efficient photothermal therapy in the NIR-II biowindow. *ACS Appl Mater Interfaces.* 2021;13(24):27963–27971.
24. Huang C, Sun Z, Cui H, et al. InSe nanosheets for efficient NIR-II-responsive drug release. *ACS Appl Mater Interfaces.* 2019;11(31):27521–27528.
25. Sun Q, Tang K, Song L, et al. Covalent organic framework based nanoagent for enhanced mild-temperature photothermal therapy. *Biomater Sci.* 2021;9(23):7977–7983.
26. Shi M, Liu Y, Huang J, et al. Multifunctional theranostic nanoplatform loaded with autophagy inhibitor for enhanced photothermal cancer therapy under mild near-infrared irradiation. *Biomater Adv.* 2022;138:212919.
27. Gomez-Pastor R, Burchfiel ET, Thiele DJ. Regulation of heat shock transcription factors and their roles in physiology and disease. *Nat Rev Mol Cell Biol.* 2018;19:1.
28. Richter K, Haslbeck M, Buchner J. The heat shock response: life on the verge of death. *Mol Cell.* 2010;40(2):253–266.
29. Galluzzi L, Baehrecke EH, Ballabio A, et al. Molecular definitions of autophagy and related processes. *EMBO J.* 2017;36(13):1811–1836.
30. Levy JMM, Towers CG, Thorburn A. Targeting autophagy in cancer. *Nat Rev Cancer.* 2017;17(9):528–542.
31. Yu L, Chen Y, Tooze SA. Autophagy pathway: cellular and molecular mechanisms. *Autophagy.* 2018;14(2):207–215.
32. Finka A, Goloubinoff P. Proteomic data from human cell cultures refine mechanisms of chaperone-mediated protein homeostasis. *Cell Stress Chaperones.* 2013;18(5):591–605.
33. Jolly C, Morimoto RI. Role of the heat shock response and molecular chaperones in oncogenesis and cell death. *J Natl Cancer Inst.* 2000;92(19):1564–1572.
34. Genest O, Wickner S, Doyle SM. Hsp90 and Hsp70 chaperones: collaborators in protein remodeling. *J Biol Chem.* 2019;294(6):2109–2120.
35. Cyran AM, Zhitkovich A. Heat shock proteins and HSF1 in cancer. *Front Oncol.* 2022;12:860320.
36. Zhao R, Zhang R, Feng L, et al. Constructing virus-like SiO/CeO/VO nanozymes for 1064 nm light-triggered mild-temperature photothermal therapy and nanozyme catalytic therapy. *Nanoscale.* 2022;14(2):361–372.
37. Wang S, Li L, Ning X, Xue P, Liu Y. pH-activated heat shock protein inhibition and radical generation enhanced NIR luminescence imaging-guided photothermal tumour ablation. *Int J Pharm.* 2019;566:40–45.
38. You C, Li Y, Dong Y, et al. Low-temperature trigger nitric oxide nanogenerators for enhanced mild photothermal therapy. *ACS Biomater Sci Eng.* 2020;6(3):1535–1542.
39. Xia Y, Li C, Cao J, et al. Liposome-templated gold nanoparticles for precisely temperature-controlled photothermal therapy based on heat shock protein expression. *Colloids Surf B Biointerfaces.* 2022;217:112686.

40. Gao G, Jiang Y-W, Sun W, et al. Molecular targeting-mediated mild-temperature photothermal therapy with a smart albumin-based nanodrug. *Small*. 2019;15(33):e1900501.
41. Tian B, Wang C, Du Y, et al. Near infrared-triggered theranostic nanoplatform with controlled release of HSP90 inhibitor for synergistic mild photothermal and enhanced nanocatalytic therapy with hypoxia relief. *Small*. 2022;18(28):e2200786.
42. Yang Y, Zhu W, Dong Z, et al. 1D coordination polymer nanofibers for low-temperature photothermal therapy. *Adv Mater*. 2017;29:40.
43. Sun J, Li Y, Teng Y, Wang S, Guo J, Wang C. NIR-controlled HSP90 inhibitor release from hollow mesoporous nanocarbon for synergistic tumor photothermal therapy guided by photoacoustic imaging. *Nanoscale*. 2020;12(27):14775–14787.
44. Song Y, Wang Y, Zhu Y, et al. Biomodal tumor-targeted and redox-responsive bi se hollow nanocubes for MSOT/CT imaging guided synergistic low-temperature photothermal radiotherapy. *Adv Healthc Mater*. 2019;8(16):e1900250.
45. Li R-T, Zhu Y-D, Li W-Y, et al. Synergistic photothermal-photodynamic-chemotherapy toward breast cancer based on a liposome-coated core-shell AuNS@NMOFs nanocomposite encapsulated with gambogic acid. *J Nanobiotechnology*. 2022;20(1):212.
46. Zhang T, Wu B, Akakuru OU, et al. Hsp90 inhibitor-loaded IR780 micelles for mitochondria-targeted mild-temperature photothermal therapy in xenograft models of human breast cancer. *Cancer Lett*. 2021;500:41–50.
47. Li R, Hu X, Shang F, et al. Treatment of triple negative breast cancer by near infrared light triggered mild-temperature photothermal therapy combined with oxygen-independent cytotoxic free radicals. *Acta Biomater*. 2022;148:218–229.
48. Sun Q, Liu F, Wen Z, et al. Combined effect of heat shock protein inhibitor geldanamycin and free radicals on photodynamic therapy of prostate cancer. *J Mater Chem B*. 2022;10(9):1369–1377.
49. Lian H, Guan P, Tan H, Zhang X, Meng Z. Near-infrared light triggered multi-hit therapeutic nanosystem for tumor specific photothermal effect amplified signal pathway regulation and ferroptosis. *Bioact Mater*. 2022;9:63–76.
50. Jiang A, Liu Y, Ma L, et al. Biocompatible heat-shock protein inhibitor-delivered flowerlike short-wave infrared nanoprobe for mild temperature-driven highly efficient tumor ablation. *ACS Appl Mater Interfaces*. 2019;11(7):6820–6828.
51. Song L, Dong X, Zhu S, et al. Tween 20 nanodots loading PI3K inhibitor, LY294002, for mild photothermal therapy of LoVo cells in vitro and in vivo. *Adv Healthc Mater*. 2018;7(22):e1800830.
52. Xia J, Qing X, Shen J, et al. Enzyme-loaded pH-sensitive photothermal hydrogels for mild-temperature-mediated combinational cancer therapy. *Front Chem*. 2021;9:736468.
53. Cao J, Qiao B, Luo Y, et al. A multimodal imaging-guided nanoreactor for cooperative combination of tumor starvation and multiple mechanism-enhanced mild temperature phototherapy. *Biomater Sci*. 2020;8(23):6561–6578.
54. Wang P, Kankala RK, Chen B, et al. Cancer cytomembrane-cloaked Prussian blue nanoparticles enhance the efficacy of mild-temperature photothermal therapy by disrupting mitochondrial functions of cancer cells. *ACS Appl Mater Interfaces*. 2021;13(31):37563–37577.
55. Shu X, Chen Y, Yan P, et al. Biomimetic nanoparticles for effective mild temperature photothermal therapy and multimodal imaging. *J Control Release*. 2022;347:270–281.
56. Qi P, Zhang J, Bao Z, et al. Nanozyme for mitochondrial damage-mediated mild-temperature photothermal therapy. *ACS Appl Mater Interfaces*. 2022;14(17):19081–19090.
57. Ding F, Gao X, Huang X, et al. Polydopamine-coated nucleic acid nanogel for siRNA-mediated low-temperature photothermal therapy. *Biomaterials*. 2020;245:119976.
58. Li X, Pan Y, Chen C, et al. Hypoxia-responsive gene editing to reduce tumor thermal tolerance for mild-photothermal therapy. *Angew Chem Int Ed Engl*. 2021;60(39):21200–21204.
59. Chen C, Ma Y, Du S, et al. Controlled CRISPR-Cas9 ribonucleoprotein delivery for sensitized photothermal therapy. *Small*. 2021;17(33):e2101155.
60. Wu C, Wang D, Cen M, et al. Mitochondria-targeting NO gas nanogenerator for augmenting mild photothermal therapy in the NIR-II biowindow. *Chem Commun*. 2020;56(92):14491–14494.
61. Ge H, Du J, Long S, et al. Near-Infrared Light Triggered H Generation for Enhanced Photothermal/Photodynamic Therapy against Hypoxic Tumor. *Adv Healthc Mater*. 2022;11(3):e2101449.
62. Ma G, Liu Z, Zhu C, et al. Responsive NIR-II AIE nanobomb for carbon monoxide boosting low-temperature photothermal therapy. *Angew Chem Int Ed Engl*. 2022;61(36):e202207213.
63. Forouzanfar F, Barreto G, Majeed M, Sahebkar A. Modulatory effects of curcumin on heat shock proteins in cancer: a promising therapeutic approach. *Biofactors*. 2019;45(5):631–640.
64. Nuñez-Rivera A, Fournier PGJ, Arellano DL, Rodriguez-Hernandez AG, Vazquez-Duhalt R, Cadena-Nava RD. Brome mosaic virus-like particles as siRNA nanocarriers for biomedical purposes. *Beilstein J Nanotechnol*. 2020;11:372–382.
65. Liu Y, Li L, Guo Q, et al. Novel Cs-based upconversion nanoparticles as dual-modal CT and UCL imaging agents for chemo-photothermal synergistic therapy. *Theranostics*. 2016;6(10):1491–1505.
66. Mantso T, Vasileiadis S, Anastopoulos I, et al. Hyperthermia induces therapeutic effectiveness and potentiates adjuvant therapy with non-targeted and targeted drugs in an in vitro model of human malignant melanoma. *Sci Rep*. 2018;8(1):10724.
67. Liang -R-R, Jiang S-Y, Zhao X. Two-dimensional covalent organic frameworks with hierarchical porosity. *Chem Soc Rev*. 2020;49(12):3920–3951.
68. Liu X, Li J, Gui B, et al. Covalent organic framework with flexible building blocks. *J Am Chem Soc*. 2021;143(4):2123–2129.
69. Guan Q, Zhou -L-L, Li Y-A, et al. Nanoscale covalent organic framework for combinatorial antitumor photodynamic and photothermal therapy. *ACS Nano*. 2019;13(11):13304–13316.
70. Wang L-K, Zhou -J-J, Lan Y-B, Ding S-Y, Yu W, Wang W. Divergent synthesis of chiral covalent organic frameworks. *Angew Chem Int Ed Engl*. 2019;58(28):9443–9447.
71. Chen W-H, Luo G-F, Lei Q, et al. Overcoming the heat endurance of tumor cells by interfering with the anaerobic glycolysis metabolism for improved photothermal therapy. *ACS Nano*. 2017;11(2):1419–1431.
72. Dai Y, Sun Z, Zhao H, et al. NIR-II fluorescence imaging guided tumor-specific NIR-II photothermal therapy enhanced by starvation mediated thermal sensitization strategy. *Biomaterials*. 2021;275:120935.
73. Fulda S, Galluzzi L, Kroemer G. Targeting mitochondria for cancer therapy. *Nat Rev Drug Discov*. 2010;9(6):447–464.

74. Stine ZE, Schug ZT, Salvino JM, Dang CV. Targeting cancer metabolism in the era of precision oncology. *Nat Rev Drug Discov.* 2022;21(2):141–162.
75. Ma Y, Zhou J, Miao Z, Qian H, Zha Z. dl-menthol loaded polypyrrole nanoparticles as a controlled diclofenac delivery platform for sensitizing cancer cells to photothermal therapy. *ACS Appl Bio Mater.* 2019;2(2):848–855.
76. Zhang K, Li P, Chen H, Bo X, Li X, Xu H. Continuous cavitation designed for enhancing radiofrequency ablation via a special radiofrequency solidoid vaporization process. *ACS Nano.* 2016;10(2):2549–2558.
77. Fu L-H, Qi C, Lin J, Huang P. Catalytic chemistry of glucose oxidase in cancer diagnosis and treatment. *Chem Soc Rev.* 2018;47(17):6454–6472.
78. Ma Y, Zhao Y, Bejjanki NK, et al. Nanoclustered cascaded enzymes for targeted tumor starvation and deoxygenation-activated chemotherapy without systemic toxicity. *ACS Nano.* 2019;13(8):8890–8902.
79. Feng W, Han X, Wang R, et al. Nanocatalysts-augmented and photothermal-enhanced tumor-specific sequential nanocatalytic therapy in both NIR-I and NIR-II biowindows. *Adv Mater.* 2019;31(5):e1805919.
80. Lu X, Gao S, Lin H, Shi J. Single-atom catalysts for nanocatalytic tumor therapy. *Small.* 2021;17(16):e2004467.
81. Wang W, Zhu Y, Zhu X, et al. Biocompatible ruthenium single-atom catalyst for cascade enzyme-mimicking therapy. *ACS Appl Mater Interfaces.* 2021;13(38):45269–45278.
82. Zhao M, Zhang N, Yang R, Chen D, Zhao Y. Which is better for nanomedicines: nanocatalysts or single-atom catalysts? *Adv Healthc Mater.* 2021;10(8):e2001897.
83. Feng Y, Qin J, Zhou Y, Yue Q, Wei J. Spherical mesoporous Fe-N-C single-atom nanozyme for photothermal and catalytic synergistic antibacterial therapy. *J Colloid Interface Sci.* 2022;606(Pt 1):826–836.
84. Lyu M, Chen M, Liu L, et al. A platelet-mimicking theranostic platform for cancer interstitial brachytherapy. *Theranostics.* 2021;11(15):7589–7599.
85. Bahmani B, Gong H, Luk BT, et al. Intratumoral immunotherapy using platelet-cloaked nanoparticles enhances antitumor immunity in solid tumors. *Nat Commun.* 2021;12(1):1999.
86. He Q, Kiesewetter DO, Qu Y, et al. NIR-responsive on-demand release of CO from metal carbonyl-caged graphene oxide nanomedicine. *Adv Mater.* 2015;27(42):6741–6746.
87. Wang S-W, Gao C, Zheng Y-M, et al. Current applications and future perspective of CRISPR/Cas9 gene editing in cancer. *Mol Cancer.* 2022;21(1):57.
88. Yun CW, Lee SH. The roles of autophagy in cancer. *Int J Mol Sci.* 2018;19:11.
89. Zhou Z, Yan Y, Hu K, et al. Autophagy inhibition enabled efficient photothermal therapy at a mild temperature. *Biomaterials.* 2017;141:116–124.
90. Chen T, Cen D, Ren Z, et al. Bismuth embedded silica nanoparticles loaded with autophagy suppressant to promote photothermal therapy. *Biomaterials.* 2019;221:119419.
91. Ma Y, Chen H, Hao B, et al. A chloroquine-loaded Prussian blue platform with controllable autophagy inhibition for enhanced photothermal therapy. *J Mater Chem B.* 2018;6(37):5854–5859.
92. Cui X, Liang Z, Lu J, et al. A multifunctional nanodiamond-based nanopatform for the enhanced mild-temperature photothermal/chemo combination therapy of triple negative breast cancer via an autophagy regulation strategy. *Nanoscale.* 2021;13(31):13375–13389.
93. Zhang X, Du J, Guo Z, et al. Efficient near infrared light triggered nitric oxide release nanocomposites for sensitizing mild photothermal therapy. *Adv Sci.* 2019;6(3):1801122.
94. Zhou Z, Yan Y, Wang L, Zhang Q, Cheng Y. Melanin-like nanoparticles decorated with an autophagy-inducing peptide for efficient targeted photothermal therapy. *Biomaterials.* 2019;203:63–72.
95. Chen H, Liu Z, Wei B, et al. Redox responsive nanoparticle encapsulating black phosphorus quantum dots for cancer theranostics. *Bioact Mater.* 2021;6(3):655–665.
96. Barnard AS. Predicting the impact of structural diversity on the performance of nanodiamond drug carriers. *Nanoscale.* 2018;10(19):8893–8910.
97. Tinwala H, Wairkar S. Production, surface modification and biomedical applications of nanodiamonds: a sparkling tool for theranostics. *Mater Sci Eng C Mater Biol Appl.* 2019;97:913–931.
98. Cui Z, Zhang Y, Xia K, et al. Nanodiamond autophagy inhibitor allosterically improves the arsenical-based therapy of solid tumors. *Nat Commun.* 2018;9(1):4347.
99. Mu Y, Yan X, Li D, et al. NUPR1 maintains autolysosomal efflux by activating SNAP25 transcription in cancer cells. *Autophagy.* 2018;14(4):654–670.
100. Wang Y, Lin Y-X, Qiao Z-Y, et al. Self-assembled autophagy-inducing polymeric nanoparticles for breast cancer interference in-vivo. *Adv Mater.* 2015;27(16):2627–2634.
101. Esin E, Telli TA, Yuce D, Yalcin S. A correlation study of fluorouracil pharmacodynamics with clinical efficacy and toxicity. *Tumori.* 2018;104(3):157–164.
102. Vázquez C, Orlova M, Angriman F, et al. Prediction of severe toxicity in adult patients under treatment with 5-fluorouracil: a prospective cohort study. *Anticancer Drugs.* 2017;28(9):1039–1046.
103. Babincová M, Vrbovská H, Sourivong P, Babinec P, Durdík Š. Application of albumin-embedded magnetic nanoheaters for release of etoposide in integrated chemotherapy and hyperthermia of U87-MG glioma cells. *Anticancer Res.* 2018;38(5):2683–2690.
104. Martin B, Seguin J, Annerau M, et al. Preparation of parenteral nanocrystal suspensions of etoposide from the excipient free dry state of the drug to enhance in vivo antitumoral properties. *Sci Rep.* 2020;10(1):18059.
105. Wang J, Liu J, Liu Y, et al. Gd-hybridized plasmonic au-nanocomposites enhanced tumor-interior drug permeability in multimodal imaging-guided therapy. *Adv Mater.* 2016;28(40):8950–8958.
106. Miyamoto R, Oda T, Hashimoto S, et al. Cetuximab delivery and antitumor effects are enhanced by mild hyperthermia in a xenograft mouse model of pancreatic cancer. *Cancer Sci.* 2016;107(4):514–520.
107. Zhang L, Su H, Cai J, et al. Platform for tumor angiogenesis-targeted chemo-thermal therapy using polydopamine-coated gold nanorods. *ACS Nano.* 2016;10(11):10404–10417.

108. Han HS, Choi KY, Lee H, et al. Gold-nanoclustered hyaluronan nano-assemblies for photothermally maneuvered photodynamic tumor ablation. *ACS Nano*. 2016;10(12):10858–10868.
109. He H, Liu L, Zhang S, et al. Smart gold nanocages for mild heat-triggered drug release and breaking chemoresistance. *J Control Release*. 2020;323:387–397.
110. Han R, Tang K, Hou Y, Yu J, Wang C, Wang Y. Ultralow-intensity near infrared light synchronously activated collaborative chemo/photothermal/photodynamic therapy. *Biomater Sci*. 2020;8(2):607–618.
111. Liu J, Sun L, Li L, Zhang R, Xu ZP. Synergistic cancer photochemotherapy via layered double hydroxide-based trimodal nanomedicine at very low therapeutic doses. *ACS Appl Mater Interfaces*. 2021;13(6):7115–7126.
112. He -P-P, Du X, Cheng Y, et al. Thermal-responsive MXene-DNA hydrogel for near-infrared light triggered localized photothermal-chemo synergistic cancer therapy. *Small*. 2022;18(40):e2200263.
113. Huang X, Shi Q, Du S, Lu Y, Han N. Poly-tannic acid coated paclitaxel nanocrystals for combinational photothermal-chemotherapy. *Colloids Surf B Biointerfaces*. 2021;197:111377.
114. Wu J, Williams GR, Niu S, et al. Nanocomposite for Cancer Theranostics. *Adv Sci*. 2019;6(14):1802001.
115. Zhao W, Li T, Long Y, et al. Self-promoted albumin-based nanoparticles for combination therapy against metastatic breast cancer via a hyperthermia-induced “platelet bridge”. *ACS Appl Mater Interfaces*. 2021;13(22):25701–25714.
116. Kim SS, Kim HK, Kim H, et al. Hyperthermal paclitaxel-bound albumin nanoparticles co-loaded with indocyanine green and hyaluronidase for treating pancreatic cancers. *Arch Pharm Res*. 2021;44(2):182–193.
117. Zhang C, Wang X, Wang J, et al. TCPP-isoliensinine nanoparticles for mild-temperature photothermal therapy. *Int J Nanomedicine*. 2021;16:6797–6806.
118. Li S, Lui K-H, Lau W-S, et al. MSOT-guided nanotheranostics for synergistic mild photothermal therapy and chemotherapy to boost necroptosis/apoptosis. *ACS Appl Mater Interfaces*. 2022;14:33712.
119. Qin Y, Liu T, Guo M, et al. Mild-heat-inducible sequentially released liposomal complex remodels the tumor microenvironment and reinforces anti-breast-cancer therapy. *Biomater Sci*. 2020;8(14):3916–3925.
120. Wang Y, Huang Q, He X, et al. Multifunctional melanin-like nanoparticles for bone-targeted chemo-photothermal therapy of malignant bone tumors and osteolysis. *Biomaterials*. 2018;183:10–19.
121. Du C, Ding Y, Qian J, Zhang R, Dong C-M. Achieving traceless ablation of solid tumors without recurrence by mild photothermal-chemotherapy of triple stimuli-responsive polymer-drug conjugate nanoparticles. *J Mater Chem B*. 2019;7(3):415–432.
122. Feng T, Zhou L, Wang Z, et al. Dual-stimuli responsive nanotheranostics for mild hyperthermia enhanced inhibition of Wnt/ $\beta$ -catenin signaling. *Biomaterials*. 2020;232:119709.
123. Mulens-Arias V, Nicolás-Boluda A, Pinto A, et al. Tumor-selective immune-active mild hyperthermia associated with chemotherapy in colon peritoneal metastasis by photoactivation of fluorouracil-gold nanoparticle complexes. *ACS Nano*. 2021;15(2):3330–3348.
124. Onbasli K, Erkisa M, Demirci G, et al. The improved killing of both androgen-dependent and independent prostate cancer cells by etoposide loaded SPIONs coupled with NIR irradiation. *Biomater Sci*. 2022;10(14):3951–3962.
125. Liu J, Liu K, Zhang L, et al. Heat/pH-boosted release of 5-fluorouracil and albumin-bound paclitaxel from Cu-doped layered double hydroxide nanomedicine for synergistical chemo-photo-therapy of breast cancer. *J Control Release*. 2021;335:49–58.
126. Zhu F, Tan G, Zhong Y, et al. Smart nanopatform for sequential drug release and enhanced chemo-thermal effect of dual drug loaded gold nanorod vesicles for cancer therapy. *J Nanobiotechnology*. 2019;17(1):44.
127. Xu L, Liu J, Xi J, et al. Synergized multimodal therapy for safe and effective reversal of cancer multidrug resistance based on low-level photothermal and photodynamic effects. *Small*. 2018;2018:e1800785.
128. Ding Y, Du C, Qian J, Dong C-M. NIR-responsive polypeptide nanocomposite generates NO gas, mild photothermia, and chemotherapy to reverse multidrug-resistant cancer. *Nano Lett*. 2019;19(7):4362–4370.
129. Dong X, Yin W, Zhang X, et al. Intelligent MoS nanotheranostic for targeted and Enzyme-pH/NIR-responsive drug delivery to overcome cancer chemotherapy resistance guided by PET imaging. *ACS Appl Mater Interfaces*. 2018;10(4):4271–4284.
130. Wang L, Yu Y, Wei D, et al. Strategy of combinational blow for overcoming cascade drug resistance via NIR-light-triggered hyperthermia. *Adv Mater*. 2021;33(20):e2100599.
131. Du C, Ding Y, Qian J, Zhang R, Dong C-M. Dual drug-paired polyprodrug nanotheranostics reverse multidrug resistant cancers via mild photothermal-cocktail chemotherapy. *J Mater Chem B*. 2019;7(35):5306–5319.
132. Mitchell MJ, Billingsley MM, Haley RM, Wechsler ME, Peppas NA, Langer R. Engineering precision nanoparticles for drug delivery. *Nat Rev Drug Discov*. 2021;20(2):101–124.
133. Kunjachan S, Pola R, Gremse F, et al. Passive versus active tumor targeting using RGD- and NGR-modified polymeric nanomedicines. *Nano Lett*. 2014;14(2):972–981.
134. Steeg PS. Targeting metastasis. *Nat Rev Cancer*. 2016;16(4):201–218.
135. Mohme M, Riethdorf S, Pantel K. Circulating and disseminated tumour cells - mechanisms of immune surveillance and escape. *Nat Rev Clin Oncol*. 2017;14(3):155–167.
136. Schlesinger M. Role of platelets and platelet receptors in cancer metastasis. *J Hematol Oncol*. 2018;11(1):125.
137. Borsig L, Wong R, Feramisco J, Nadeau DR, Varki NM, Varki A. Heparin and cancer revisited: mechanistic connections involving platelets, P-selectin, carcinoma mucins, and tumor metastasis. *Proc Natl Acad Sci U S A*. 2001;98(6):3352–3357.
138. Franco AT, Corken A, Ware J. Platelets at the interface of thrombosis, inflammation, and cancer. *Blood*. 2015;126(5):582–588.
139. Haemmerle M, Stone RL, Menter DG, Afshar-Kharghan V, Sood AK. The platelet lifeline to cancer: challenges and opportunities. *Cancer Cell*. 2018;33(6):965–983.
140. Labelle M, Begum S, Hynes RO. Platelets guide the formation of early metastatic niches. *Proc Natl Acad Sci U S A*. 2014;111(30):E3053–E3061.
141. Glehen O, Gilly FN, Boutitie F, et al. Toward curative treatment of peritoneal carcinomatosis from nonovarian origin by cytoreductive surgery combined with perioperative intraperitoneal chemotherapy: a multi-institutional study of 1290 patients. *Cancer*. 2010;116(24):5608–5618.
142. Valle SJ, Alzahrani N, Alzahrani S, Traiki TB, Liauw W, Morris DL. Enterocutaneous fistula in patients with peritoneal malignancy following cytoreductive surgery and hyperthermic intraperitoneal chemotherapy: incidence, management and outcomes. *Surg Oncol*. 2016;25(3):315–320.



143. Robey RW, Pluchino KM, Hall MD, Fojo AT, Bates SE, Gottesman MM. Revisiting the role of ABC transporters in multidrug-resistant cancer. *Nat Rev Cancer*. 2018;18(7):452–464.
144. Fan W, Yung BC, Chen X. Stimuli-responsive NO release for on-demand gas-sensitized synergistic cancer therapy. *Angew Chem Int Ed Engl*. 2018;57(28):8383–8394.
145. Dong X, Cheng R, Zhu S, et al. WO-WSe nanoradiosensitizer increases local tumor ablation and checkpoint blockade immunotherapy upon low radiation dose. *ACS Nano*. 2020;14(5):5400–5416.
146. Yi X, Duan Q-Y, Wu F-G. Low-temperature photothermal therapy: strategies and applications. *Research*. 2021;2021:9816594.
147. Behzadi S, Serpooshan V, Tao W, et al. Cellular uptake of nanoparticles: journey inside the cell. *Chem Soc Rev*. 2017;46(14):4218–4244.
148. Housman G, Byler S, Heerboth S, et al. Drug resistance in cancer: an overview. *Cancers*. 2014;6(3):1769–1792.
149. Curtin NJ. DNA repair dysregulation from cancer driver to therapeutic target. *Nat Rev Cancer*. 2012;12(12):801–817.
150. Rocha CRR, Silva MM, Quinet A, Cabral-Neto JB, Menck CFM. DNA repair pathways and cisplatin resistance: an intimate relationship. *Clinics*. 2018;73(suppl 1):e478s.
151. Galluzzi L, Senovilla L, Vitale I, et al. Molecular mechanisms of cisplatin resistance. *Oncogene*. 2012;31(15):1869–1883.
152. Cavazzana M, Bushman FD, Miccio A, André-Schmutz I, Six E. Gene therapy targeting haematopoietic stem cells for inherited diseases: progress and challenges. *Nat Rev Drug Discov*. 2019;18(6):447–462.
153. Ma -C-C, Wang Z-L, Xu T, He Z-Y, Wei Y-Q. The approved gene therapy drugs worldwide: from 1998 to 2019. *Biotechnol Adv*. 2020;40:107502.
154. Karlsson J, Tzeng SY, Hemmati S, et al. Photocrosslinked bioreducible polymeric nanoparticles for enhanced systemic siRNA delivery as cancer therapy. *Adv Funct Mater*. 2021;31:17.
155. Jung B-K, Lee YK, Hong J, Ghandehari H, Yun C-O. Mild hyperthermia induced by gold nanorod-mediated plasmonic photothermal therapy enhances transduction and replication of oncolytic adenoviral gene delivery. *ACS Nano*. 2016;10(11):10533–10543.
156. Zhang C, Yong Y, Song L, et al. @Poly(ethylene imine) nanoplatforms for imaging guided gene-photothermal synergistic therapy of cancer. *Adv Healthc Mater*. 2016;5(21):2776–2787.
157. Odda AH, Cheang T-Y, Alesary HF, et al. A multifunctional  $\alpha$ -FeO@PEDOT core-shell nanoplatform for gene and photothermal combination anticancer therapy. *J Mater Chem B*. 2022;10(9):1453–1462.
158. Tang W, Han L, Lu X, et al. A nucleic acid/gold nanorod-based nanoplatform for targeted gene editing and combined tumor therapy. *ACS Appl Mater Interfaces*. 2021;13(18):20974–20981.
159. Pan L, Liu J, He Q, Shi J. MSN-mediated sequential vascular-to-cell nuclear-targeted drug delivery for efficient tumor regression. *Adv Mater*. 2014;26(39):6742–6748.
160. Zhang X, Yang Y, Kang T, et al. NIR-II absorbing semiconducting polymer-triggered gene-directed enzyme prodrug therapy for cancer treatment. *Small*. 2021;17(23):e2100501.
161. Su G-Q, Su G, Huang Z-H. Adenovirus-mediated tissue-targeted expression of the CDglyTk gene for the treatment of breast cancer. *Mol Med Rep*. 2012;6(2):321–329.
162. Tang H, Xu X, Chen Y, et al. Reprogramming the tumor microenvironment through second-near-infrared-window photothermal genome editing of PD-L1 mediated by supramolecular gold nanorods for enhanced cancer immunotherapy. *Adv Mater*. 2021;33(12):e2006003.
163. Zhou Z, Ni K, Deng H, Chen X. Dancing with reactive oxygen species generation and elimination in nanotheranostics for disease treatment. *Adv Drug Deliv Rev*. 2020;158:73–90.
164. Ni K, Lan G, Veroneau SS, Duan X, Song Y, Lin W. Nanoscale metal-organic frameworks for mitochondria-targeted radiotherapy-radiodynamic therapy. *Nat Commun*. 2018;9(1):4321.
165. Ni K, Aung T, Li S, Fatuzzo N, Liang X, Lin W. Nanoscale metal-organic framework mediates radical therapy to enhance cancer immunotherapy. *Chem*. 2019;5(7):1892–1913.
166. Xue C, Li M, Liu C, et al. NIR-actuated remote activation of ferroptosis in target tumor cells through a photothermally responsive iron-chelated biopolymer nanoplatform. *Angew Chem Int Ed Engl*. 2021;60(16):8938–8947.
167. Li L, Song D, Qi L, et al. Photodynamic therapy induces human esophageal carcinoma cell pyroptosis by targeting the PKM2/caspase-8/caspase-3/GSDME axis. *Cancer Lett*. 2021;520:143–159.
168. Zhang Y, Liu J, Yu Y, et al. Enhanced radiotherapy using photothermal therapy based on dual-sensitizer of gold nanoparticles with acid-induced aggregation. *Nanomedicine*. 2020;29:102241.
169. Zhang J, Yang L, Huang F, et al. Multifunctional hybrid hydrogel enhanced antitumor therapy through multiple destroying DNA functions by a triple-combination synergistic therapy. *Adv Healthc Mater*. 2021;10(21):e2101190.
170. Ma Q, Cheng L, Gong F, et al. Platinum nanoworms for imaging-guided combined cancer therapy in the second near-infrared window. *J Mater Chem B*. 2018;6(31):5069–5079.
171. Tang W, Dong Z, Zhang R, et al. Multifunctional two-dimensional core-shell MXene@gold nanocomposites for enhanced photo-radio combined therapy in the second biological window. *ACS Nano*. 2019;13(1):284–294.
172. Yin W, Bao T, Zhang X, et al. Biodegradable MoO nanoparticles with efficient near-infrared photothermal and photodynamic synergetic cancer therapy at the second biological window. *Nanoscale*. 2018;10(3):1517–1531.
173. Chen P-L, Huang P-Y, Chen J-Y, et al. A self-delivery chimeric peptide for high efficient cell membrane-targeting low-temperature photothermal/photodynamic combinational therapy and metastasis suppression of tumor. *Biomaterials*. 2022;286:121593.
174. Wang K, Jiang L, Qiu L. Near infrared light triggered ternary synergistic cancer therapy via L-arginine-loaded nanovesicles with modification of PEGylated indocyanine green. *Acta Biomater*. 2022;140:506–517.
175. Wang J, Sun J, Hu W, et al. Bimetallic core-shell nanostructure as an H<sub>2</sub>O<sub>2</sub>-driven oxygen generator to alleviate tumor hypoxia for simultaneous bimodal imaging and enhanced photodynamic therapy. *Adv Mater*. 2020;32(22):e2001862.
176. Guo W, Chen Z, Chen J, et al. Biodegradable hollow mesoporous organosilica nanotheranostics (HMON) for multi-mode imaging and mild photo-therapeutic-induced mitochondrial damage on gastric cancer. *J Nanobiotechnology*. 2020;18(1):99.
177. Li P, Lin B, Chen Z, et al. Biodegradable hollow mesoporous organosilica nanotheranostics (HMONs) as a versatile platform for multimodal imaging and phototherapeutic-triggered endolysosomal disruption in ovarian cancer. *Drug Deliv*. 2022;29(1):161–173.

178. Li G, Zhong X, Wang X, et al. Titanium carbide nanosheets with defect structure for photothermal-enhanced sonodynamic therapy. *Bioact Mater.* 2022;8:409–419.
179. Gong F, Cheng L, Yang N, et al. Preparation of TiH nanodots by liquid-phase exfoliation for enhanced sonodynamic cancer therapy. *Nat Commun.* 2020;11(1):3712.
180. Qiu K, Wang J, Rees TW, Ji L, Zhang Q, Chao H. A mitochondria-targeting photothermogenic nanozyme for MRI-guided mild photothermal therapy. *Chem Commun.* 2018;54(100):14108–14111.
181. Qian M, Cheng Z, Luo G, et al. Molybdenum diphosphide nanorods with laser-potentiated peroxidase catalytic/mild-photothermal therapy of oral cancer. *Adv Sci.* 2022;9(1):2101527.
182. Tao Q, He G, Ye S, et al. Mn doped Prussian blue nanoparticles for T/T MR imaging, PA imaging and Fenton reaction enhanced mild temperature photothermal therapy of tumor. *J Nanobiotechnol.* 2022;20(1):18.
183. Ma X, Chen B, Wu H, et al. A tumour microenvironment-mediated BiMnO hollow nanospheres glutathione depletion for photothermal enhanced chemodynamic collaborative therapy. *J Mater Chem B.* 2022;10(18):3452–3461.
184. Liu J, Wang A, Liu S, et al. Nanozyme for pH-responsive and irradiation-enhanced cascade-catalytic tumor therapy. *Angew Chem Int Ed Engl.* 2021;60(48):25328–25338.
185. Xiong G, Huang D, Lu L, et al. Near-infrared-II light induced mild hyperthermia activate cisplatin-artemisinin nanoparticle for enhanced chemo/chemodynamic therapy and immunotherapy. *Small Methods.* 2022;6(9):e2200379.
186. Zhao Y, Ding B, Xiao X, et al. Virus-Like FeO@BiS nanozymes with resistance-free apoptotic hyperthermia-augmented nanozymic activity for enhanced synergetic cancer therapy. *ACS Appl Mater Interfaces.* 2020;12(10):11320–11328.
187. Ning B, Liu Y, Ouyang B, et al. Low-temperature photothermal irradiation triggers alkyl radicals burst for potentiating cancer immunotherapy. *J Colloid Interface Sci.* 2022;614:436–450.
188. Ouyang B, Liu F, Ruan S, et al. Localized free radicals burst triggered by NIR-II Light for augmented low-temperature photothermal therapy. *ACS Appl Mater Interfaces.* 2019;11(42):38555–38567.
189. Feng N, Li Q, Bai Q, et al. Development of an Au-anchored Fe Single-atom nanozyme for biocatalysis and enhanced tumor photothermal therapy. *J Colloid Interface Sci.* 2022;618:68–77.
190. Sun L, Wang X, Gong F, et al. Silicon nanowires decorated with platinum nanoparticles were applied for photothermal-enhanced sonodynamic therapy. *Theranostics.* 2021;11(19):9234–9242.
191. Han X, Zhao C, Wang S, Pan Z, Jiang Z, Tang X. Multifunctional TiO/C nanosheets derived from 3D metal-organic frameworks for mild-temperature-photothermal-sonodynamic-chemodynamic therapy under photoacoustic image guidance. *J Colloid Interface Sci.* 2022;621:360–373.
192. Huang L, Li Z, Zhao Y, et al. Enhancing photodynamic therapy through resonance energy transfer constructed near-infrared photosensitized nanoparticles. *Adv Mater.* 2017;29:28.
193. Zhou Q, Shao S, Wang J, et al. Enzyme-activatable polymer-drug conjugate augments tumour penetration and treatment efficacy. *Nat Nanotechnol.* 2019;14(8):799–809.
194. Chen S, Zhong Y, Fan W, et al. Enhanced tumour penetration and prolonged circulation in blood of polyzwitterion-drug conjugates with cell-membrane affinity. *Nat Biomed Eng.* 2021;5(9):1019–1037.
195. Son S, Kim JH, Wang X, et al. Multifunctional sonosensitizers in sonodynamic cancer therapy. *Chem Soc Rev.* 2020;49(11):3244–3261.
196. Liu M, Khan AR, Ji J, Lin G, Zhao X, Zhai G. Crosslinked self-assembled nanoparticles for chemo-sonodynamic combination therapy favoring antitumor, antimetastasis management and immune responses. *J Control Release.* 2018;290:150–164.
197. Zhang L, Shen S, Cheng L, et al. Mesoporous gold nanoparticles for photothermal controlled anticancer drug delivery. *Nanomedicine.* 2019;14(11):1443–1454.
198. Liu Y, Zhen W, Jin L, et al. All-in-one theranostic nanoagent with enhanced reactive oxygen species generation and modulating tumor microenvironment ability for effective tumor eradication. *ACS Nano.* 2018;12(5):4886–4893.
199. Wang Y, Shi L, Ye Z, et al. Reactive oxygen correlated chemiluminescent imaging of a semiconducting polymer nanoplatform for monitoring chemodynamic therapy. *Nano Lett.* 2020;20(1):176–183.
200. Guo Y, Jia H-R, Zhang X, et al. A glucose/oxygen-exhausting nanoreactor for starvation- and hypoxia-activated sustainable and cascade chemo-chemodynamic therapy. *Small.* 2020;16(31):e2000897.
201. Bao Y-W, Hua X-W, Zeng J, Wu F-G. Bacterial template synthesis of multifunctional nanospindles for glutathione detection and enhanced cancer-specific chemo-chemodynamic therapy. *Research.* 2020;2020:9301215.
202. Liu G, Zhu J, Guo H, et al. Mo C-derived polyoxometalate for NIR-II photoacoustic imaging-guided chemodynamic/photothermal synergistic therapy. *Angew Chem Int Ed Engl.* 2019;58(51):18641–18646.
203. Dong S, Xu J, Jia T, et al. Upconversion-mediated ZnFeO nanoplatform for NIR-enhanced chemodynamic and photodynamic therapy. *Chem Sci.* 2019;10(15):4259–4271.
204. O'Neill PM, Barton VE, Ward SA. The molecular mechanism of action of artemisinin--the debate continues. *Molecules.* 2010;15(3):1705–1721.
205. Lai HC, Singh NP, Sasaki T. Development of artemisinin compounds for cancer treatment. *Invest New Drugs.* 2013;31(1):230–246.
206. Li J, Cao F, Yin H-L, et al. Ferroptosis: past, present and future. *Cell Death Dis.* 2020;11(2):88.
207. Dai Y, Zhao H, He K, et al. Nanomedicine for fluorescence/photoacoustic tumor imaging and targeted photothermal-photonic thermodynamic therapy. *Small.* 2021;17(42):e2102527.
208. Wang W, Zhang X, Ni X, et al. Semiconducting polymer nanoparticles for NIR-II fluorescence imaging-guided photothermal/thermodynamic combination therapy. *Biomater Sci.* 2022;10(3):846–853.
209. Riley RS, June CH, Langer R, Mitchell MJ. Delivery technologies for cancer immunotherapy. *Nat Rev Drug Discov.* 2019;18(3):175–196.
210. Waldman AD, Fritz JM, Lenardo MJ. A guide to cancer immunotherapy: from T cell basic science to clinical practice. *Nat Rev Immunol.* 2020;20(11):651–668.
211. June CH, O'Connor RS, Kawalekar OU, Ghassemi S, Milone MC. CAR T cell immunotherapy for human cancer. *Science.* 2018;359(6382):1361–1365.
212. Ribas A, Wolchok JD. Cancer immunotherapy using checkpoint blockade. *Science.* 2018;359(6382):1350–1355.

213. Galon J, Bruni D. Approaches to treat immune hot, altered and cold tumours with combination immunotherapies. *Nat Rev Drug Discov.* 2019;18(3):197–218.
214. Huang Y, Kim BYS, Chan CK, Hahn SM, Weissman IL, Jiang W. Improving immune-vascular crosstalk for cancer immunotherapy. *Nat Rev Immunol.* 2018;18(3):195–203.
215. Chen Q, Sun T, Jiang C. Recent advancements in nanomedicine for ‘cold’ tumor immunotherapy. *Nanomicro Lett.* 2021;13(1):92.
216. Liu X, Feng Y, Xu J, et al. Combination of MAPK inhibition with photothermal therapy synergistically augments the anti-tumor efficacy of immune checkpoint blockade. *J Control Release.* 2021;332:194–209.
217. Zhang N, Song J, Liu Y, et al. Photothermal therapy mediated by phase-transformation nanoparticles facilitates delivery of anti-PD1 antibody and synergizes with antitumor immunotherapy for melanoma. *J Control Release.* 2019;306:15–28.
218. Tan T, Hu H, Wang H, et al. Bioinspired lipoproteins-mediated photothermia remodels tumor stroma to improve cancer cell accessibility of second nanoparticles. *Nat Commun.* 2019;10(1):3322.
219. Huang L, Li Y, Du Y, et al. Mild photothermal therapy potentiates anti-PD-L1 treatment for immunologically cold tumors via an all-in-one and all-in-control strategy. *Nat Commun.* 2019;10(1):4871.
220. Chen Q, Hu Q, Dukhovlina E, et al. Photothermal therapy promotes tumor infiltration and antitumor activity of CAR T cells. *Adv Mater.* 2019;31(23):e1900192.
221. Qu D, Qin Y, Liu Y, et al. Fever-inducible lipid nanocomposite for boosting cancer therapy through synergistic engineering of a tumor microenvironment. *ACS Appl Mater Interfaces.* 2020;12(29):32301–32311.
222. Nicolas-Boluda A, Laurent G, Bazzi R, Roux S, Donnadiou E, Gazeau F. Two step promotion of a hot tumor immune environment by gold decorated iron oxide nanoflowers and light-triggered mild hyperthermia. *Nanoscale.* 2021;13(44):18483–18497.
223. Hu Z, Ott PA, Wu CJ. Towards personalized, tumour-specific, therapeutic vaccines for cancer. *Nat Rev Immunol.* 2018;18(3):168–182.
224. Zhang Y, Lin S, Wang X-Y, Zhu G. Nanovaccines for cancer immunotherapy. *Wiley Interdiscip Rev Nanomed Nanobiotechnol.* 2019;11(5):e1559.
225. Melero I, Gaudernack G, Gerritsen W, et al. Therapeutic vaccines for cancer: an overview of clinical trials. *Nat Rev Clin Oncol.* 2014;11(9):509–524.
226. Miao L, Zhang Y, Huang L. mRNA vaccine for cancer immunotherapy. *Mol Cancer.* 2021;20(1):41.
227. Liu J, Miao L, Sui J, Hao Y, Huang G. Nanoparticle cancer vaccines: design considerations and recent advances. *Asian J Pharm Sci.* 2020;15(5):576–590.
228. Fang X, Lan H, Jin K, Gong D, Qian J. Nanovaccines for cancer prevention and immunotherapy: an update review. *Cancers.* 2022;14:16.
229. Huang D, Wu T, Lan S, Liu C, Guo Z, Zhang W. In situ photothermal nano-vaccine based on tumor cell membrane-coated black phosphorus-Au for photo-immunotherapy of metastatic breast tumors. *Biomaterials.* 2022;289:121808.
230. Li Y, Zhang K, Wu Y, et al. Antigen capture and immune modulation by bacterial outer membrane vesicles as in situ vaccine for cancer immunotherapy post-photothermal therapy. *Small.* 2022;18(14):e2107461.
231. Galluzzi L, Buqué A, Kepp O, Zitvogel L, Kroemer G. Immunogenic cell death in cancer and infectious disease. *Nat Rev Immunol.* 2017;17:2.
232. Feng Z-H, Li Z-T, Zhang S, et al. A combination strategy based on an Au nanorod/doxorubicin gel via mild photothermal therapy combined with antigen-capturing liposomes and anti-PD-L1 agent promote a positive shift in the cancer-immunity cycle. *Acta Biomater.* 2021;136:495–507.
233. Huang X, Zhong Y, Li Y, et al. Black phosphorus-synergic nitric oxide nanogasholder spatiotemporally regulates tumor microenvironments for self-amplifying immunotherapy. *ACS Appl Mater Interfaces.* 2022;14(33):37466–37477.
234. Deng X, Guan W, Qing X, et al. Ultrafast low-temperature photothermal therapy activates autophagy and recovers immunity for efficient antitumor treatment. *ACS Appl Mater Interfaces.* 2020;12(4):4265–4275.
235. Zhang Y, Ma S, Liu X, et al. Supramolecular assembled programmable nanomedicine as in situ cancer vaccine for cancer immunotherapy. *Adv Mater.* 2021;33(7):e2007293.
236. Wu J, Chen J, Feng Y, et al. An immune cocktail therapy to realize multiple boosting of the cancer-immunity cycle by combination of drug/gene delivery nanoparticles. *Sci Adv.* 2020;6:40.
237. Kast F, Klein C, Umaña P, Gros A, Gasser S. Advances in identification and selection of personalized neoantigen/T-cell pairs for autologous adoptive T cell therapies. *Oncoimmunology.* 2021;10(1):1869389.
238. Schuster SJ, Bishop MR, Tam CS, et al. Tisagenlecleucel in adult relapsed or refractory diffuse large B-cell lymphoma. *N Engl J Med.* 2019;380(1):45–56.
239. Overchuk M, Zheng G. Overcoming obstacles in the tumor microenvironment: recent advancements in nanoparticle delivery for cancer theranostics. *Biomaterials.* 2018;156:217–237.
240. Chen Z, Pan H, Luo Y, et al. Nanoengineered CAR-T biohybrids for solid tumor immunotherapy with microenvironment photothermal-remodeling strategy. *Small.* 2021;17(14):e2007494.
241. Shi B, Li D, Yao W, et al. Multifunctional theranostic nanoparticles for multi-modal imaging-guided CAR-T immunotherapy and chemophotothermal combinational therapy of non-Hodgkin’s lymphoma. *Biomater Sci.* 2022;10(10):2577–2589.
242. Lin X, Li F, Gu Q, et al. Gold-seaurchin based immunomodulator enabling photothermal intervention and  $\alpha$ CD16 transfection to boost NK cell adoptive immunotherapy. *Acta Biomater.* 2022;146:406–420.

International Journal of Nanomedicine

Dovepress

Publish your work in this journal

The International Journal of Nanomedicine is an international, peer-reviewed journal focusing on the application of nanotechnology in diagnostics, therapeutics, and drug delivery systems throughout the biomedical field. This journal is indexed on PubMed Central, MedLine, CAS, SciSearch®, Current Contents®/Clinical Medicine, Journal Citation Reports/Science Edition, EMBase, Scopus and the Elsevier Bibliographic databases. The manuscript management system is completely online and includes a very quick and fair peer-review system, which is all easy to use. Visit <http://www.dovepress.com/testimonials.php> to read real quotes from published authors.

Submit your manuscript here: <https://www.dovepress.com/international-journal-of-nanomedicine-journal>